

The copyright of this thesis vests in the author. No quotation from it or information derived from it is to be published without full acknowledgement of the source. The thesis is to be used for private study or non-commercial research purposes only.

Published by the University of Cape Town (UCT) in terms of the non-exclusive license granted to UCT by the author.

List of Figures and Tables

Figure 2-1: IWA Water Balance (Farley & Trow, 2003)	2-1
Figure 2-2: Grain size distribution for bedding material (SANS 2001-DP1:2011).....	2-5
Figure 2-3: Pipe bedding details for flexible pipe (SANS 2001-DP1:2011)	2-6
Figure 2-4: Normalised plot of the Ergun equation (Ergun, 1952).....	2-9
Figure 2-5: Characterisation of different flow regimes in fixed beds by means of pressure drop-flow rate behaviour (Hlushkou & Tallarek, 2006)	2-9
Figure 2-6: Three fundamental governing principles characterising behaviour of leaks (Fox et al., 2014)	2-10
Figure 2-7: Soil Properties (Niven & Khalili, 1998)	2-12
Figure 2-8: Schematic Diagram of Transition from Stable in Situ Fluidisation to Cavity Formation. (Niven & Khalili, 1998).....	2-13
Figure 2-9: Sketch of the experimental setup (Zoueshtiagh and Merlen, 2007).....	2-14
Figure 2-10: Patterns formed at the sand fluid interface (Zoueshtiagh & Merlen, 2007).....	2-15
Figure 2-11: Schematic of test apparatus for fluidization tests(Alsaydalani & Clayton, 2013)	2-16
Figure 2-12: Different stages of Fluidisation (Alsaydalani & Clayton, 2013)	2-17
Figure 2-13: Schematic diagram of the experimental apparatus(Van Zyl <i>et al.</i> , 2013).....	2-18
Figure 2-14: Schematic diagram of the fluidisation phenomenon: (a) packed bed; (b) fluidised bed (Van Zyl <i>et al.</i> , 2013).....	2-19
Figure 2-15: Geometry of the fluidised zone for set 3 at different flow rates: (a) 130 litres/h; (b) 220 litres/h; (c) 320 litres/h (Van Zyl <i>et al.</i> , 2013)	2-19
Figure 2-16: Experimental Setup (Bailey, 2015).....	2-21
Figure 2-17: Velocity vector plot in ballotini glass beads (Bailey, 2015)	2-22
Figure 2-18: Pore pressure head measurements (Bailey, 2015)	2-23
Figure 3-1: Schematic diagram of Experimental Setup	3-1
Figure 3-2: Manufactured apparatus.....	3-2
Figure 3-3: Inner box aligned with geotextile	3-2
Figure 3-4 : Outer tank	3-3
Figure 3-5 : Inner tank	3-3
Figure 3-6: Bottom tank design	3-4
Figure 3-7 : Delivery pipe connected to PRV and Flow meter.....	3-4
Figure 3-8 : Delivery pipe connected to hose	3-4
Figure 3-9: Pipe Sample connected to detachable hole through end cap.....	3-5
Figure 3-11: Compacting sand at 300mm interval	3-6
Figure 3-10: Lifting sand bag with Gantry	3-6
Figure 3-13: Spirit Level to ensure the tank stand.....	3-6
Figure 3-12: Tank filled with sand.	3-6
Figure 3-14: Fibertex geotextile samples.....	3-7
Table 3-1: Sand Physical Properties (Pike, 2015)	3-8
Figure 3-15: Sieve Analysis Test Results (Pike, 2015)	3-8
Figure 3-16: Decagon EC-5 moisture sensor and Em5b logger	3-9
Figure 3-17: 7 EC-5 sensors and 2 EM-5 loggers used in the experiments.....	3-10
Figure 3-18 : Weighing of lids.....	3-11
Figure 3-19: Calibration of EC-5 sensors	3-11



Table 3-2: Data collection table for calibration	3-12
Figure 3-20: Plot of calibration data with soil specific calibration equation	3-12
Figure 3-21: Decagon Em5b data logger	3-13
Figure 3-22 : ECH2O Utility Main Screen	3-14
Figure 3-23: Moisture sensors positions	3-15
Figure 3-24: Setup with sensors fixed on the supporting frames.....	3-15
Figure 3-25 : Sensus DN20 iPERL smart meters	3-16
Figure 3-26: iPERL Magnetic field technology	3-16
Figure 3-27 : SIRT handheld device and Sensus RF 2 communication modes.....	3-17
Figure 3-28 : Position of the iPERL water meters.....	3-18
Figure 3-29: Drainage outlets of tank	3-18
Table 3-3: Experiments details summary	3-20
Figure 3-30: Orientation adopted for leak location	3-21
Figure 3-31: Upward pointing Leak	3-21
Figure 3-32: Leak pointing Sideways.....	3-22
Figure 3-33: Typical Trench Details for (SANS 1200 DB).....	3-23
Table 4-1: Parameters details for experiments on the effect of flow rates	4-1
Figure 4-1: Locations of EC-5 sensors and iPERLS	4-1
Figure 4-2: Moisture Content Readings for 200 l/h Flowrate	4-2
Figure 4-3: Leakage Outflow Readings for 200 l/h.....	4-3
Figure 4-4: Moisture Content Readings for 400 l/h Flowrate	4-3
Figure 4-5: Leakage Outflow Readings for 400 l/h.....	4-4
Figure 4-6: Moisture Content Readings for 800 l/h Flowrate	4-5
Figure 4-7: Leakage Outflow Readings for 800 l/h.....	4-6
Table 4-2: Parameters details for experiments on the effect of leak orientation	4-6
Figure 4-8: Moisture Content Readings for 200 l/h Flowrate	4-7
Figure 4-9: Leakage Outflow Readings for 200 l/h.....	4-8
Figure 4-10: Moisture Content Readings for 800 l/h Flowrate.....	4-9
Figure 4-11: Leakage Outflow Readings for 800 l/h.....	4-10
Figure 4-12: Moisture Content Readings for 200 l/h Flowrate.....	4-11
Figure 4-13: Leakage Outflow Readings for 200 l/h.....	4-11
Figure 4-14: Moisture Content Readings for 800 l/h Flowrate.....	4-12
Figure 4-15: Leakage Outflow Readings for 800 l/h.....	4-13
Table 4-4: Parameter details for experiments on the effect of soil permeability	4-14
Figure 4-16: Moisture Content Readings for 200 l/h Flowrate.....	4-15
Figure 4-17: Leakage Outflow Readings for 200 l/h.....	4-15
Figure 4-18: Moisture Content Readings for 800 l/h Flowrate.....	4-16
Figure 4-19: Leakage Outflow Readings for 800 l/h.....	4-17
Figure 4-20: Moisture Content Readings for 200 l/h Flowrate.....	4-18
Figure 4-21: Leakage Outflow Readings for 200 l/h.....	4-18
Figure 4-22: Moisture Content Readings for 800 l/h Flowrate.....	4-19
Figure 4-23: Leakage Outflow Readings for 800 l/h.....	4-20
Figure 4-24: Damaged sensor above leak.....	4-21
Figure 4-25: Formation of cavity on the surface	4-22
Figure 4-27: Leakage at drainage outlets.....	4-23

Figure 4-26 Minor Leak at the bottom of tank 4-23
Figure 4-28: PVC board drilled by water jet 4-24
Figure 4-29: Accumulated sand..... 4-24
Figure 4-30: Leak jet pointing slightly sideways instead of vertically upwards. 4-25



1. Introduction

1.1 Background to study

Water distribution systems are of utmost importance in any country, not only as a domestic need, but they also serve the nation in many economic sectors like tourism, industrial and agriculture. Yet, water distribution systems constitute one of the most vulnerable parts of civil infrastructure systems. The world is already fronting an acute water crisis and it is anticipated to get even worse. Water resources are becoming scarce and there is significant increase in water demand due to the speedily growing world population. One important contributing factor is losses from water supply and distribution systems which can often exceed 50% of production (Rogers, 2014). In fact, effective water management is important because leaks in water distribution pipes are causing substantial water losses and wastage. For example in South Africa, water losses were estimated to stretch up to 70% in some municipalities and many of these regions are characterised by extensive socioeconomic underdevelopment (Muller, 2009). Numerous investigations are being carried out to understand leakage in water distribution pipes and to reduce water losses with a view to satisfying the increase in water demand.

The surrounding soil around water pipes is an important factor when studying leaks in water distribution systems and plays a key role in leakage management worldwide (Van Zyl *et al.*, 2013). Some recent research has been based on understanding the interaction between soil and leakage in water distribution systems. In the context of soil and leak interaction, the hydraulics of both soil and leakage need an in-depth study. Leak hydraulics is governed by Torricelli's flow through an orifice equation. For soil hydraulics, Van Zyl and Clayton (2007) concluded that the flow-pressure relationship is unlikely to be linear. Non-linear flow is assumed to occur mainly because of turbulent flow, hydraulic fracturing and soil fluidisation (Van Zyl *et al.*, 2013).

Not much research has been done to understand under what conditions a leak will become visible above the ground. Water pipes are normally buried below a meter of graded soils that may facilitate water draining away from the surface. In a recent experimental study (Van Zyl *et al.*, 2013), it was found that even jets directed vertically upward did not penetrate about 30 cm of an ideal soil, while sustaining a pressure of 25 m in the pipe. The work showed that the fluidised zone is responsible for dissipating the majority of the energy of the water jet and thus, limiting the leak's ability to reach the soil surface. These leaks are considered as background leakage, are difficult to find, and ultimately remain undetected for months or years.

1.2 Problem Statement

In most of the recent studies involving leakage in water distribution systems, the interaction between a leaking pipe and its surrounding soil has not been addressed as in real water reticulation systems. The experiments and models analysed different factors like bed heights, orifice sizes and flow rates under ideal soil conditions. The soil-leak interaction is reported to be complex mainly because Darcy flow does not occur as leakage water moves in the surrounding

soil. Hence, it is justifiable to investigate the impact of soil as in real situations rather than in an idealised scenario. The main reason for studying soil fluidisation is due to the energy loss which occurs between the orifice and the soil surface when leakage water moves through the soil.

Therefore, studying the soil-interaction when water pipes are buried under real conditions can prove to be useful to have a better understanding on leak development and eventually, its effect on leak discoverability. Moreover, it is valuable to identify how much leakage water is actually lost through the walls of the typical trench before it appears to the ground surface. This project is based on an investigation to understand soil-leak interaction when a pipe is buried under real conditions and to evaluate the impact of factors affecting leakage propagation and hence, its ability to reach the ground surface.

1.3 Objectives of Research

The aim of this research is to understand soil-leak interaction and design an equipment to understand the movement of water leaking in distribution pipes. In addition, as a preliminary study, it will identify and evaluate the impact of a few basic parameters affecting leakage flow paths and hence, a leak's ability to reach the surface. The study will involve setting up a pipe with a manufactured leak in different trench conditions in the hydraulics laboratory. The research's main steps towards the goal are therefore to:

- Investigate and understand soil-leak interaction from previous studies;
- Design and construct an experimental set up to evaluate movement of water around a leaking pipe;
- Run experiments to investigate the movement of water considering a number of variables; and
- Analyse results to evaluate the impact of leakage flow in different conditions and integrate them in the context of leak detection.

1.4 Thesis Layout

Chapter 1: Introduction

Chapter 1 explains the background and problem statement for the study. The objectives of the research are also listed.

Chapter 2: Literature Review

This chapter discusses the literature which is relevant to the study and also includes, previous studies on soil leak interaction in water distribution systems.

Chapter 3: Methodology

Chapter 3 describes the equipment manufactured for this study and the methods used for data collection.

Chapter 4: Results and Discussions

This chapter includes discussions of the results obtained from the experiments.

Chapter 5: Conclusions

The last chapter summarises the outcomes of this study and recommendations for future experiments relating to this study are addressed.

2. Literature Review

In this chapter, all theoretical approaches gained from several readings in relation to the topic are brought together under appropriate headings in a systematic order. The discussions include water losses, leakage, leakage hydraulics, soil hydraulics, complexity at orifice-soil interface and soil fluidisation. The literature ends with some recent studies done on water flow outside leaks.

2.1 Background

2.1.1 Water Losses

All water networks worldwide involve water losses and it is a major concern for many developing nations including South Africa. Water loss is normally defined as the difference between total production and total consumption. Figure 2-1 shows the standard water balance from the International Water Association (IWA). Leakage makes up a large part of water losses and other causes include meter inaccuracies and unauthorised consumption (Farley & Trow, 2003).

System input volume (corrected for known errors)	Authorised consumption	Billed authorised consumption	Billed metered consumption (including water exported)	Revenue water
			Billed unmetered consumption	
		Unbilled authorised consumption	Unbilled metered consumption	Non-revenue water (NRW)
			Unbilled unmetered consumption	
	Water losses	Apparent losses	Unauthorised consumption	
			Customer metering inaccuracies	
		Real losses	Leakage on transmission and/or distribution mains	
			Leakage and overflows at utility's storage tanks	
	Leakage on service connections up to point of customer metering			

Figure 2-1: IWA Water Balance (Farley & Trow, 2003)

From Figure 2-1, it can be noted that water losses normally exist as real and apparent losses. Real losses are the physical water losses between the system input and the consumer's meter, and comprise of water lost through leaks, bursts and overflows (Seago et al., 2004). Real losses are the main components of water losses and can be divided into two types of leakage which are pipe bursts and background leakage (Seago et al., 2004). Pipe bursts are leaks that break through the

surface of the ground and hence, are easily spotted and fixed. On the contrary, background leakage are leaks which are mainly pressure dependent and are difficult to detect without exact excavation. Background leakage are mainly caused by installation failures and are usually found at service connections. These background leaks can be reduced through pressure management.

Apparent losses often referred to as non-physical losses occur from unauthorised consumption and customer metering inaccuracies. The increase in water losses from water networks is of great concern for municipalities in South Africa. Mc Kenzie et al. conducted a study (2012) that showed data collected from 132 out of 237 South African municipalities, results showed that 36.8% of the total system input volume has been classified as Non-Revenue Water (NRW) and approximately 70% of this NRW comprised of physical leakage (McKenzie et al., 2012).

Studies estimated that 32 billion cubic meters of water are lost annually in water distribution networks through leakage (Global Water Leakage Summit, 2008). Leakage is not just a waste of valuable water resource but also constitutes points of entries for pollutants into pipe lines and hence, often causing health hazards. Leakage compromises between the quality and safety of drinking water (Packer et al., 2002). A lot research is being done to mitigate intrusions into water pipelines. For example, Yang et al. (2014) investigated the effect of porous media on the intrusion rate in water distribution pipes.

In order to control leakages in water distribution systems, it is important to understand the functioning of the system. Studies have revealed that leakage and pressure management are related and that leakage can be reduced through effective pressure management (Marunga et al., 2006; T. Walski *et al.*, 2006; Clayton & van Zyl, 2007). In the same way as pressure influences leakage, the undefined surrounding media also influences leakage. Hence, a better understanding of the behaviour of the soil-leak interaction zone is necessary.

2.2 Flow through Orifice

2.2.1 Leakage Hydraulics

Many studies (Cassa et al., 2010; Mutikanga, 2012) have reported that one of the main factors affecting leakage is the pressure in the system. The conventional relationship between leakage and pressure is described by the orifice equation. This expression can be derived from first principles using the principle of energy conservation (Greyvenstein & Van Zyl, 2005; Walski *et al.*, 2009; Guo *et al.*, 2013).

Velocity of the jet is given by Torricelli's theorem (Chadwick, Morfett and Borthwick, 2004)

$$v = \sqrt{2gh} \quad (2.1)$$

Where v is velocity of the jet, g is the gravitational constant (9.81m.s^{-1}) and h is the pressure head between the orifice and the free surface. The flow rate is the product of the area of the orifice and the velocity through the orifice, resulting in equation 2.2:

$$Q = A\sqrt{2gh} \quad (2.2)$$

Where A is the area of orifice and Q is the discharge through orifice.

The discharge is less than the theoretical value and hence a discharge coefficient is added to equation:

$$Q = C_d A \sqrt{2gh} \quad (2.3)$$

(Note: The discharge coefficient, C_d is normally given by: $C_d = C_v C_c$ where C_v is the velocity coefficient and C_c the contraction coefficient.)

Typical values of C_v are between 0.95 and 0.99 and for C_c between 0.6 and 1 (Daugherty and Franzini, 1965). C_c accounts for the contraction in area of the upstream and downstream end of the orifice downstream. This contraction is known as the vena contractor (Daugherty & Franzini, 1965). C_v accounts for the assumption that the velocity flowing through the orifice is the same at the upstream end of the orifice as it is in the vena contractor.

2.2.2 Pressure and Leakage

Given that pressure has a great influence on the leakage rate in the distribution systems, the orifice equation was subsequently converted into a simpler form where the leakage exponent (N_1) was introduced Lambert (2001).

$$Q = CH^{N_1} \quad (2.4)$$

Where C is a fixed leakage coefficient and N_1 is the leakage exponent.

A number of field studies have shown that N_1 can be considerably larger than 0.5 and typically varies between 0.5 and 2.79 with a median of 1.15 (Farley and Trow, 2003). The reasons for the nonconformity of the leakage exponent (N_1) from the theoretical value of 0.5 is not well understood for its complexity. In recent studies, factors like leak hydraulics, pipe material behaviour, soil hydraulics, and water demand were reported as reasons for the range of leakage exponents (N_1) (Van Zyl and Clayton, 2007). With regards to soil hydraulics which is more relevant to this research, the researchers reported that the interaction between a leaking pipe and the surrounding soil is a very complex problem. They described a number of reasons for the non-linear (non-Darcy) relationship between head loss and the flow through leaks in pipes namely orifice-soil particles interaction; turbulent flow in soil; changing geometry of the fluidising zone; the void creation in soils and rock by the pressurised fluid known as hydraulic fracturing; and piping.

2.2.3 Orifice blockage

Around a leaking pipe, there is granular soil particles which can obstruct the orifice opening at some stages during fluidisation and then the flow behaviour is expected to be disturbed. Massimilla et al. (1963) studied the rate of fluid-particle flow from fluidised beds through small orifices. They examined the effect of the ratio of orifice to particle diameter on the flow behaviour. The result of this study showed that for beds of greater than 70% liquid the rate of

flow was similar to that of 100% of liquid. They indicated that under such conditions, the orifice flow equation (2.3) can be used. However, at some critical bed solids concentration (35-50 %) the particles started to interfere with the orifice and the coefficient of discharge for the flow decreased. They observed a reduction in the value of the coefficient of discharge by about 22 % of that at high liquid rate.

The soil-orifice interaction modifies the downstream jet behaviour when in some instances part of the orifice is blocked (Massimilla et al., 1963; Clayton & van Zyl, 2007). Water seeping through these particles meets with more resistance than water flowing freely through an unblocked orifice. Under such situations, it is expected that more energy is required to deliver more flow.

2.3 Fluidisation outside Water Pipes

Many definitions are given for the term fluidisation in different disciplines. It can occur in the field of civil engineering and other fields such as chemical engineering, costal engineering and geology. In civil engineering, fluidisation is initiated as a result of uncontrolled seepage flow.

In recent studies (Ma, 2011; Alsaydalani & Clayton, 2013), fluidisation occurring outside cracked water pipes was termed “internal fluidisation”. In practice, internal fluidisation is believed to occur when water from a leaking pipe moves through the orifice and infiltrates into the surrounding soil. As water penetrates the granular soil near the orifice, the pore pressure increases and continues to increase as the flow rate through the orifice is increased. At some point, the increased pore pressure equals and surpasses the weight of the above granular bed and initiates internal fluidisation (Alsaydalani & Clayton, 2013). Three dissimilar regions were observed just outside the water leak and are classified as the fluidised zone, the mobile bed zone and the static bed zone. In the fluidised zone, the granular material becomes completely displaced. The mobile bed zone envelopes the fluidised zone and the granular material is in continuous motion. Finally, in the static bed zone, there is no granular material movement (Van Zyl *et al.*, 2013). The pressure changes and particle movements in the different zones are later described in the literature where the study by Van Zyl et al. (2013) is further detailed.

2.4 Buried Pipes Design Considerations

In order to design an experiment with a buried water pipe in the hydraulics laboratory, it is important to follow the specifications for pipeline trench in SANS 2001-DP1:2011. The bedding surrounding the buried pipe should be placed without voids so that the pipe does not move or deflect. The extent to which the material must be compacted is described by a compatibility factor in Part 3 of SANS 2001-DP1:2011. The bedding grains should be evenly graded meaning that 90% of the material by mass should be retained on a single sieve size as illustrated in Figure 2-2.

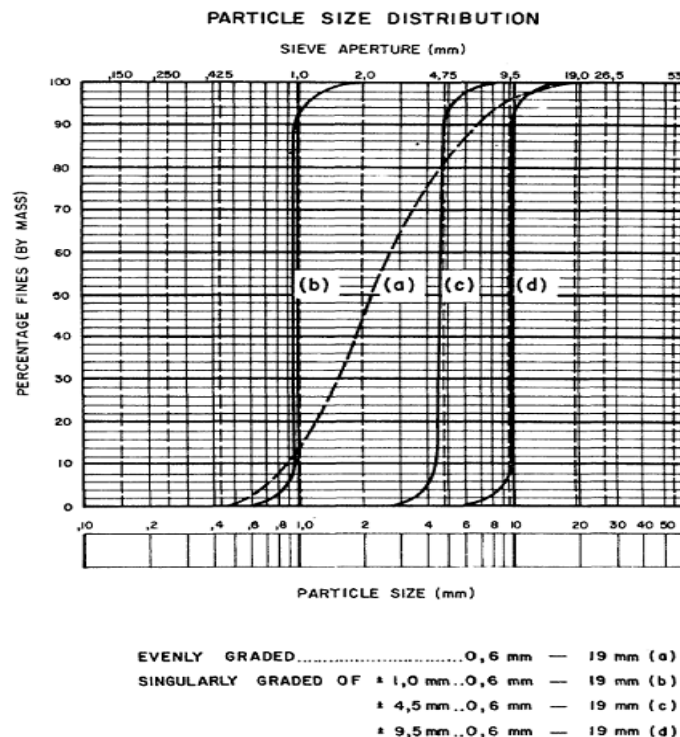
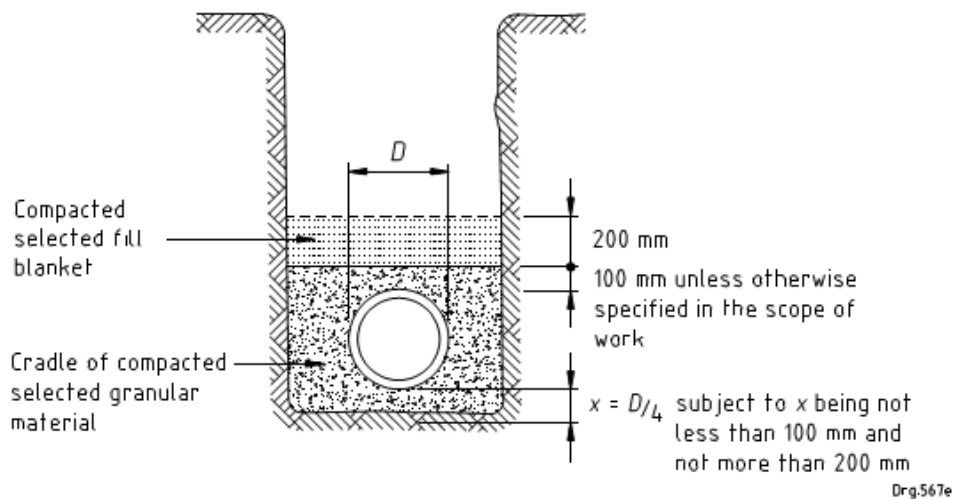


Figure 2-2: Grain size distribution for bedding material (SANS 2001-DP1:2011)

A selected fill blanket is characterised as the cradle up the sides and over the top of a pipe, such that the barrel is supported continuously and firmly on the sides and protected over the top by a dense cushion of material as shown in Figure 2-2. The selected material should be granular, non-cohesive that is singularly graded between 0,6 mm and 19 mm, free-draining, and should have a compatibility factor not exceeding 0,4 unless otherwise specified. Moreover, the selected fill material is required to have a maximum Plasticity Index (PI) of 6, and to be free from vegetation and from lumps and stones of diameter larger than 30 mm. The main fill is the approved filling material placed in a pipe trench. Flexible pipes should be supported on a continuous bed of selected granular material of minimum compacted depth of 100mm as well as covering the full width of the trench. Figure 2-3 below shows the setup as per SANS 2001-DP1:2011.



NOTE D is the external diameter of the pipe barrel.

Figure 2-3: Pipe bedding details for flexible pipe (SANS 2001-DP1:2011)

2.5 Flow through Granular Soil

Water normally moves through soil by means of seepage action. Water has to overcome a drag force along the surfaces of contact between the water and the sidewalls of the pore spaces in the soil. This force is conveyed to the solid particles and is also called seepage force (Spangler & Handy, 1982). Fluid flow through a granular media can be classified to be either laminar or turbulent depending on the flow velocity and is characterised by Reynolds's number (Re) (Harr, 1962):

$$Re = \frac{VD\rho_f}{\mu} \quad (2.6)$$

Where Re is the Reynolds number, V is the average velocity between particles (flow per unit cross section of soil), D the average particle diameter, ρ_f the fluid density, and μ the dynamic viscosity of fluid which is the resistance a fluid exerts to shearing flows.

2.5.1 Laminar Flow

Laminar flow through granular materials may be described as smooth flow in which flow lines, not necessarily parallel, remain distinct and follow the general vector direction of overall flow (Watson & Burnett, 1993).

Darcy (1856) established the first law of flow through a saturated porous medium, which is known as Darcy's law. He carried out a series of experiments using a vertical column filled with sand particles and allowed water to flow through the sand column. Based on these experiments,

Darcy concluded that the rate of flow through the porous media is linearly proportional to the total head loss across the sand column (Darcy, 1856).

$$Q = K A \left(\frac{\Delta H}{L} \right) \quad (2.7)$$

Where A is the cross sectional area of the flow, K is the hydraulic conductivity and L is the packed bed height of the column.

The equation was further simplify as follows:

$$v = ki \quad (2.8)$$

Where v is flow velocity, i is the hydraulic gradient and k is the hydraulic conductivity.

The value k can be calculated using equation proposed by Allen Hazen (Aysen, 2002):

$$k = c_H D_{10}^2 \quad (2.9)$$

Where D_{10} is the grain diameter corresponding to 10% of the fine grains (obtained from the particle size distribution curve in Figure 2-2) and c_H is Hazen's coefficient. (Aysen, 2002)

The range of the validity of Darcy Law was examined and it was found that the law is valid for a wide range of soils and hydraulic gradients (Terzaghi, 1943). Furthermore, Taylor (1948) has indicated that flow through most soil is generally laminar. He found that under a hydraulic gradient of unity, typical for most flow situations, soil with a grain size of 0.5 mm or smaller will always have laminar flow (Taylor, 1948).

However, in cases of flow through coarse sand and gravels, Darcy's law is not strictly applicable and the flow is expected to be non-laminar (Cedergren, 1989).

2.5.2 Turbulent Flow

At higher flow velocity, turbulent flow may occur in porous media and tends to have a non-linear relationship. Therefore, Darcy's equation cannot be used for turbulent flow (Craig, 2004). Turbulent flow occurs at the high Reynolds numbers for which inertial forces predominate over viscous forces. Turbulent flow is not observed in a porous medium until the pore Reynolds number (Re) is 60 to 150 (Bear, 1972).

A non-linear relationship between flow and head, was suggested where Darcy's law was modified for high flow velocities (Forchheimer, 1901). A second order term in the velocity was added:

$$I = aV + bV^2 \quad (2.10)$$

The values of the constants a and b can be obtained for a given physical system by solutions of the Navier-Stokes equations relating pressure and velocity fields, for the corresponding boundary conditions (Hlushkou D & Tallarek 2006).

In 1998, Venkataraman & Rao tabulated the previous four decades of work done in solving for a and b values. The survey included a large variety of granular mediums ranging from fine sands to different types of rocks with varying particle diameters. They examined the porosity and



permeability values for these granular mediums. Venkataraman & Rao (1998) verified the correctness of a and b experimental data with theoretical relationships by Ward (1964) and Ahmed & Sunada (1969). Ward (1964) used the method of dimensional analysis whereas Ahmed & Sunada (1969) used the Navier-Stokes equations to obtain expressions for a and b . The theoretical relationships were reported to match with the experimental results from the various investigations of Venkataraman and Rao (1998). Considering Ward's expressions for coefficients a and b :

$$a = \frac{1}{k} \quad (2.11)$$

$$b = \frac{6.72(1-n)}{g\phi_s D n^2} \quad (2.12)$$

Where n is porosity, g is the acceleration due to gravity, (ϕ_s) is the particle shape factor and D is the particle diameter.

A non-linear relationship between pressure drop and fluid velocity was also studied by Ergun (1952) in the field of chemical engineering where a column, similar to that of Darcy, was filled with granular material and a gas was allowed to flow through the bed. Factors like flow rate, size and shape of the particle, porosity of the bed, and fluid properties were measured. By equating the fluid energy loss to the sum of viscous energy and kinetic energy losses, an equation giving the pressure loss per length of a packed bed was developed:

$$\frac{\Delta P}{L} = A \frac{\mu}{\phi_s^2 d_p^2} \cdot \frac{(1-\varepsilon)^2}{\varepsilon^3} U + B \frac{\rho_f}{\phi_s d_p} \cdot \frac{(1-\varepsilon)}{\varepsilon^3} U^2 \quad (2.13)$$

Where μ is the dynamic viscosity of fluid, d_p is the particle diameter, ρ_f is the fluid density, ρ_s is the solids density, ϕ_s is the particle shape factor, ε is the porosity, U is the superficial velocity.

The Ergun model is used to describe pressure loss with different packing. This is due to the fact that it takes into account the effect of pressure losses (Niven, 2003):

- Due to viscous energy loss resulting from laminar flow at low velocity.
- Due to kinetic energy or inertial losses from the onset of flow separation effects within the porous media at higher flow velocity.

Figure 2-4 validates the capability of the Ergun model to cover, in good agreement with the experimental data, a wide range of velocities in a packed granular beds from laminar to turbulent flow (Bird et al. 2002; Hlushkou & Tallarek 2006). The transition from laminar to turbulent flow has been described by Ergun to be gradual and smooth.

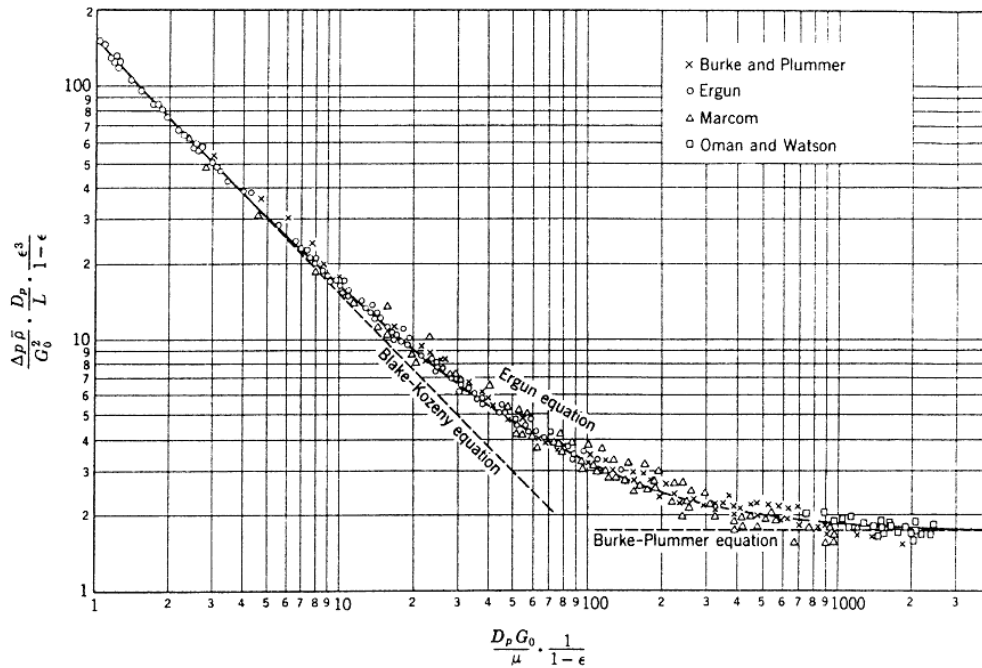


Figure 2-4: Normalised plot of the Ergun equation (Ergun, 1952)

Hlushkou and Tallarek (2006) indicated three regimes of liquid flow through porous media which are illustrated in Figure 2-5. It is interesting to note the range for transitional or nonlinear laminar flow in which viscous and inertial forces effects exist and pressure loss varies nonlinearly with fluid velocity, but flow remains laminar. Pressure loss due to kinetic energy loss dominates at high Reynolds number (Re).

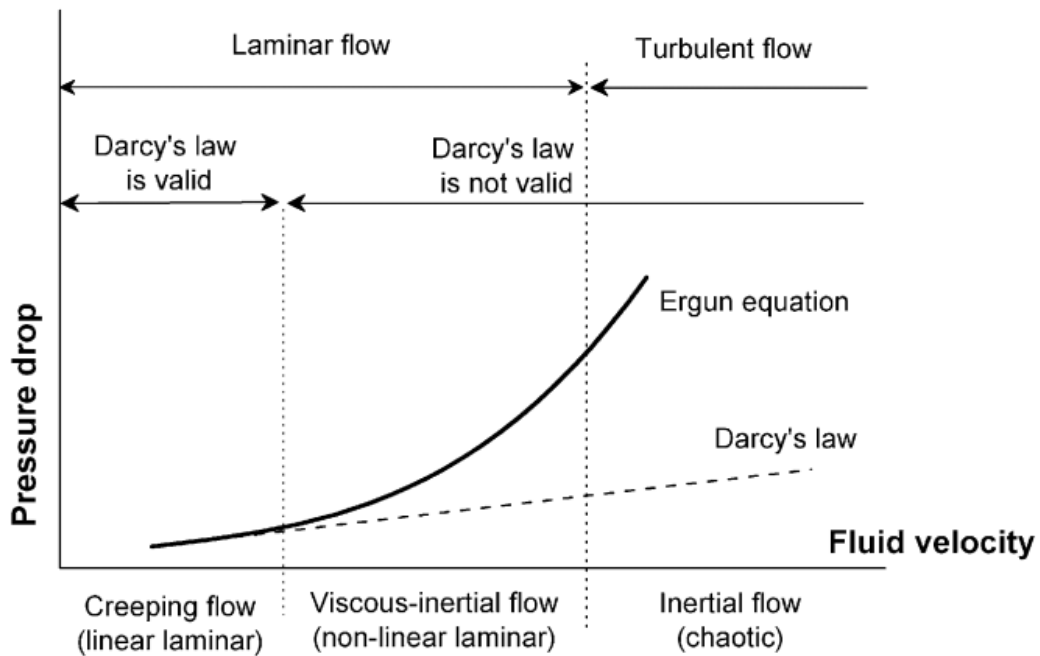


Figure 2-5: Characterisation of different flow regimes in fixed beds by means of pressure drop-flow rate behaviour (Hlushkou & Tallarek, 2006)



2.5.3 Pore Pressures and Effective Stress

Pore pressure and effective stress exist in granular soils when water penetrates through the soil. Pore pressure and effective stress can be described by creating flow nets which consist of the velocity vectors and the equipotential pressure lines (Craig, 2004). The velocity vectors are drawn first in the direction of flow from the source through the soil and then the pressure lines are drawn perpendicularly. Velocity vectors decrease when moving away from the flow source. The lower velocities are result of the lower pressures which exist further away from the flow source.

The effective stress in a soil is the force which binds the particles together i.e. the stress in a soil minus the pore water pressure (Craig, 2004). Terzaghi (1925) proposed a relationship for effective stress (Craig, 2004):

$$\sigma' = \sigma - u \quad (2.14)$$

Where σ' is the effective stress, σ is the stress and u is the pore pressure. Typically the pore pressure increases in the presence of pressurised water. The expression plays an important role in understanding the inter-grain stress regarding pore pressures.

In the case where the pore pressure is negative, the effective stress can increase if the pore pressure increases which occurs when a fluid is drawn upwards above the water level by the forces between the soil particles and the fluid. These forces overcome the gravitational forces that act on the fluid. This upward movement of water is known as capillary action (Aysen, 2002).

2.6 Complexity at Soil-Leak Interaction Interface

Flow through the granular soils and the leak opening can be termed as combined flow in internal fluidisation. The complexity of this combined flow has been mentioned in several studies (Ledwith et al., 1990; Walski et al., 2006; Clayton & van Zyl, 2007; Zoueshtiagh & Merlen, 2007).

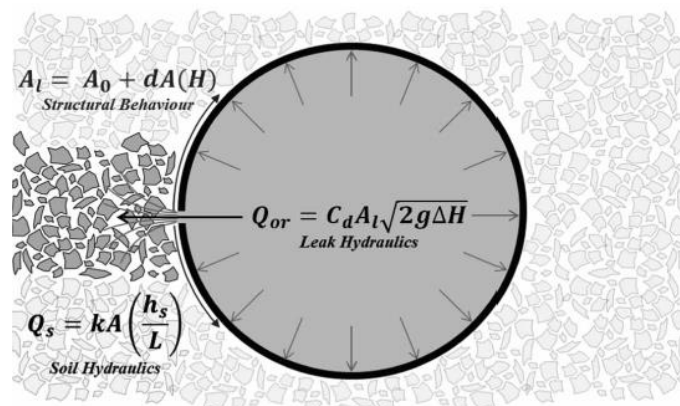


Figure 2-6: Three fundamental governing principles characterising behaviour of leaks (Fox et al., 2014)

Ledwith & Weisman (1990) investigated the pipe pressures and flow rates required for internal fluidisation by means of a 2-D internal fluidisation experiment. In the experiments, the sand varied between fine, medium and coarse grains at bed heights of 254 and 420 mm. 12 different orifice diameters from 1.59 to 6.35 mm were tested. One thought-provoking result was that high pressures could be maintained in the pipe before the soil became fully fluidised. Also, at the initiation of internal fluidisation the internal pipe pressure dropped significantly.

Walski et al. (2006) investigated head losses due to flow through an orifice and flow through soil. They derived a dimensionless "orifice/soil" (OS) number assuming Darcy flow:

$$OS = \frac{h_o}{h_s} = \frac{KAQ}{2gL} \left(\frac{1}{C_d A_o} \right)^2 \quad (2.15)$$

Where h_o is head loss through orifice, h_s is head loss through soil, K is the hydraulic conductivity of the soil, A is the area of flow in the soil, Q is the flow rate, L is the length of the flow path in the soil, C_d is the coefficient of discharge of the orifice, and A_o is the area of the orifice.

When OS is less than unity, they claimed that soil head losses dominate. When OS is larger than unity orifice head losses were thought to dominate. An OS with a magnitude of 1 indicates that both the soil losses and orifice losses are important. Based on their observations, they concluded that "in most real-world cases, the OS number is large" so that the orifice head losses dominate. However, other literature indicates that seepage head may dominate and indeed, that it is possible to maintain significant heads in a water pipe whilst fluidising a shallow bed of soil.

Zoueshtiagh & Merlen (2007) experimented with a vertical internal fluidising water jet surrounded by a granular bed. The authors categorised the internal fluidisation occurrence into three distinct regimes. The regimes described the different stages leading up to and into the occurrence of internal fluidisation, where these stages were dependant on the granular bed behaviour. The authors described Regime (1) as where seepage flow exists in the granular bed and the bed itself remains motionless, with low flow rates through the orifice. Regime (2) experiences higher flow rates where there is an inherent distortion on the granular bed surface. Zoueshtiagh & Merlen (2007) refer to this regime as the transitional situation where a complex interaction exists at the orifice-soil particle interface. Regime (3) experienced even higher flow rates. In Regime (3) they found fluidisation to occur up to and on the granular bed surface. They described the fluidised zone as being similar to that of a vertical cylindrical chimney.

Van Zyl & Clayton (2007) pointed out that coupling of the orifice equation (Equation 2.3) and the soil seepage equation (Equation 2.7) does not properly define the combination of flows in the OS expression by Walski et al. (2006). They stated that the orifice flow analysis and soil seepage analysis are incompatible. The orifice-soil interaction is very complex and whether the seepage flow through the granular bed is laminar as in Darcy flow or whether it is turbulent is still a contentious issue.

Based on the above discussions, it can be concluded that the soil-leak interaction is complex and it is unlikely that the relationship between head and flow rate is a linear relationship. The reasons

for the complexity can be attributed to orifice blocking, turbulent flow in the soil bed, and initiations of additional mechanisms such as piping, hydraulic fracturing and internal fluidisation.

2.7 Previous Studies on Soil-Leak Interaction

2.7.1 In Situ Fluidisation by a single Internal Vertical Jet (Niven & Khalili, 1998)

Niven and Khalili (1998) performed an experiment which examined the scour of granular material initiated with a jet of water, located vertically downward within the bed of material, creating an internal fluidised zone. Within this experiment, the granular material and jet diameters of water flow were varied in order to test its effects on the fluidisation geometry.

The equipment used for this experiment consisted of three different sized containers used in conjunction with a specific granular material, a tank made of Plexiglas (280mm × 280mm × 240mm), a tank constructed of glass (750mm × 340mm × 460mm) and a cylindrical tank (400mm radius and a depth of 1100mm). The water supply was provided via either a glass or metal jet connected to the local water supply, anchored by a ratchet system enabling it to be lowered vertically into the tanks. Other equipment such as thermometers and a rotameter bank were used to monitor the temperature of the water and the flow rate.

Within the experiment five samples of granular material and the properties of the following samples are displayed below in Figure 2-7.

Property	FS	MCS	CS	VCS	SM
Description	Fine sand	Medium to coarse sand	Coarse sand	Very coarse sand	Silty clayey sand
Median (d_{50}) diameter (mm)	0.231	0.595	0.884	1.62	0.313
Mean diameter (mm)	0.207	0.540	0.775	1.31	0.383
Pore volume ($L\ kg^{-1}$)	0.28	nd	nd	nd	0.25 ± 0.04
Measured hydraulic conductivity (ms^{-1})	$3.9E-4 \pm 0.5E-4$	nd	nd	nd	$6.4E-5 \pm 0.5E-5$
Calculated U_{mffv} (ms^{-1}) at $\epsilon=0.43$, eq'n (5) *	$5.1E-4$	$3.4E-3$	$7.5E-3$	0.025	$9.4E-4$
Calculated U_{mffT} (ms^{-1}), eq'n (7) *	$5.2E-4$	$3.4E-3$	$7.0E-3$	0.018	$9.5E-4$

nd = not determined

*Assumptions: $d_p = d_{50}$; $\rho_f = 1000\ kg\ m^{-3}$; $\rho_s = 2650\ kg\ m^{-3}$; $\mu = 0.001\ kg\ m^{-1}s^{-1}$ and $\phi_s = 0.8$

Figure 2-7: Soil Properties (Niven & Khalili, 1998)

From the observations of the experiments several facts regarding fluidisation had been determined:

- As the depth of jet was lowered into the sample of granular material the fluidisation geometry changed from an open stable profile, progressing to an unstable asymmetric profile and finally a submerged fluidised cavity;
- The process of fluidisation caused the accumulation of granular material in the formation of circular ring surrounding the zone of fluidisation;
- The depth required for this transition was dependent upon the particle size of the granular medium. The finer the particle size the larger the transition depth, within the experiment the medium to very coarse sands had a transition depth of 10 to 50mm, whilst the finer sands had a transition depth of at least 230mm.

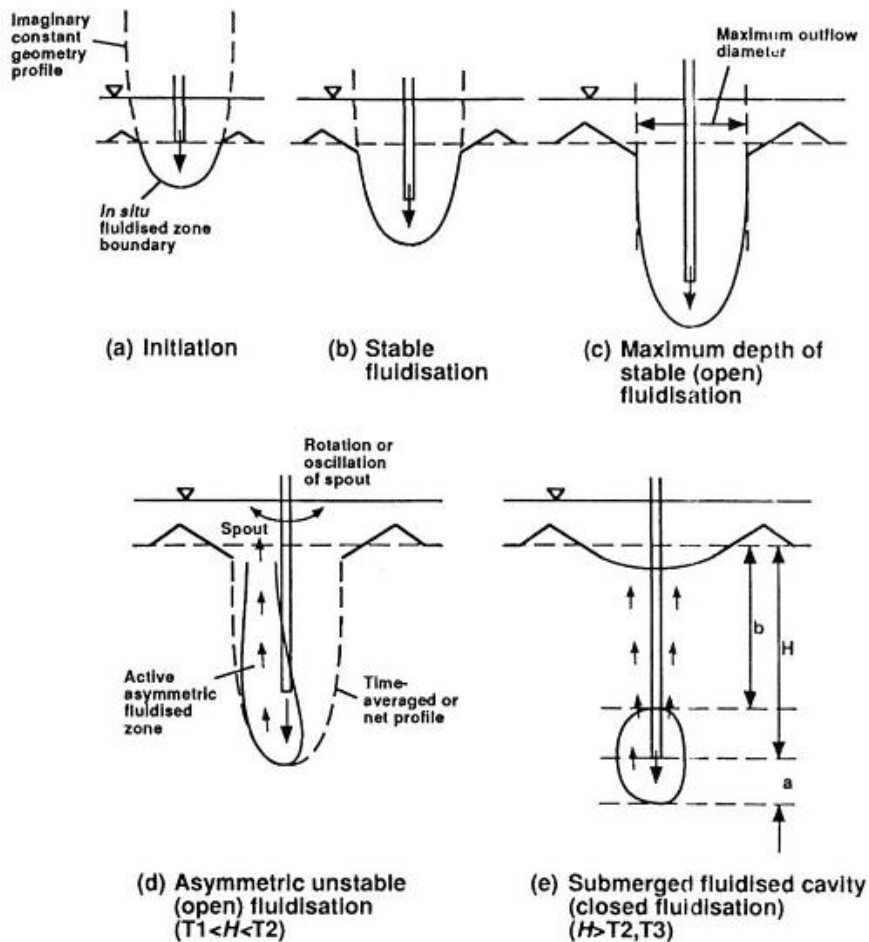


Figure 2-8: Schematic Diagram of Transition from Stable in Situ Fluidisation to Cavity Formation. (Niven & Khalili, 1998)

2.7.2 Effect of a vertically flowing water jet underneath a granular bed (Zoueshtiagh and Merlen, 2007)

In this study, the effects of a water jet penetrating vertically upwards underneath a granular bed was investigated. The results of the experiments were compared theoretically and numerically with previous studies. The varying parameters of the experiments were bed heights, orifice diameters and flow rates.

Figure 2-9 below shows the experimental setup which consisted of a vertical Plexiglas cylinder with an internal diameter of 240 mm. Interchangeable sub-cylinders had internal diameters of 3, 15 or 35 mm and fitted centrally on a disk. A grid of 210 μm was placed above each sub-cylinder to avoid bed material from entering the water source. The water level in the cylinder was kept above the varying height of the bed, to ensure complete bed saturation. The bed was monitored using a CCD video camera set at two locations.

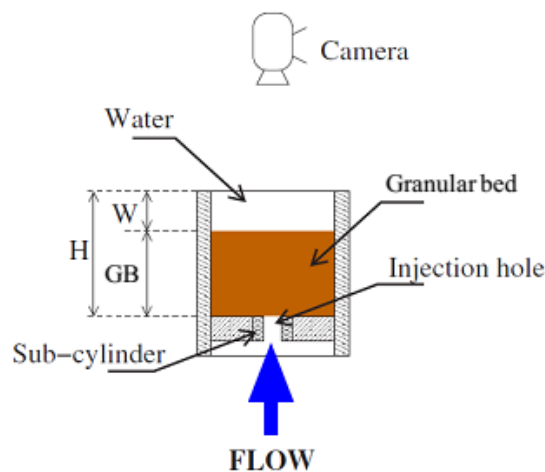


Figure 2-9: Sketch of the experimental setup (Zoueshtiagh and Merlen, 2007)

Three different regimes were suggested according to the flow rates entering into the system. Regime 1 was a motionless bed occurring at low flow rates. Regime 2 occurred when the bed deformed locally. This was only apparent at large enough flow rates, and formed a bump shape on the bed surface. Most importantly, the authors stated that in this regime there was likely to be internal fluidisation located at the injection of the jet. This regime therefore had potential for further research on internal fluidisation. Regime 3 was observed to have local fluidisation to the surface of the granular bed. This regime occurred at flow rates greater than those of Regime 2. Material in this regime moved in a “chimney” shape motion above the orifice and up to the bed surface while the material surrounding the chimney was at rest and acted as a solid porous skeleton. Figure 2-10 contains two images captured directly above the granular bed at different stages in Regime 3. Image B reflects a higher flow rate than image A.

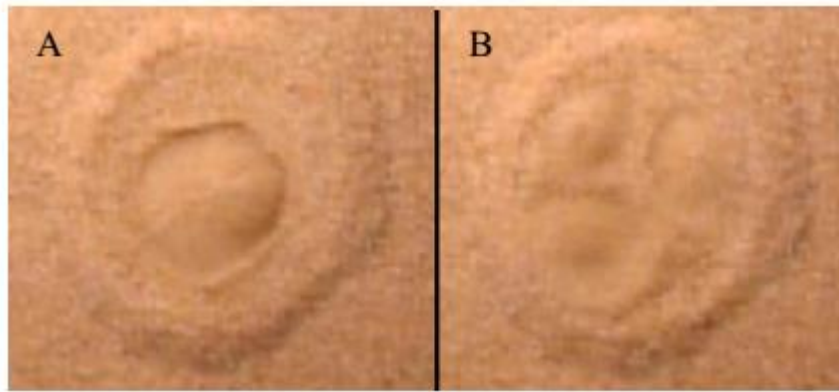


Figure 2-10: Patterns formed at the sand fluid interface (Zoueshitiagh & Merlen, 2007)

The main findings of the study by Zoueshitiagh & Merlen (2007) are:

- Chimney diameter was almost independent of the orifice size at a given flow rate;
- The flow rate required for the start of internal fluidisation was dependent on the bed height;
- In the case of sand grains, the water supply pressure at the start of internal fluidisation was approximately 3 times the pressure needed to maintain internal fluidisation; and
- In the case of glass beads, the water supply pressure at the start of internal fluidisation was only 1.24 times the pressure needed to maintain internal fluidisation.

2.7.3 Internal Fluidisation in Granular Soils (Alsaydalani & Clayton, 2013)

In this study, the phenomenon of internal fluidisation was investigated by positioning a water jet vertically upwards penetrating a granular bed of sand. The three independent variables were:

- Water jet flow rates;
- Orifice sizes; and
- Granular Soil (Shape and Particle size).

The experiments were conducted in a Plexiglas tank, of dimensions 1060mm x 550mm x 153mm. A machined aluminium box was attached to the bottom of the tank. This box was designed with an idealised longitudinal crack that served as the orifice. It had dimensions 330mm x 152mm x 105mm. The remaining equipment included a pump, pressure gauges, measuring cylinders, tubes and a sight tube panel assembly. Figure 2-11 is a schematic of test apparatus for fluidisation tests. The experiment was monitored using sight tubes and Particle Image Velocimetry (PIV). The sight tubes were used for pore pressure measurement during the preliminary tests. This measurement was done through six holes which were drilled through the back wall of the tank. The holes were located directly above the orifice at 10, 53, 102, 150, 220 and 300 mm. Needles with a 2 mm inner diameter were then fed in through the holes. The needles were connected to the sight tubes where the pressures relating to the water elevation could be read. The PIV technique was used to monitor the behaviour of internal fluidisation. The PIV consisted of a light

source, a camera, a board with gridlines, and image processing software to track the movement of the particles.

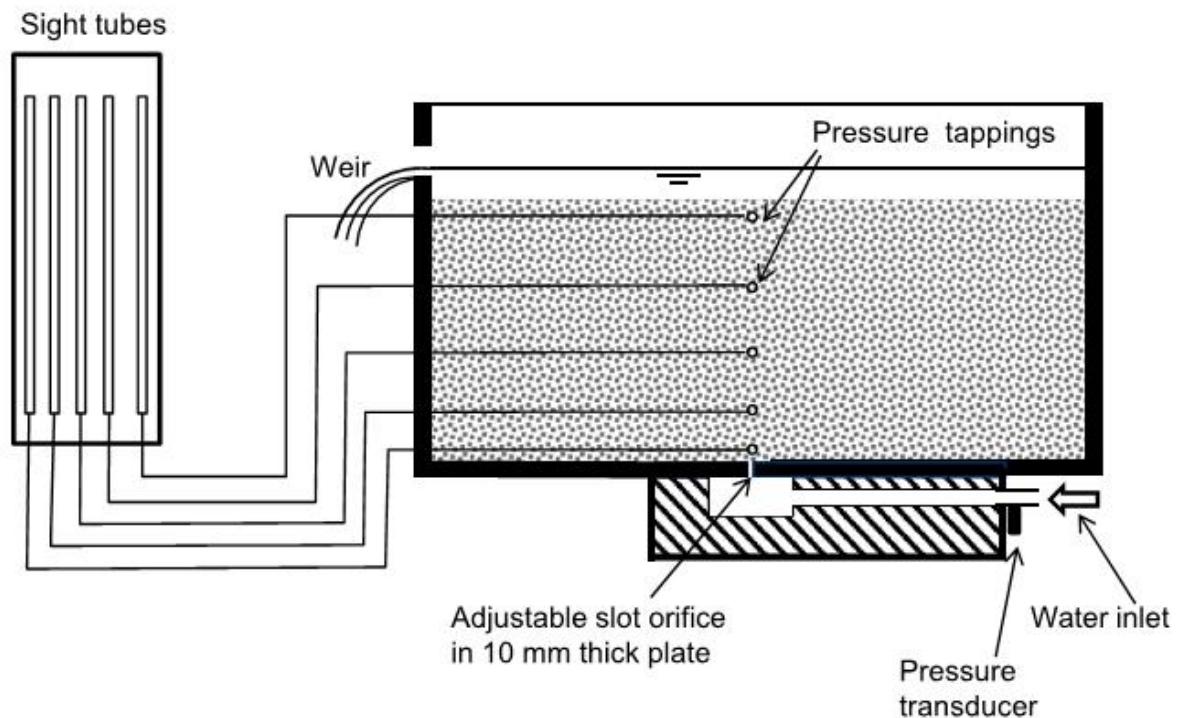


Figure 2-11: Schematic of test apparatus for fluidization tests(Alsaydalani & Clayton, 2013)

Two types of granular mediums i.e. Silica sand and Leighton Buzzard Sand (LBS) were tested separately. These mediums have average particle diameters of 0.9 mm and 1.6 mm respectively. With the use of a funnel, the mediums were rained into the seepage tank which was partially filled with water. This prevented any air pockets from forming within the granular bed.

Experiments were run with increasing flow rates until complete fluidisation up to the granular bed surface was observed. Alsaydalani and Clayton (2013) described the process as follows: initially there was no observable grain movement. As the flow rate was increased though, an uplift mechanism occurred, moving particles away from the orifice and providing a small internal fluidised zone where particles could move rapidly and freely. As the flow rate increased further, the internal fluidised zone grew larger until eventually with an even greater flow rate the fluidised zone reached the granular bed surface. Figure 2-12 shows the sequence of fluidisation observed in the experiment.

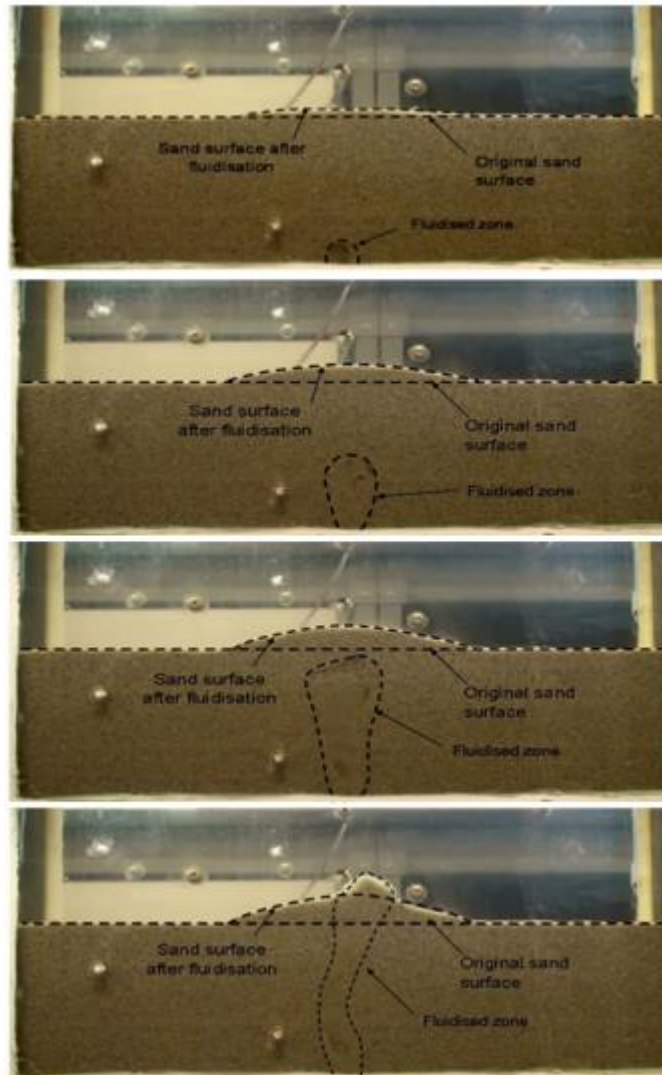


Figure 2-12: Different stages of Fluidisation (Alsaydalani & Clayton, 2013)

The following findings were reported from the study:

- A static cavity which was a localised zone of displaced particles, formed prior to the onset of fluidisation. The cavity allowed particles to circulate which at higher flow rates caused fluidisation;
- Greater flow rates were required to initiate fluidisation in a coarser granular bed. Particle size did therefore have an effect on fluidisation;
- The size of the orifice had no effect on the fluidised zone; and
- The weight of material displaced at the start of fluidisation was approximately equivalent to the uplift force exerted by the fluidising jet.

2.7.4 Soil fluidisation outside leaks in water distribution pipes- preliminary observations (Van Zyl *et al.*, 2013)

This research was done as a preliminary study to investigate the effect soil has on a leaking water pipe. Van Zyl *et al.* (2013) investigated an internal fluidising water jet positioned vertically upwards, penetrating a bed of glass beads (glass Ballotini). The jet was produced by a single round orifice of varying diameters (2, 4 and 8mm). The experiment was conducted in an 8 mm thick walled Perspex tank with the dimensions 1 000mm x 200mm x 500mm high. The interchangeable orifice was placed 2 mm from the front wall of the tank and protruded 98 mm vertically into the tank. The position of the orifice can be seen in both the side and front views of the experimental setup shown in Figure 2.13. In their experiments the excess water pressure in the bed was measured. This was done by a number of 1 mm diameter drilled holes in the front wall of the tank. The holes are labelled “pressure tapings” in Figure 2-13. Blunted hypodermic syringe needles with 0.9 mm internal diameters were introduced through these holes. The needles were then connected to sight tubes where pressure readings could be taken. The holes were drilled on one side of the orifice centreline, due to the symmetry of the fluidised zone.

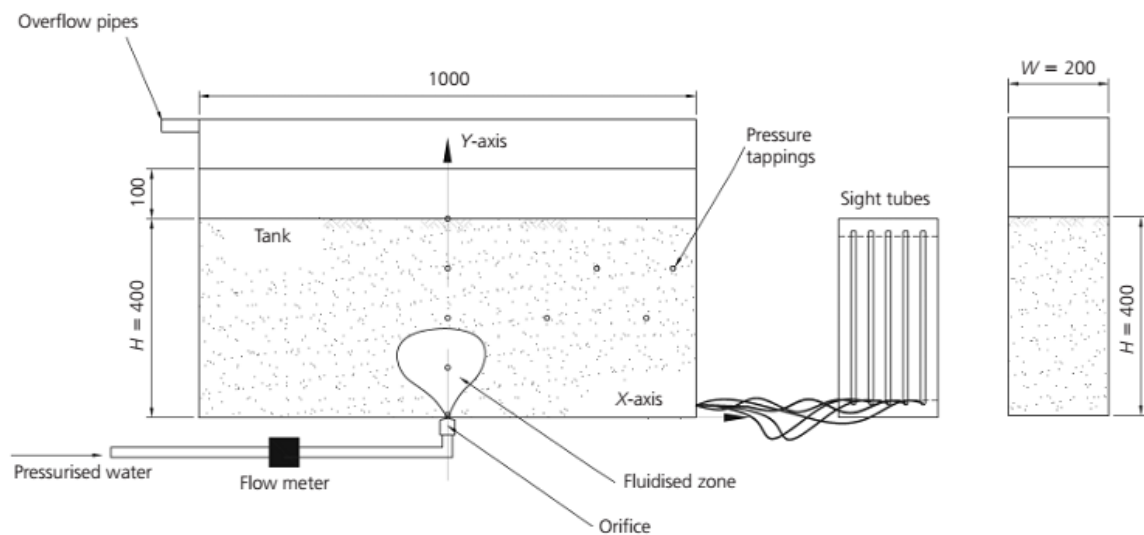


Figure 2-13: Schematic diagram of the experimental apparatus (Van Zyl *et al.*, 2013)

The experiment was prepared by filling the tank with water first and then adding the Ballotini to a depth of 400 mm. The flow rate was increased in steps from a minimum of 220 l/h to a maximum of 850 l/h. An electromagnetic flow meter was placed upstream of the orifice to record the flow rates. The size of the internal fluidised zone for the allocated flow rates and the corresponding pressure head in the Ballotini bed was recorded.

Internal soil fluidisation was defined as the phenomenon by which solid state material from the sand bed around the leakage of a pipe is saturated and changed into a liquid-like material (Van Zyl *et al.*, 2013). When a jet of liquid from the orifice passes through a bed of soil material and induces a force strong enough to counter the force keeping the particles together and the gravitational force on the particles, resulting in particles free to move with the fluid from the leakage (Van Zyl *et al.*, 2013). Figure 2-14 below shows the phenomenon where the particles become separated and in motion with the pore fluid.

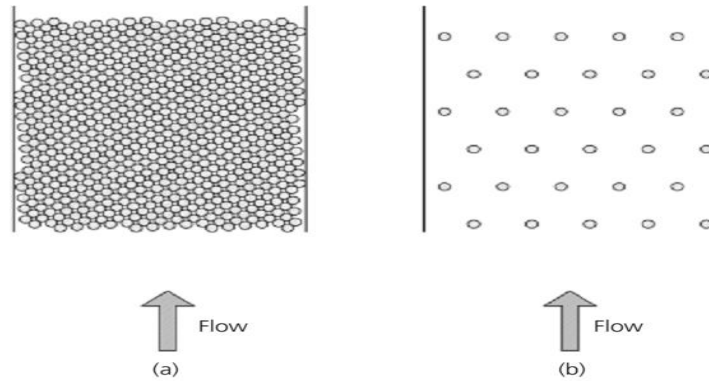


Figure 2-14: Schematic diagram of the fluidisation phenomenon:
(a) packed bed; (b) fluidised bed (Van Zyl *et al.*, 2013)

One of the objectives of the experiments was to assess the geometry of the internal fluidised zone and so the orifice setup in this experiment differed slightly. A 60 mm long, 6 mm diameter tube was cut in half laterally and fixed to the front wall of the seepage tank. This allowed for accurate visual inspection through the Perspex wall of the tank. Three distinct zones were observed in these experiments: the fluidised, mobile and static bed zones. These zones can be seen at three different flow rates in Figure 2-15.

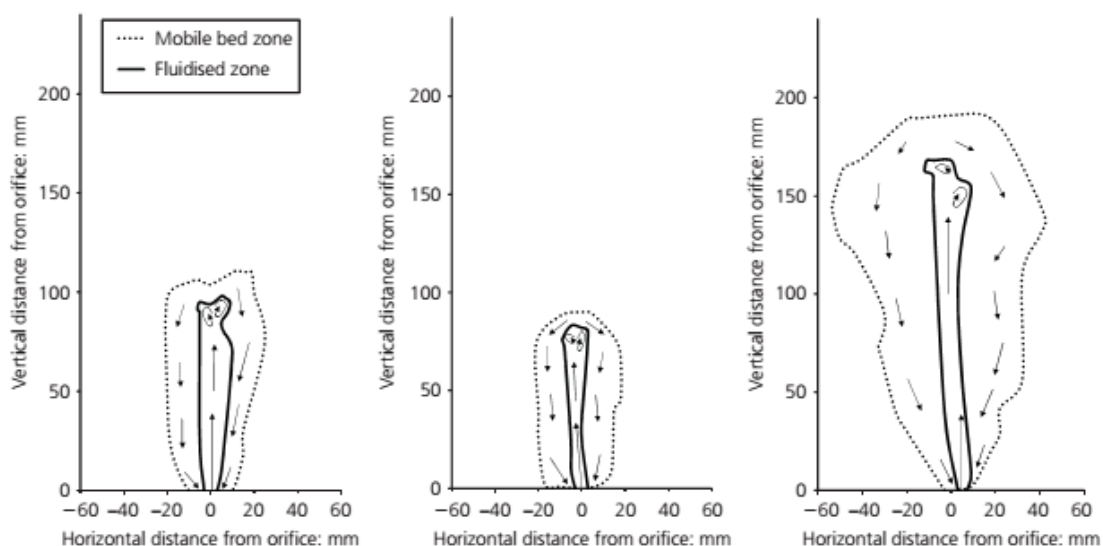


Figure 2-15: Geometry of the fluidised zone for set 3 at different flow rates: (a) 130 litres/h; (b) 220 litres/h; (c) 320 litres/h (Van Zyl *et al.*, 2013)

Fluidised zone: This zone was a high velocity water jet, starting from the orifice and ending in a vortex movement. Ballotini particles entered the zone at the orifice. They were then deposited back into the mobile bed zone at the head (top) of the jet. The body of the fluidised zone was found to be stable, whereas the head tended to move from side to side.

Mobile zone: This zone surrounded the fluidised zone. Ballotini particles were observed moving steadily from the fluidised zone head down towards the orifice at which point they were picked up by the fluidised zone again.

Static zone: This was the outermost zone, where the Ballotini remained unaffected by the water jet.

In the study, the following findings were reported:

- The majority of the head loss existed in the fluidised bed and mobile bed zones. Orifice head loss was less in these two zones, but still substantially more than the head loss in the static bed zone, which had the least;
- It is the orifice flow rate rather than the orifice diameter which controls the excess pore water pressure at various depths in the bed, as well as the height of the fluidised zone;
- Under ideal conditions, the soil surrounding water distribution pipes is unlikely to have much impact on the pressure-leakage relationship; and
- High pressure heads can be sustained by a granular bed without visible piping at the ground surface and this may well be the reason for many leaks going undetected.

2.7.5 Experimental investigation of internal fluidisation due to a vertical water leak jet in a uniform medium (Bailey, 2015)

In this study, an experimental method for measuring excess pore pressure and flow velocity in a uniform glass beads medium surrounding the leak was developed. Figure 2-16 below shows the experimental setup which consisted of a glass tank with a central inlet in its base and four overflow holes in its walls, and was filled with glass ballotini. The inlet on the tank was a vertically drilled circular hole in its base and was fitted with a bored stainless steel tube, through which the water flowed. The tube had a diameter of 3mm for a length of over 10D to ensure uniform flow. Water was directed via valves and a flow meter to the inlet, simulating a pipe leak. The glass ballotini was used as an idealised soil medium.

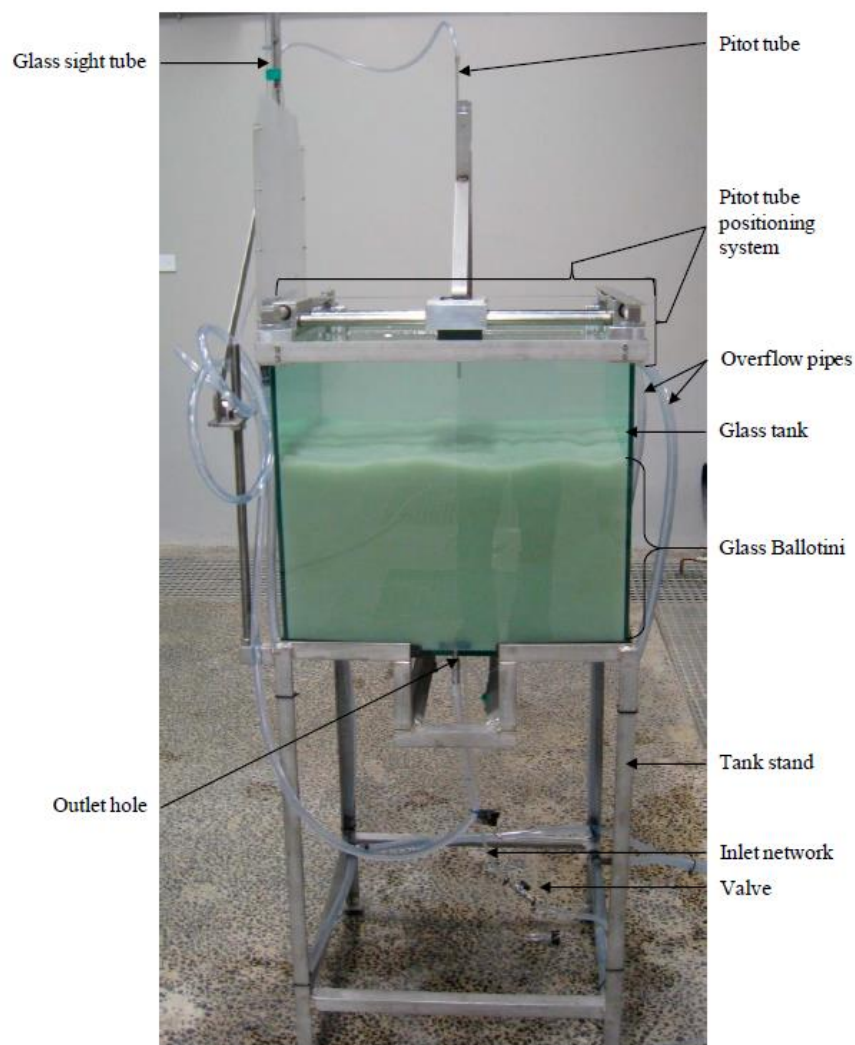


Figure 2-16: Experimental Setup (Bailey, 2015)

Figure 2-17 shows the measured velocity distribution. The largest velocities were found in the fluidised zone in a vertical direction just outside the inlet opening. Outside of the fluidised zone the velocities were substantially smaller. It was found that some of the velocity vectors near the inlet were directed down towards the inlet. The flow from the top of the fluidised zone circulates down towards the inlet. This circulating flow is generally located in the mobile bed zone, which surrounds the fluidised zone.

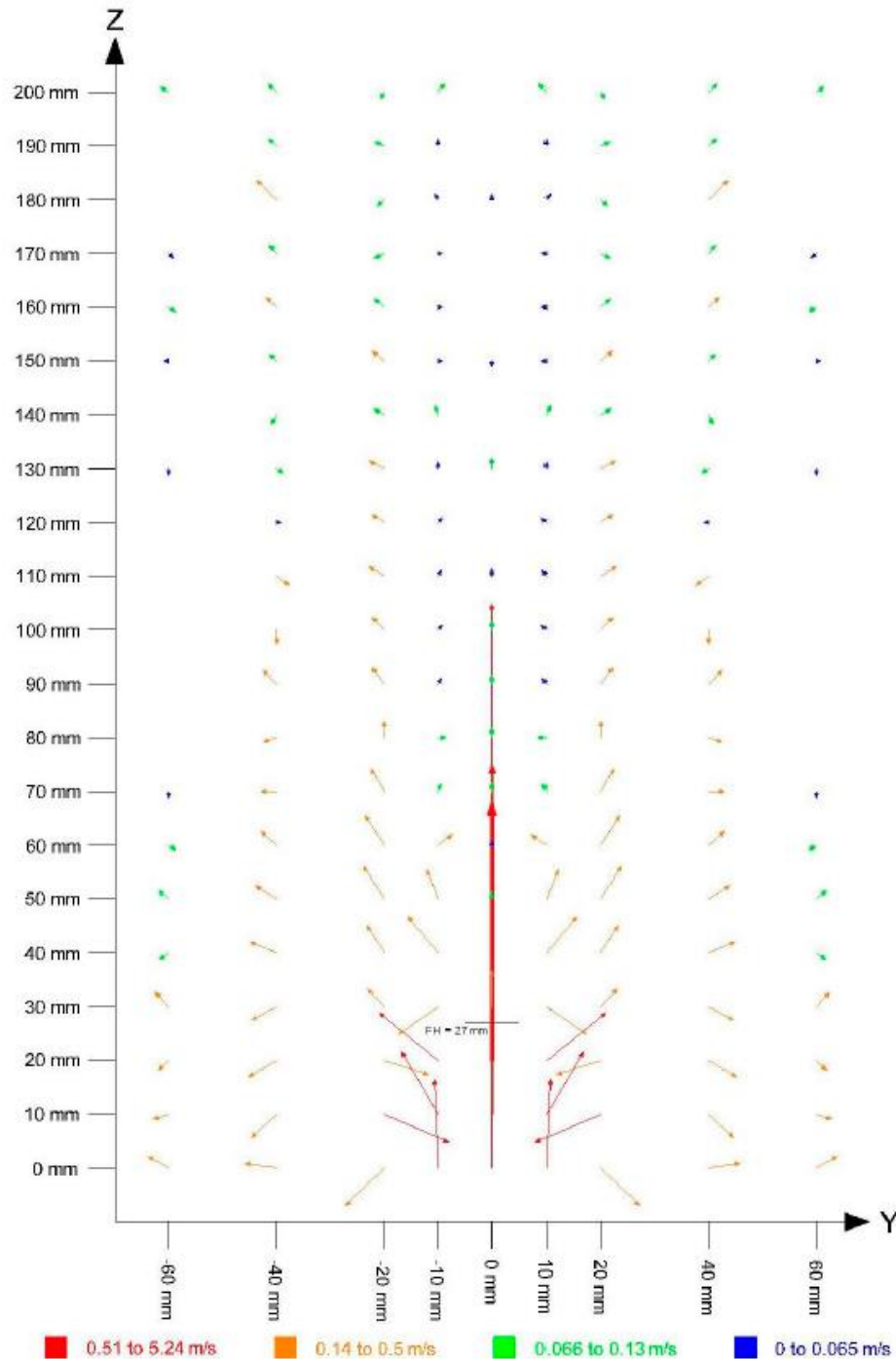


Figure 2-17: Velocity vector plot in ballotini glass beads (Bailey, 2015)

Figure 2-18 shows the increase in excess pore pressure in the ballotini bed due to the leak flow. The red line in the graph represents the pressure measurements vertically above the inlet. As shown in Figure 2-18 the maximum pressure head in the ballotini bed of 110.6 mm was found to occur directly above the inlet at height $Z=20$ mm. Thus the maximum pressure exists near the top of the fluidised zone where the ballotini bed is in suspension due to the jet flowing through the inlet. The graph also shows how the pore pressures rapidly decrease from the maximum pressure point with increasing height.

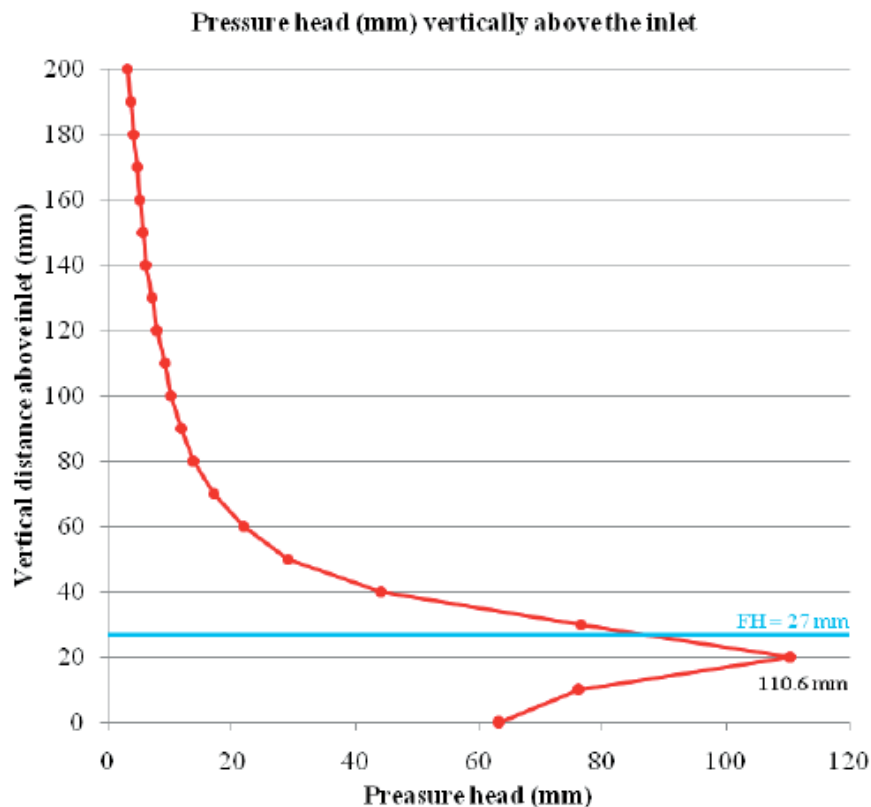


Figure 2-18: Pore pressure head measurements (Bailey, 2015)

The main findings of the study by Bailey and Van Zyl (2015) are:

- Large vertical velocities were found in the fluidised zone and outside of the fluidised zone the velocities were much lower;
- The maximum pore pressure of 110.6 mm was found to be near to the head or top of the fluidised zone. Outside of the fluidised zone the pressures decreased rapidly. Above a height of 100 mm the excess pore pressure reduces linearly with height; and
- The internal fluidisation occurring outside the leak rapidly reduces the available energy in the fluid, and this is likely to reduce the probability of a leak reaching the soil surface in the field and thus making it more difficult for the leak to be found.

3. Methodology

Investigation methods were designed to meet the objectives of the research and study the effects of various factors affecting water leakage routes. In this chapter, the technique for experimental set ups are described followed by the methods used to collect data to investigate the flow of water outside the distribution pipes.

3.1 Experimental Setup

The experiments were designed to simulate a buried pipe as in realistic field conditions with a leak opening to allow water to flow into the surrounding soil. A pressurised water supply system was used to transport water to the pipe in the trench. The pipe was placed 100mm from the bottom of the trench with a drilled leak opening that produced water jets into the surrounding sand. Figure 3-1 below shows a schematic diagram of the experimental setup.

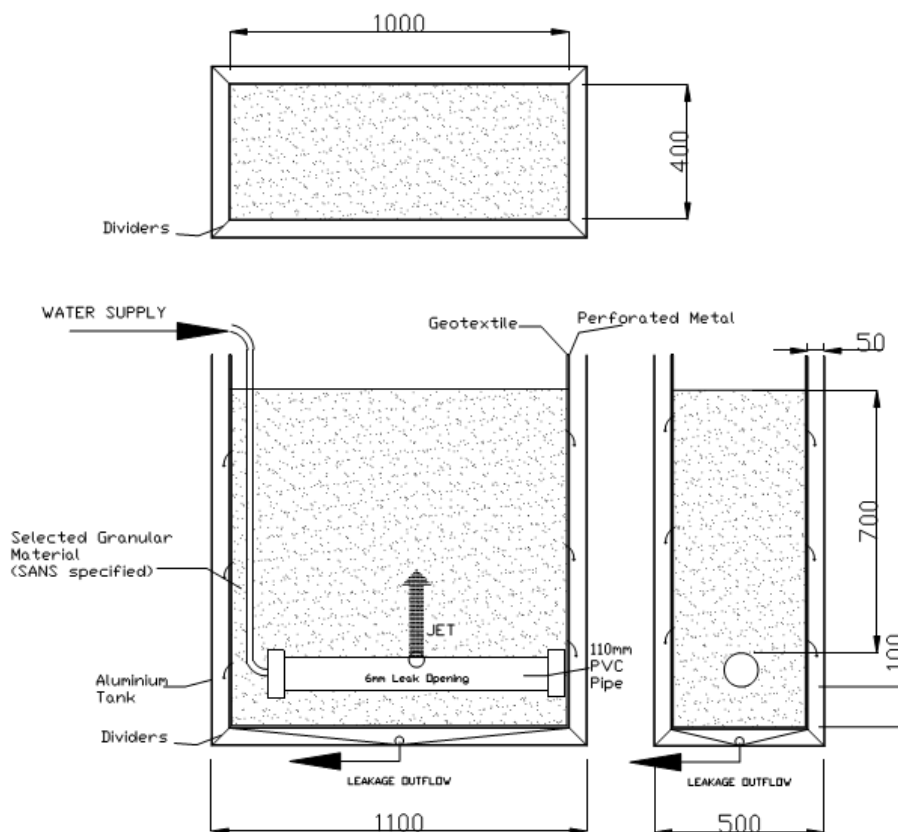


Figure 3-1: Schematic diagram of Experimental Setup

The experimental setup consisted essentially of an inner box according to the standard trench dimensions for a 110 mm diameter pipe. The inner box was constructed from perforated stainless steel metal sheets to allow water move easily through and was then aligned with a geotextile to represent the permeability of the surrounding soil as shown in Figures 3-2 and 3-3 below.

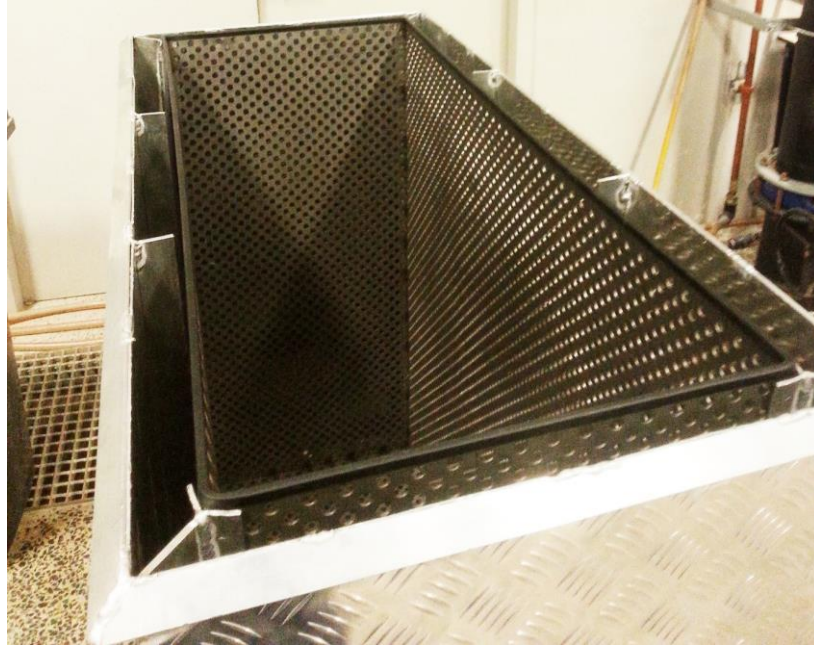


Figure 3-2: Manufactured apparatus

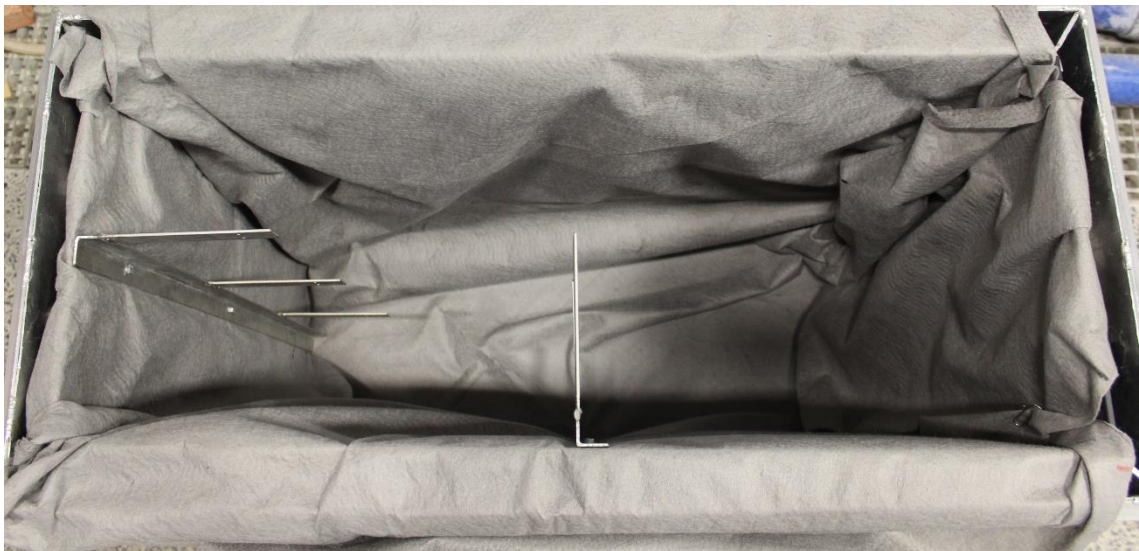


Figure 3-3: Inner box aligned with geotextile

The water moving through the geotextile and inner box would drain down in between the gaps of the inner and the solid outer aluminium box, where it would ultimately run out through drainage pipes connected to water flow meters. The gaps between the inner and outer box were separated at the edges of the box and made up isolated chambers that allowed the quantity of water passing through each of the five walls (4 sides and 1 bottom wall) to be measured separately. Figures 3-4 and 3-5 below show the outer and inner manufactured tanks respectively.



Figure 3-4 : Outer tank



Figure 3-5 : Inner tank

At the bottom of the outer box, a ramp was manufactured to provide a slant so that water draining at the bottom would run immediately to a drainage point as shown in Figure 3-6.



Figure 3-6: Bottom tank design

The experiments made use of municipal water supply and the pressure fluctuated between 5 and 6 bar. A reinforced hose transported the municipal water into a 110mm diameter uPVC pipe as shown in Figure 3-8. It should be noted that this delivery supply pipe system has 3 draw offs and was used in previous lab experiments. It was considered suitable to be used in this research experiment by ignoring the other 2 draw offs as using one does not affect the flow or pressure in the system.



Figure 3-7 : Delivery pipe connected to PRV and Flow meter



Figure 3-8 : Delivery pipe connected to hose

In order to prevent pressure and flow rate fluctuations, a pressure reducing valve (PRV) was connected to the municipal supply pipeline. The pressure was set to 4 bar which is normally below the municipal pressure level.

A saddle was used to connect the pipe to PRV together with a pressure gauge. A rigid pipe was mounted to connect a mechanical flow meter to the PRV. The flow meter measured the flow rate into the system. Figure 3-9 shows how a pipe sample was placed in tank before filling the tank with sand.



Figure 3-9: Pipe Sample connected to detachable hole through end cap

The uPVC pipe was closed with end caps and placed in a 400x1000x900 mm inner box. These dimensions were selected so that it adheres to a standard trench size for a normal 110mm distribution pipe in real reticulation system. The pipe sample was placed over a compacted bedding of 100mm depth.

The backfill sand was transferred from the sand bag into the container with the help of a gantry. The sand was compacted using a simple geotechnical compactor at each 200-300mm depth to ensure uniformity. The inner tank was filled completely up to the surface (900mm depth) with the backfill sand as shown below in Figure 3-13. Additionally, it was also important to ensure that the tank was always horizontal with respect to the ground.



Figure 3-10: Lifting sand bag with Gantry



Figure 3-11: Compacting sand at 300mm interval



Figure 3-12: Tank filled with sand.

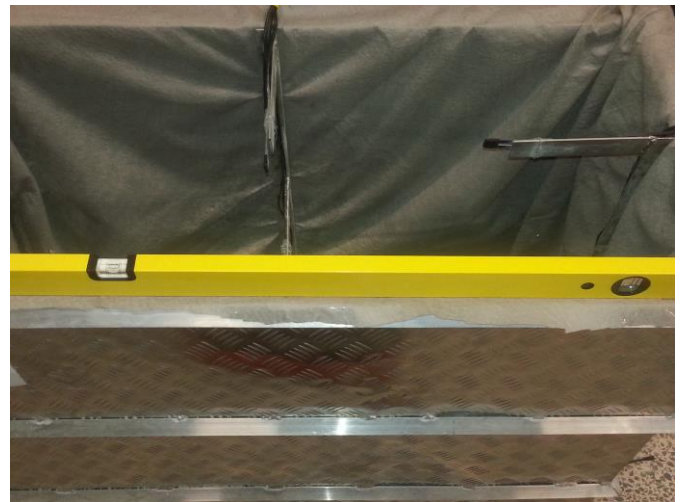


Figure 3-13: Spirit Level to ensure the tank stand

3.2 Geotextiles and Sand Properties

In order to simulate a surrounding soil condition, geotextiles were installed in the inner box. Hence, water flowing through the textile would represent the water flowing through the side and bottom walls of a typical trench with a buried pipe. Non-woven needle punched fibertex geotextiles made from polypropylene staple fibre were used in this research. Figure 3-14 shows the different types of fibertex geotextiles.



Figure 3-10: Fibertex geotextile samples

In this experimental investigation, F-25 and F-1000 Fibertex were used. For 50mm water head, Fibertex F-25 has a water flow of 77 l/s/m² and Fibertex F-1000 has a water flow of 16 l/s/m². The detailed specifications like physical, mechanical, hydraulic properties of the products can be found in Appendix A.

The sand used in the experiments were previously used by Stefan Pike (2015) who investigated the scouring effect in water pipes in the hydraulic lab at University of Cape Town. As such, the characterisation of the sand had already been determined and the same data was used in this research. Silica sands, originating from the Consol Industrial Mineral mine in Philippi, Western Cape, South Africa was used. This sand was selected so as to maintain approximately the same particle density, Bond Work Index, hardness and angularity (Pike, 2015). The physical properties of the sand are listed in Table 3-1 below.

Table 3-1: Sand Physical Properties (Pike, 2015)

Sand Property	
D ₅₀ (mm)	1.6
Coefficient of uniformity (D ₆₀ /D ₁₀)	1.62
Particle density (kg/m ³)	2661
Max Dry bulk density (kg/m ³)	1643
Minimum Void Ratio	0.62
Minimum Porosity %	38.26
Permeability (cm/s)	0.44

Figure 3-15 below shows the grading curve from the sieve analysis test by Stefan Pike (2015) for three sand types. It has to be noted that only the medium grained sand, that is, D₅₀=1.6 mm was used in this research as preliminary test.

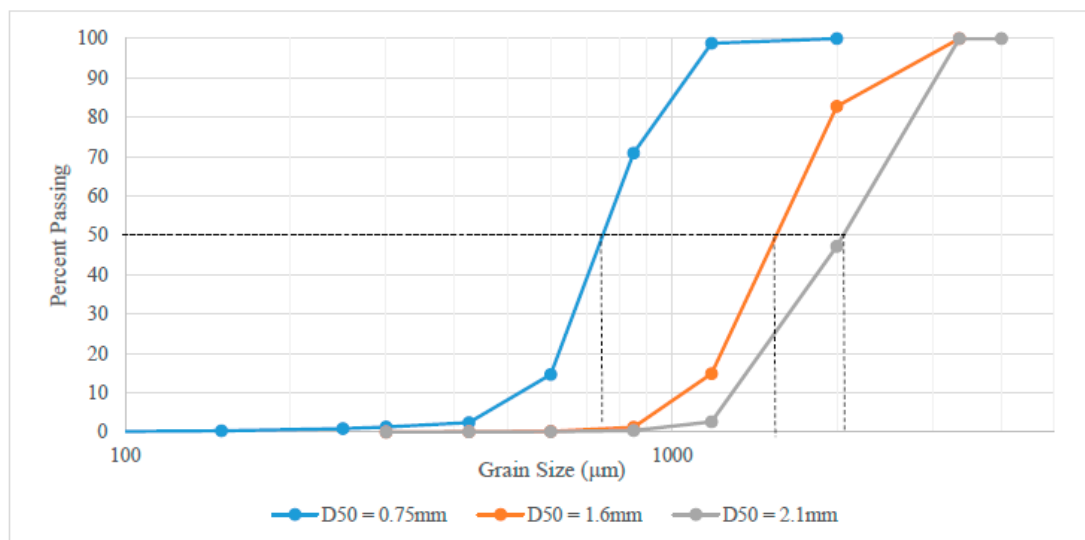


Figure 3-11: Sieve Analysis Test Results (Pike, 2015)

3.3 Data Collection and Analysis

3.3.1 Measurement of Soil Moisture

The aim of the experiments was to analyse water leakage paths and moisture sensors were considered to be suitable to determine the movement of water inside the tank. The Decagon EC-5 moisture sensor was chosen for this research. The EC-5 sensor is used to measure volumetric moisture content of soils for scientific research. The EC-5 measures volumetric water content via the dielectric constant of the soil using capacitance technology. The EC-5 has a small area of influence. The EC-5 delivers research-grade accuracy at an economical price and measures water content in any soil or soilless media. Figure 3-16 shows a Decagon EC-5 sensor with its logger.



Figure 3-12: Decagon EC-5 moisture sensor and Em5b logger

In this research, 7 EC-5 sensors were used in the inner box to determine the moisture readings at different locations for 1-minute time intervals. Figure 3-17 shows the 7 EC-5 sensors and 2 data loggers. The EM-5 consist of 5 ports and hence, can read 5 sensors simultaneously.



Figure 3-13: 7 EC-5 sensors and 2 EM-5 loggers used in the experiments

3.3.1.1 Calibration of EC-5 Sensors

Decagon EC-5 sensors were installed to gauge the Volumetric Water Content (VWC) of the soil. According to the soil sensor calibrations tests done by Decagon Devices (2009), the following equation would universally suit all mineral soils:

$$VMC = 11.9 \times 10^{-4} mV - 0.401 \quad (3.1)$$

This equation, however, did not give realistic results for the soil in use. The following calibration method was used to obtain an equation which is specific to the experimental soil:

1. A soil sample was packed into a container;
2. The EC-5 sensor was inserted vertically directly into the full soil container;
3. Raw data was collected from the sensor, that is, with no calibration applied and recorded in Table 3-2;
4. A volumetric soil sample was then collected. The entire soil core was placed into drying container and the container was capped. Any water loss from the soil between sampling and the first weighing introduces error to the volumetric water content calculation;
5. The mass of the wet soil + container was measured and recorded in Table 3-2;



Figure 3-14 : Weighing of lids

6. Water was added to the calibration soil. 1 mL of water for every 10 mL of soil volume and was thoroughly mixed to obtain a homogenous distribution of water;
7. The sensor readings were recorded and steps repeated until soil neared saturation;
8. The volumetric soil samples were dried by placing all of the already-weighed, wet samples into an oven at 105 °C for 24 hours;



Figure 3-15: Calibration of EC-5 sensors

9. After 24 hours the soil drying containers were removed from the oven; and
10. The mass of the dry soil + containers (without lids) were measured and recorded.

The volumetric water content is defined as the volume of water per volume of bulk soil. Table 3-2 shows the data collected for the soil specific EC-5 sensor calibration.

Table 3-2: Data collection table for calibration

Sample No	Sensor Output	Lid Mass(g)	Sample Vol(cm ³)	Lid+ Wet Soil(g)	Lid + Dry Soil(g)	Mass/Vol Water (g)	VWC (cm ³ /cm ³)
1	530	8.068	16.97	48.85	48.82	0.03	0.00177
2	556	8.136	16.97	48.602	46.385	2.217	0.13064
3	739	8.17	16.97	48.711	44.208	4.503	0.26535
4	773	8.189	16.97	54.845	47.349	7.496	0.44172
5	1005	8.117	16.97	62.525	51.645	10.88	0.64113

The VWC is defined as the volume of water per volume of bulk soil:

$$\theta = V_W/V_t \quad (3.2)$$

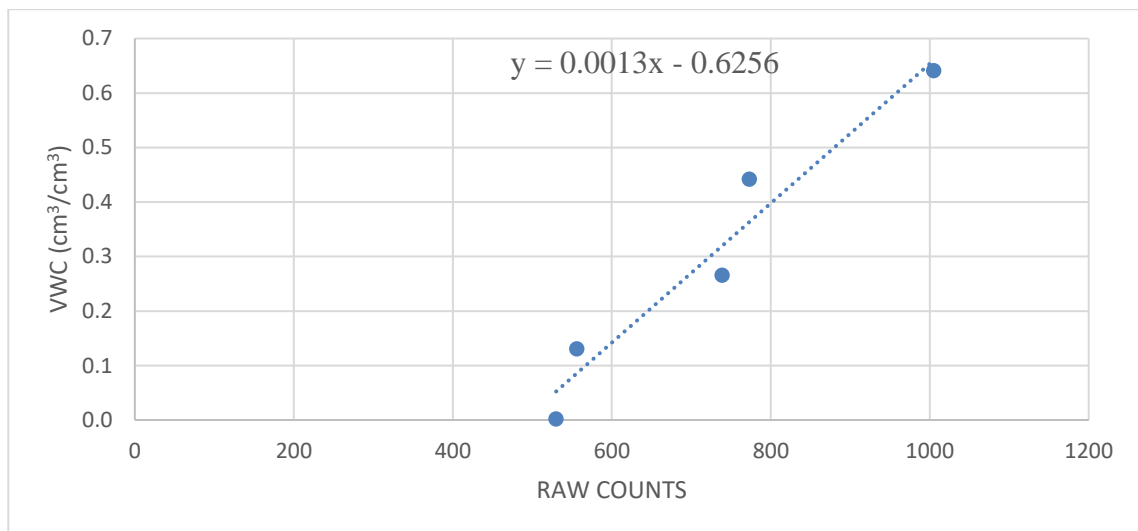
Where θ is volumetric water content (cm³/cm³), V_w is the volume of water (cm³) and V_t is the total volume of bulk soil sample (cm³). To find V_w , we calculated the volume of the water that is lost from the soil sample during oven drying:

$$m_W = m_{wet} - m_{dry} \quad (3.3)$$

$$V_W = m_w/\rho_w \quad (3.4)$$

Where m_w is the mass of water, m_{wet} is the mass of moist soil (g), m_{dry} is the mass of the dry soil, and ρ_w is the density of water (1 g/cm³).

The calibration function was plotted and shown in Figure 3-20. A trend line was used to construct a mathematical model of the relationship. The calibration function was then applied when collecting data with the EC-5.

**Figure 3-16: Plot of calibration data with soil specific calibration equation**

3.3.1.2 Em5b Data Logger

The Em5b is a 5-channel, self-contained data logger. Em5b is designed primarily to make soil moisture measurements and is the cost effective.



Figure 3-17: Decagon Em5b data logger

3.3.1.3 ECH2O Utility

ECH2O Utility is the software that was used to configure the Em5b loggers. The software allowed downloading and processing of the measured data.

The measurement interval worked relative to the real-time, 24-hour clock inside the Em5b. When choosing a measurement interval of 120 minutes, the Em5b stores data every two hours, on the hour. The resulting data shows sensor measurements hourly at 12:00 am, 2:00 am - 10:00 pm. The Em5b makes a measurement from each of the 5 sensor ports every 60 seconds, regardless of the measurement interval value. When the Em5b internal clock reaches the time to store a reading, the average value of all the 60-second sensor readings is stored. For example, if you set the measurement interval to 60, the Em5b stores an average of the past 60 sensor readings. If you choose an interval of 1440, the Em5b stores one value that represents the average sensor value for the entire 24-hour period. The Em5b stores 3348 data scans. When the logger has filled its data memory, it begins overwriting the oldest data in the memory.

ECH2O Utility provides a user-friendly interface for configuring and downloading the Em5b logger. Once connected, the main screen looks similar to Figure 3-22.

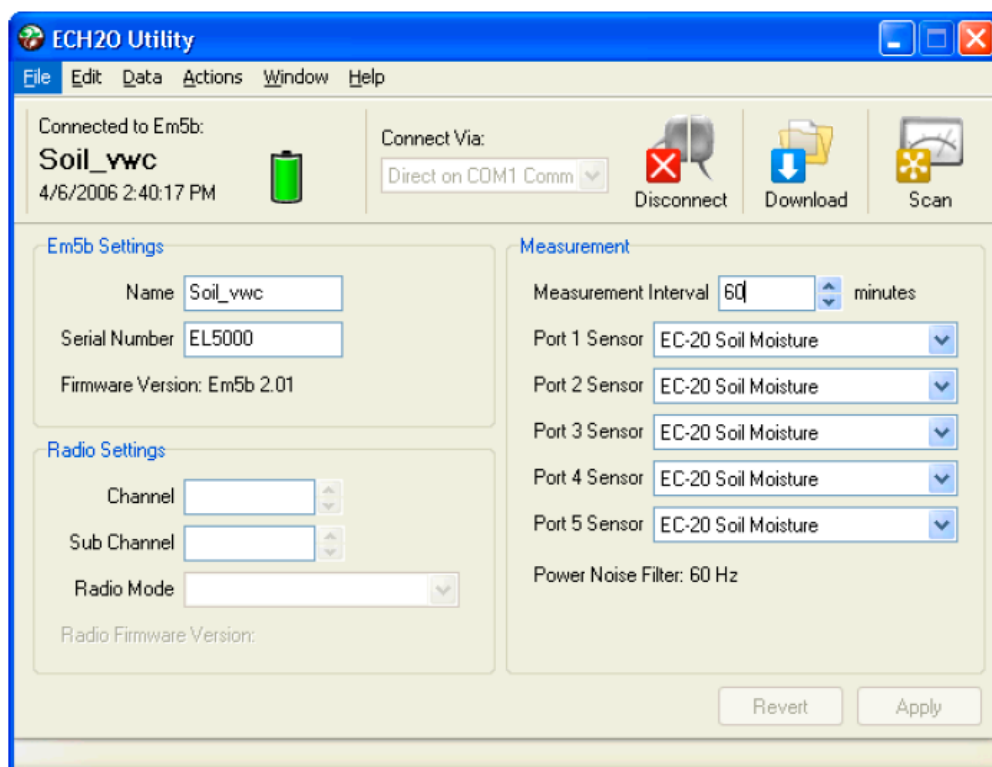


Figure 3-18 : ECH2O Utility Main Screen

ECH2O Utility can save the data in different file formats. The data was downloaded as Raw Data Excel File (.xls) and analysed.

3.3.1.4 Positioning Moisture Sensors

The measurement of moisture content in the tank was critical in this research to determine the movement of the leakage flow outside the leaking pipe. Figures 3-23 and 3-24 show the positions of the sensors used in the experiments. The sensors were required to be at fixed locations for each set of experiments and therefore, two support frames were manufactured to support the sensors at specific locations. Frame 1 was fixed half way along the longer section of the tank and Frame 2 was placed half way the shorter section. Frame 1 consisted of 4 moisture sensors. Sensor 1 (S1) was positioned at a height of 150 mm so that it was situated exactly next to the leaking pipe. Sensor 2 (S2) was 150mm higher than S1 and located just above an upward pointing leak. Sensors 3 and 4 were fixed 300mm away from the each other as shown in Figure 3-23. Frame 2 was fixed on the shorter side of the trench box and consisted of 3 sensors which were positioned at 300mm intervals from the bottom. As such, sensors 4 and 7 were located near the surface of the tank and were able to measure when the leakage water actually hits the surface. Figures 3-23 and 3-24 below illustrate the positions of the 7 sensors in the experiments.

3.3.2 Measurement of Leakage Outflow

The experimental setup allowed leakage outflow to be determined from 5 drainage points (4 vertical sides and 1 bottom). The drainage pipes were connected to Sensus DN20 iPERL water meters. The iPERL smart meters were chosen for this research work because of several important features. iPERL delivers constant accuracy in a wide range of installation conditions and can be installed in any orientation without the need for linear pipe leads in or out. iPERL also has an automatic detection of the direction of flow, further enabling the choice of installation positions. The meters allowed a minimum water flow rate of 100 L/h. Figure 3-25 below shows a Sensus DN20 iPERL meter used to measure leakage outflow in the experiments.



Figure 3-21 : Sensus DN20 iPERL smart meters

Unlike other solid state meters, iPERL uses remnant magnetic field technology which provides a linear measurement range even down to very low flow rates. The magnetic field acting on the water flowing through the flow channel generates an electrical voltage; this is proportional to the velocity of the water (principle of magnetic-inductive flow measurement).

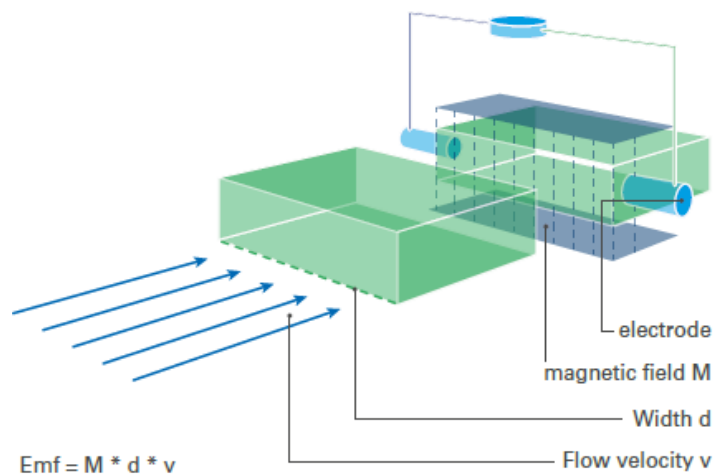


Figure 3-22: iPERL Magnetic field technology

iPERL is equipped with either standards compliant low power 868 MHz or 433 MHz integrated radio technology. The innovative communications provide for walk-by / drive-by collection, plus the ability to interrogate meters for more detailed data, including the log of up to 2880 data points and alarms. Sensus RF is an advanced radio system for retrieving data from meter endpoints and providing it for further processing and analysis.

SIRT (Sensus Interface Radio Tool) was used to obtain data from the smart meters. SIRT is a radio modem for SensusRF radio connection to a handheld via Bluetooth and using SensusREAD software. SensusREAD is the Sensus software for mobile terminals used to collect data from metering devices.

Figure 3-27 shows a handheld SIRT device and how Sensus RF offers two communication modes in unidirectional and bidirectional.



Figure 3-23 : SIRT handheld device and Sensus RF 2 communication modes

3.3.2.1 Drainage outlets

In order to measure the outflow leakage from the different side walls of the tank, 5 iPERL water meters were used. Figures 3-28 and 3-29 illustrate the positions of the 5 drainage outlets which were connected to hoses and the iPERL. M2 and M3 meters recorded the outflow from the longer sections while meters M1 and M5 recorded for the shorter sections of the tank. M4 was connected to the outlet which was collecting draining water from the bottom of the tank.

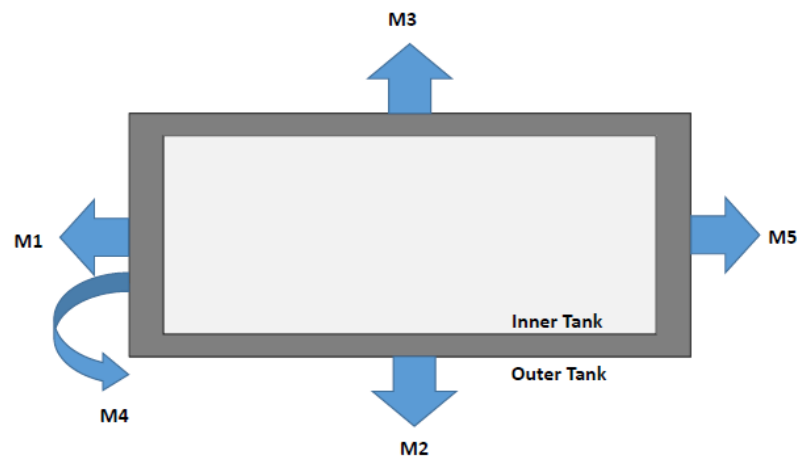


Figure 3-24 : Position of the iPERL water meters



Figure 3-25: Drainage outlets of tank

3.3.3 Timing of the Experiments

In order to examine the effects of the different parameters on leakage flow paths, proper time intervals had to be determined. During a pilot experiment, it was allowed to run for 24 hour period. It was deemed crucial to consider the amount of water being lost and costs involved during the running of the experiments. The outflow through the drainage pipes was observed to stabilise after a few hours in the pilot experiment. A time interval of 4 hrs was considered to be suitable for running the experiments. The setting up of the apparatus involved pouring and removing of sand manually which was very time-consuming. In addition, the wet sand had to be removed and placed into trays for drying in the oven over a 24h time period. Hence, significant time was allocated for the excavation, inspection, drying and general equipment maintenance.

3.4 Experimental Design

The soil-leak interaction in water distribution is very complex in nature and the process of leakage flow paths outside distribution pipes can be affected by several factors. In this research, it was decided to vary a few basic parameters to understand leakage flow paths.

The parameters affecting leakage flow paths investigated in this project were:

- Flow rate;
- Orientation of leak jet; and
- In-situ soil permeability.

Specific experiments were designed to understand the effects of the above-mentioned parameters. These factors were selected to be tested based on the literature and other potentially influencing factors were kept constant throughout the whole research. These included:

- Orifice size and shape;
- Burial depth;
- Pipe material;
- Sand grain size.

3.4.1 Experimental Planning

Five experiment Setups were planned and designed to examine the effect of flow rate, soil permeability and leak orientations on leakage flow paths. Table 3-3 below summarises the experiments that were carried out in this research. The experiments have been assigned set numbers to indicate the influence of each parameter. The flow rate was varied in each Setup from a minimum of 200 l/h to a maximum of 800 l/h while keeping the other parameters constant.

For Setup 1, the experiment tested the influence of flow rate with an upward pointing water jet and lower geotextile permeability. Setup 1(a), (b), (c) corresponds to a change in flowrate from a minimum to a maximum respectively in the system. For Setup 2 (a, b), the orifice was rotated 90° so that it would shoot the water jet sideways in the trench box. In Setup 2 (c, d), the leak was rotated 180° downwards and the results allowed to analyse the differences for leak orientations at different flowrates. In Setup 3(a, b), the flow rate and leak orientation were kept constant as in the control experiment while changing the thinner geotextile surrounding the inner tank with a thicker one to decrease the water flow through the perforated sides from a magnitude of 77 l/s/m² to 16 l/s/m². For Setup 3 (c, d), the inner box was aligned with the thinner textile on the shorter sides and the thicker textile on the longer and bottom sides. This Setup was planned according to real installation conditions where along the shorter side of a typical trench, there would be graded soil material and in-situ soil on the longer side. Hence, the last Setup allowed the investigation of water leakage paths resulting in real installation conditions.

Table 3-3: Experiments details summary

Experiment Setup	Parameters		
	Flow Rate (l/h)	Leak Orientation (°)	Soil Permeability (l/s/m ²)
1(a) (b) (c)	200	0	77
	400	0	77
	800	0	77
2(a) (b)	200	90	77
	800	90	77
(c) (d)	200	180	77
	800	180	77
3(a) (b)	200	0	16
	800	0	16
(c) (d)	200	0	16 / 77
	800	0	16 / 77

3.5 Individual Experiments

3.5.1 Effect of Flow Rate

From literature, the flow rate in the pipe plays a significant role on leakage flow which in turn increases the size of the fluidisation zone in the surrounding soil. Similarly, leakage flow rate increases the velocity of the particles within the fluidisation zone (Van Zyl *et al.*, 2013).

From Table 3-3 experimental Setup 1(a), (b), (c) have flow rates 200 l/h, 400 l/h and 800 l/h respectively. The soil moisture from the 7 sensors and the leakage outflow from iPERL meters were taken for a low flow rate of 200 l/h and then, the flow rate was increased to analyse the effect of changing flow rate on leakage flow paths. The flow rate was increased at 4 hours intervals, and the data from both data loggers were downloaded accordingly.

3.5.2 Effect of Leak Orientation

The aim of experimental Setups 2 was to determine the effect of leak orientation on the leakage flow paths. From the literature, the location of the leak affects the leakage flow outside the pipe. From literature, positions of the fluidisation zone around the pipe in the tank will depend on the leak orientation. Figure 3-30 shows how the location of the leak was interpreted in this particular research. For an upward pointing leak, the angle is 0° , sideways is 90° and bottom leak is 180° .

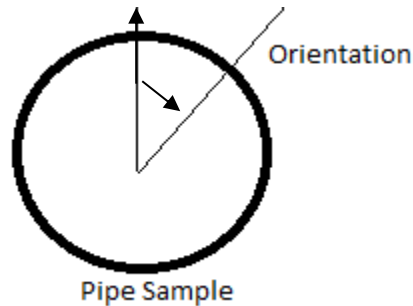


Figure 3-26: Orientation adopted for leak location

Figure 3-31 illustrates a pipe setup for the upward pointing leak while Figure 3-32 shows how the pipe was rotated to obtain a pipe leaking sideways.



Figure 3-27: Upward pointing Leak

Figure 3-32 also shows a 100 x 100 x 10 mm squared uPVC which was inserted to protect the inner tank from the water jet. The distance between the jet and sidewall of the tank was only

200mm and as such, it was likely that the high velocity jet would damage the tank if the experiment was run for longer time periods. The results obtained from this setup were interesting and are described in detail in section 4.3.3.

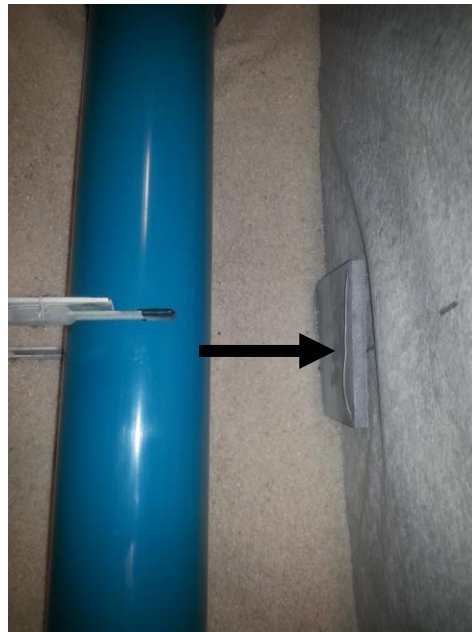


Figure 3-28: Leak pointing Sideways

3.5.3 Effect of Soil Permeability

From literature, it was important to understand how leakage water flows on the different sides of the trench walls. The apparatus was designed to allow for the modification of the side and bottom walls by changing the geotextile. Fibertex F-25 and F-1000 have different permeability properties and were used to check the influence of the wall permeability.

Experimental Setups 3 (a, b) were designed with geotextile F-1000 which was a thicker textile with lower permeability property. The experiment allowed to differentiate the results of leakage flow paths between a trench walls of higher and lower permeability.

Experimental Setups 3 (c, d) adopted a different approach by aligning the shorter sides of the trench box with the thinner textile and the longer and bottom sides with the thicker textile. Figure 3-33 shows a typical trench details for a normal distribution pipe. The excavated soils are normally replaced by selected granular and backfill soils while the surrounding soils are still the compacted and undisturbed soil. Hence, experimental Setups 3 (c, d) considered the fact that the soils on the shorter side of the trench box are likely to be more permeable than the longer section if a pipe running along a trench in real installation conditions is considered. Figure 3-33 shows the typical trench details for backfill of a trench in cross-section.

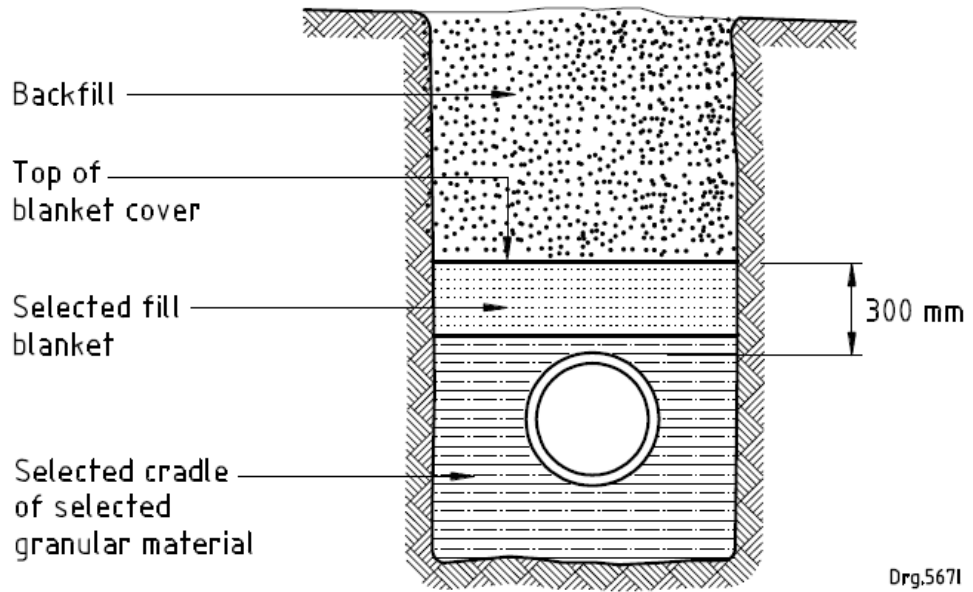


Figure 3-29: Typical Trench Details for (SANS 1200 DB)

4. Results and Discussions

Chapter 4 reports the results of the five sets of experiments that were described in Section 3.5. The results of the experiments are discussed by integrating their influence on water leakage routes. The chapter concluded with a few experimental observations.

4.1 Flow rate

The effect of flow rate on leakage flow paths was determined for the first set of experiments. Table 4-1 indicates the parameters used in this set up. Three different flow rates are used in the experiments namely, 200 l/h, 400 l/h and 800 l/h respectively.

Table 4-1: Parameters details for experiments on the effect of flow rates

Experiment Setup	Parameters		
	Flow Rate (l/h)	Leak Orientation (°)	Soil Permeability (l/s/m ²)
1(a)	200	0	77
1(b)	400	0	77
1(c)	800	0	77

Sections 4.1.1 – 4.1.3 display the results of the EC-5 moisture sensors and iPERLs smart meters in different graphs. Figure 4-1 shows for the locations of the sensors and smart meters.

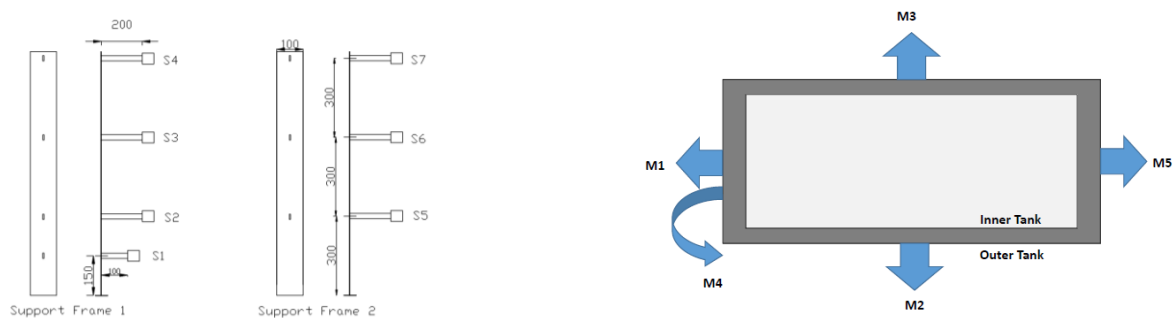


Figure 4-1: Locations of EC-5 sensors and iPERLS

4.1.1 Inlet Flow rate: 200 L/h

Figure 4-2 shows the results of the 7 moisture sensors for a flow rate of 200 l/h. The volumetric moisture content (VMC) was measured 1 minute intervals. Figure 4-2 shows that Sensor S1 showed the greatest influence and started to measure volumetric moisture content (VMC) after 15 mins. Sensor S1 was the closest sensor to the leaking pipe. A minor jump from $0.15 \text{ cm}^3/\text{cm}^3$ to $0.225 \text{ cm}^3/\text{cm}^3$ in moisture reading of S1 was noted between 15 and 30 minutes and then, it recorded a steady increase in VWC for the next 3hrs before reaching a constant value of approximately $0.35 \text{ cm}^3/\text{cm}^3$. Sensor S2 started recording VMC after 1 hour and reached a constant value $0.175 \text{ cm}^3/\text{cm}^3$ at the end. The other 5 sensors did not record any VMC and it can be deduced that leakage water did not reach the other sensors in this test. It can be suggested that more leakage water was flowing next to the pipe and to the bottom of the tank. Sensor S2 was located 100 mm above the upward pointing circular leak and leakage water reached the sensor by capillary action.

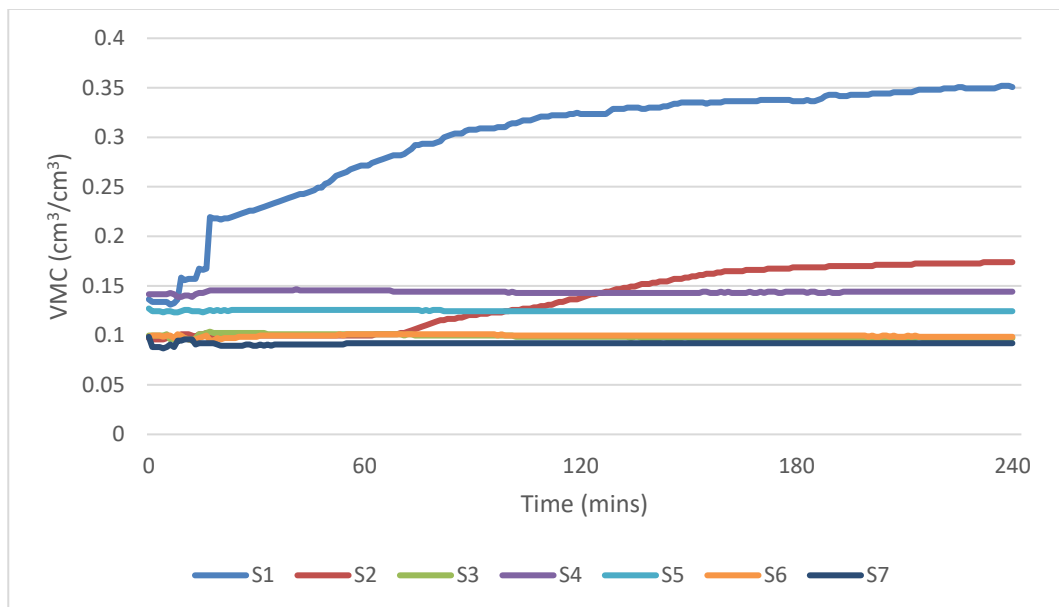


Figure 4-2: Moisture Content Readings for 200 l/h Flowrate

Figure 4-3 shows leakage water outflow readings through the smart meters. Meter M4 was the only meter recording flow indicating that water was only flowing through the bottom of the trench box and there was no flow through the side walls. The reading on the meter reached a constant value of approximately $0.0032 \text{ m}^3/\text{min}$ which matched to the inlet flow of 200 l/h ($0.0033 \text{ m}^3/\text{min}$).

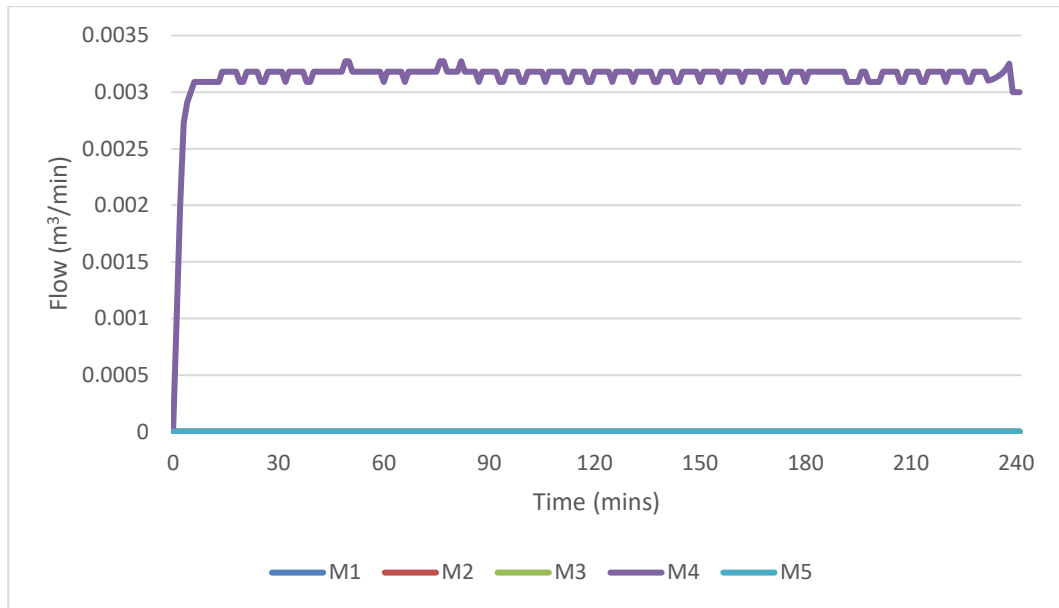


Figure 4-3: Leakage Outflow Readings for 200 l/h

4.1.2 Inlet Flow rate: 400 L/h

Figure 4-4 illustrates the VMC readings for an increased flow rate of 400 l/h. Sensor S1 recorded the highest VMC. At the start of test, the VMC of S1 increased from 0.2 cm^3/cm^3 to 0.5 cm^3/cm^3 and reached to a relatively constant value of 0.6 cm^3/cm^3 at the end of the 4 hrs test. S2 recorded VMC between 0.20 and 0.28 cm^3/cm^3 during the test. The remaining 5 sensors recorded no change in VMC throughout the test.

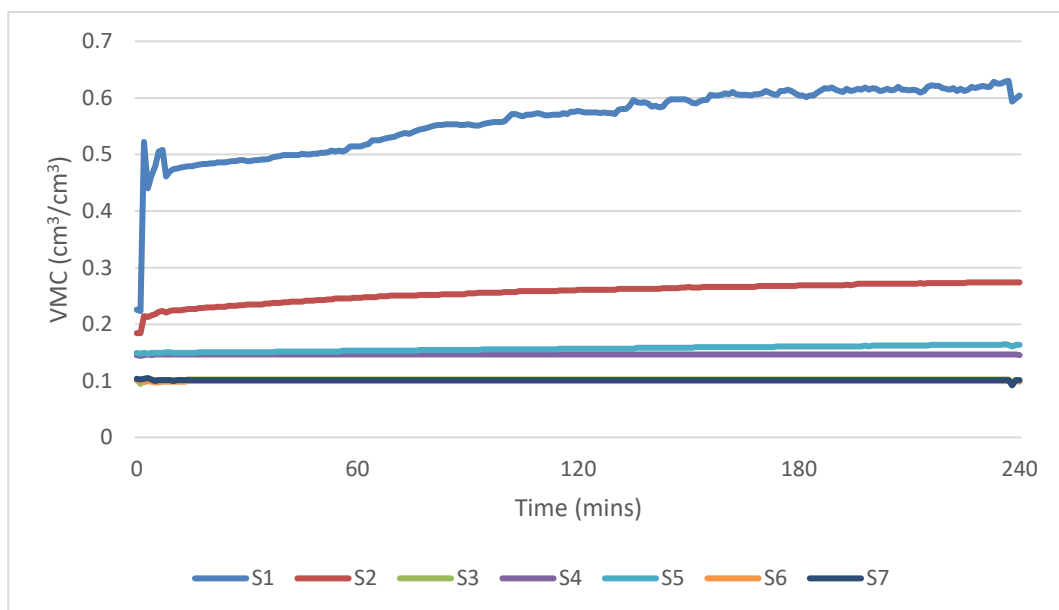


Figure 4-4: Moisture Content Readings for 400 l/h Flowrate

Figure 4-5 shows the outflow leakage recorded for the different drainage outlets for experiment 1(b). Similar to experiment 1(a), only Meter M4 recorded water flow through, that is, water was only flowing through the bottom of the trench. Doubling the flowrate from 200 l/h to 400 l/h had little effect on the flow of water through the walls of the trench box. The water flowing through Meter M4 stabilised at a value of 0.0059 m³/min which equals roughly the inlet flow of 400 l/h (0.0066 m³/min). The reason for the slight difference in conservative flow could be because of the minor water losses at the connection point of the reinforced hose and drainage outlet.

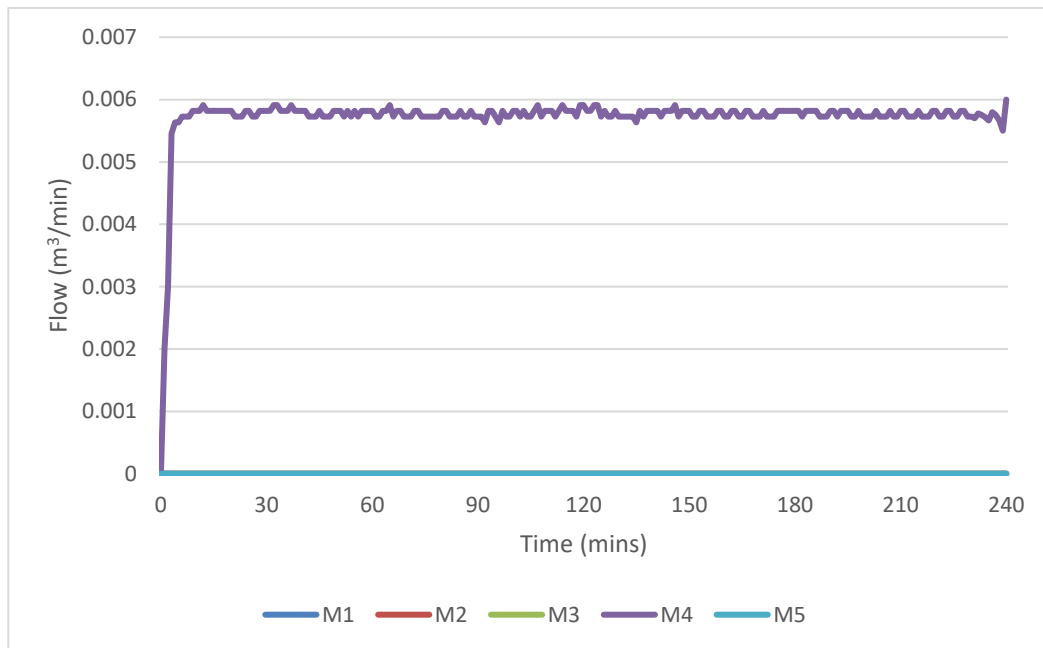


Figure 4-5: Leakage Outflow Readings for 400 l/h

4.1.3 In-let Flow rate: 800 L/h

Figure 4-6 shows the results of the sensors for a flow rate of 800 l/h. The results showed a difference from the previous two tests with lower flow rates. Only 2 sensors did not record any readings of VMC. S4 and S7 did not record any change in VMC and these sensors were near the sand surface. Sensor S1 was recording a constant value of around 0.38 cm³/cm³ VMC throughout the test. Sensor S2 fluctuated between 0.2 and 0.3 cm³/cm³. These fluctuations indicated that the water flowing near Sensor S2 was changing abruptly. Interestingly enough, S3 recorded the highest VMC values for this experiment. S3 was positioned at 400mm above the leak orifice and the results indicate that the water jet was shooting high up around Sensor S3 but not reaching the surface since Sensor S4 did not record any VMC readings.

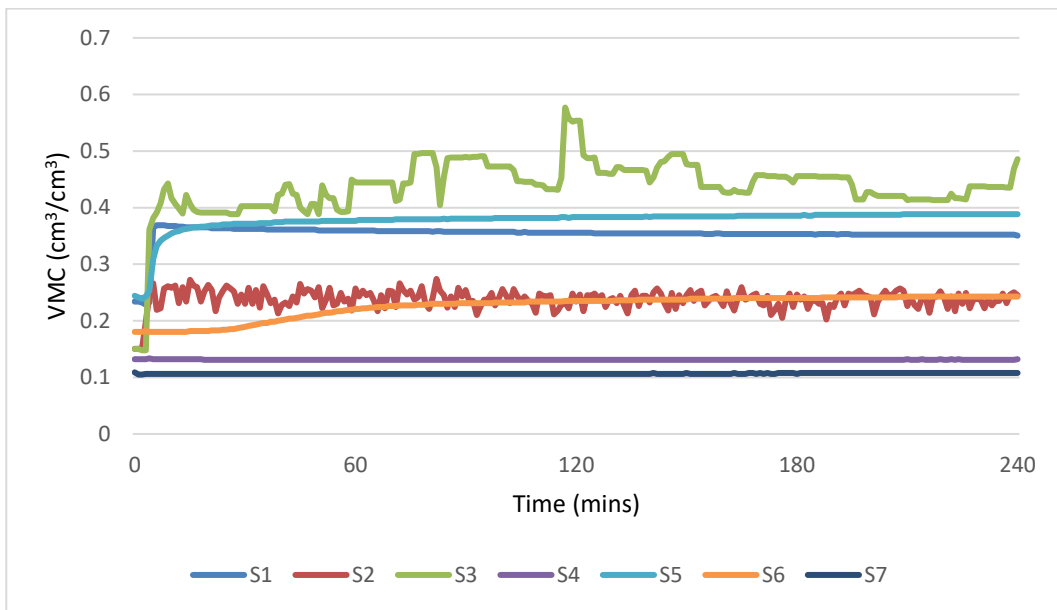


Figure 4-6: Moisture Content Readings for 800 l/h Flowrate

Figure 4-6 shows leakage outflow readings through the different walls of the trench box. It shows that all meters recorded water flow through the draining pipes and no meter was reading zero. Meters M1 and M4 recorded the higher flow rates in this experiment, that is, 0.0059 and 0.0057 m³/min respectively. Meters M2, M3 and M5 were reading below 0.001 m³/min. The longer side walls of the trench recorded low flow rates.

The total outflow was approximated as $(0.0059 + 0.0005 + 0.0002 + 0.0057 + 0.0008) = 0.0131$ m³/min which equalled to the inlet flow of 800 l/h (0.0132 m³/min).

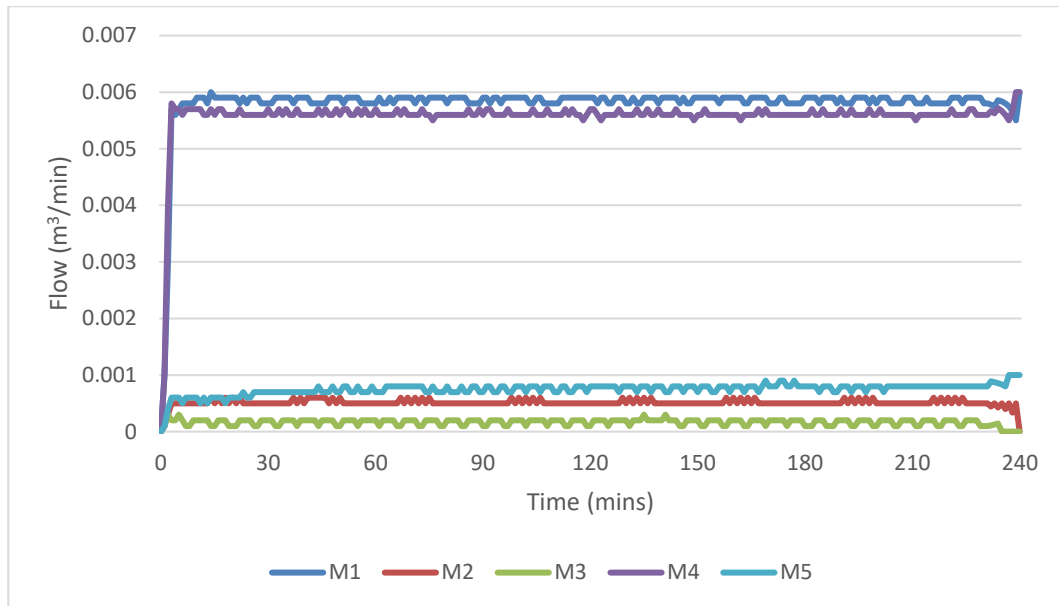


Figure 4-7: Leakage Outflow Readings for 800 l/h

4.2 Effect of Leak Orientation

The effect of leak orientation on water leakage flow paths was determined in the second set of experiments. The pipe was allowed to leak sideways by rotating 90° and downwards by rotating 180° . Table 4-2 indicates the parameters used in this setup. The flow rates used in this experiment are 200 l/h and 800 l/h respectively.

Table 4-2: Parameters details for experiments on the effect of leak orientation

Experiment Setup	Parameters		
	Flow Rate (l/h)	Leak Orientation ($^\circ$)	Soil Permeability (l/s/m ²)
(a)	200	90	77
(b)	800	90	77
(c)	200	180	77
(d)	800	180	77

4.2.1 Leak Orientation 90° , Inlet Flow rate: 200 L/h

Figure 4-8 shows the results of the moisture sensors recorded for a flow rate of 200 l/h. Sensor S1 showed the greatest influence and measured a VMC of $0.3 \text{ cm}^3/\text{cm}^3$ in the 4 hours of the test. Sensor S2 recorded a drop in VMC after 30 mins of the test and then increased at a constant value $0.175 \text{ cm}^3/\text{cm}^3$ at the end. The other 5 sensors did not record any VMC changes and it can be

deduced that leakage water did not reach other sensors in this test. It can be concluded that more leakage water was flowing next to the pipe and to the bottom of the tank.

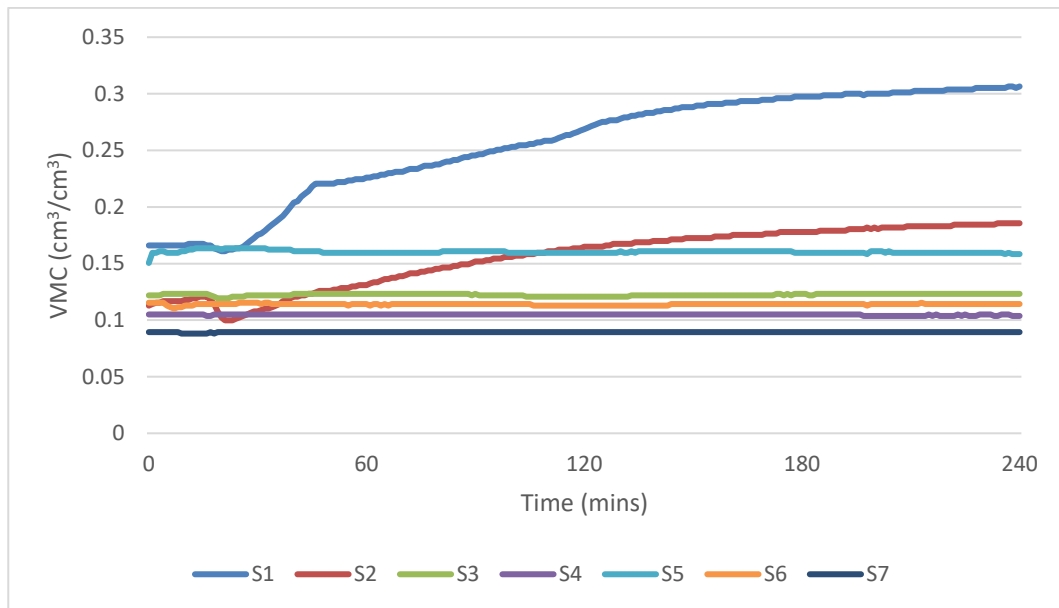


Figure 4-8: Moisture Content Readings for 200 l/h Flowrate

Figure 4-8 shows leakage outflow readings through the iPERL meters for this test. It shows that only Meter M4 recorded flow and the other meters' readings were zero. As such, leakage water was only flowing through the bottom of the trench box as was the case for experiment 1 for the same flow rate. The reading on the meter reached a constant value of approximately 0.0035 m³/min which equalled the inlet flow of 200 l/h (0.0033 m³/min).

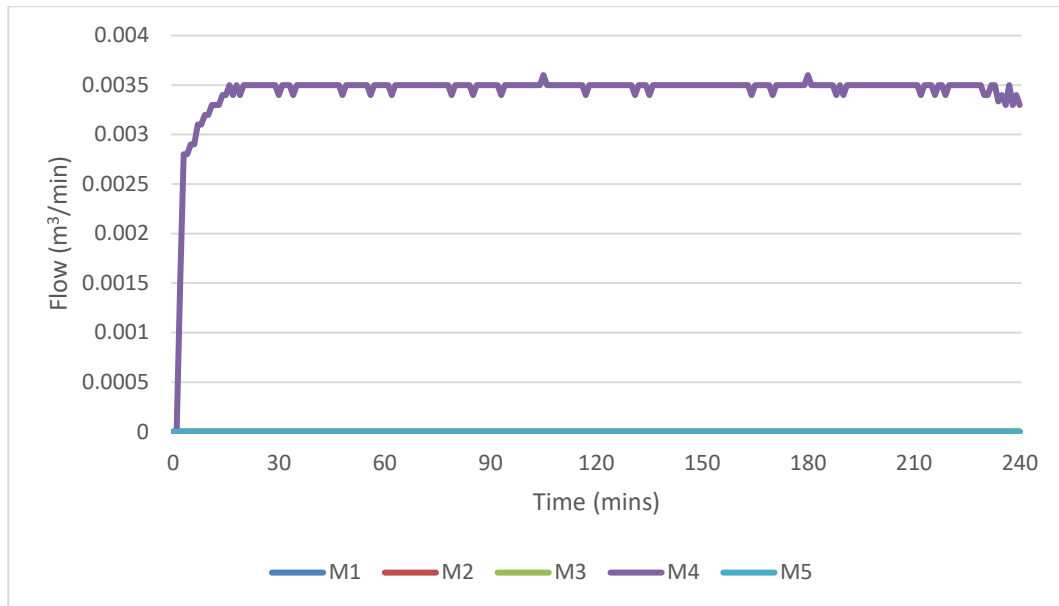


Figure 4-9: Leakage Outflow Readings for 200 l/h

4.2.2 Leak Orientation 90°, Inlet Flow rate: 800 L/h

Figure 4-10 shows the results of the sensors for a flow rate of 800 l/h. Sensors S1 and S2 recorded a maximum value at the beginning of the experiment and remained almost constant throughout the test. S1 attained a maximum value of $0.8 \text{ cm}^3/\text{cm}^3$ after 15 mins and then, was at a constant value of around $0.77 \text{ cm}^3/\text{cm}^3$ throughout the test. S2 attained a maximum value of $0.65 \text{ cm}^3/\text{cm}^3$ and then, was at a constant value of around $0.62 \text{ cm}^3/\text{cm}^3$. Interestingly enough, Sensor S5 recorded VMC values for this experiment. It was positioned at a height of 300mm on support frame 2. The other 4 sensors did not record any VMC readings. The results in Figure 4-9 indicates that most water was flowing at the bottom of tank and did not reach sensors S3 and S6 which were placed at a height of 600mm from the bottom of the tank.

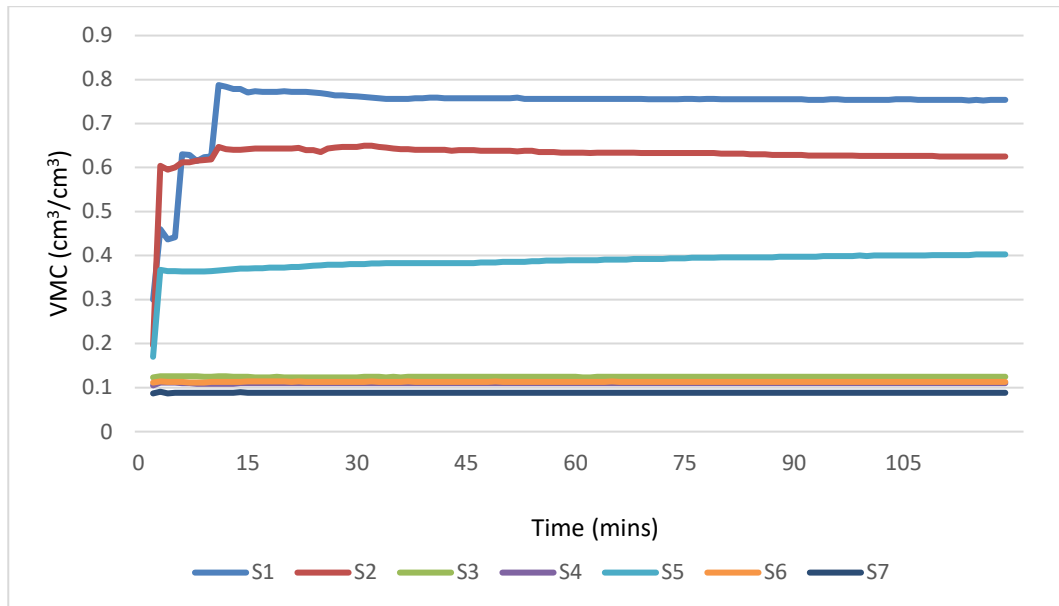


Figure 4-10: Moisture Content Readings for 800 l/h Flowrate

It has to be noted that with a flow rate of 800 l/h could not be tested for 4 hours because the leak was on the side and the high velocity jet started to destroy the geotextile after running the test for 2 hrs.

Figure 4-11 shows leakage outflow readings through the walls of the trench box for a flow rate of 800 l/h. It shows that all meters recorded water flow through the pipe and no meter was reading zero. Meters M1 and M4 recorded the highest flow rates in this experiment, that is, 0.0059 and 0.0057 m³/min respectively. Meters M2, M3 and M5 were reading flows below 0.001 m³/min. Similarly to experiment 1(c), the results of this experiment regarding leakage outflow was intriguing because there was relatively much higher flow through one of the shorter side of the tank than other. On the contrary, both of the longer side walls of the trench recorded low flow rates.

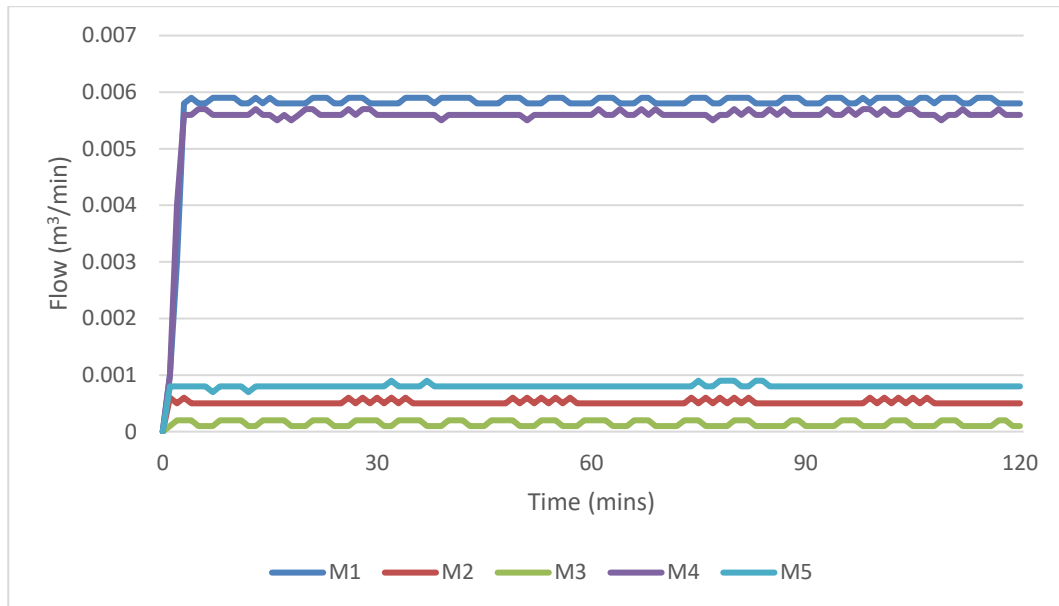


Figure 4-11: Leakage Outflow Readings for 800 l/h

The total outflow was approximated as $(0.0059 + 0.0005 + 0.0002 + 0.0057 + 0.0009) = 0.0132$ m^3/min which equalled the inlet flow of 800 l/h ($0.0132 \text{ m}^3/\text{min}$).

4.2.3 Leak Orientation 180°, Inlet Flow rate: 200 L/h

Figure 4-12 shows the results of the moisture sensors recorded for a flow rate of 200 l/h and leak orientation 180°. Only Sensor S1 measured changes in VMC. A minor jump from 0.15 to 0.27 cm^3/cm^3 in moisture content reading of S1 is noted at the beginning of the test and then, it increased steadily before reaching a constant value of approximately 0.37 cm^3/cm^3 at the end of test. The other 6 sensors did not record any VMC and it can be concluded that leakage water did not reach the other sensors in this test. It is shown from the results that most of the leakage water is flowing at the bottom of the trench with a downward pointing leak and low flow rate.

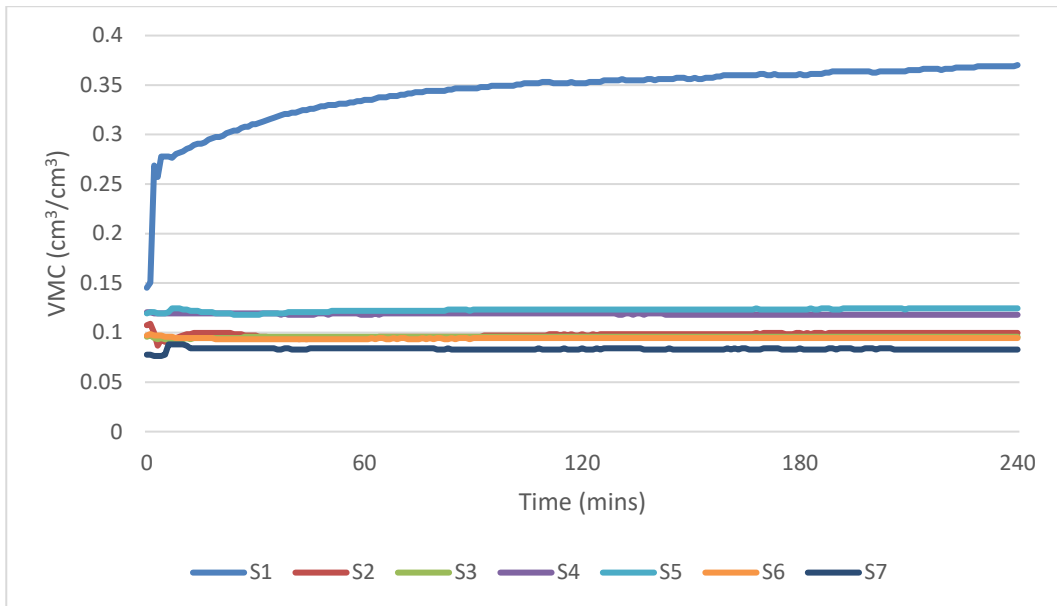


Figure 4-12: Moisture Content Readings for 200 l/h Flowrate

Figure 4-13 shows leakage outflow readings through the meters for 200 l/h flow rate and leak orientation 180° . It shows that only Meter M4 recorded flow and the other meters' readings were zero. As such, leakage water was only flowing through the bottom of the trench box and there was no flow through the side walls. The reading on the meter reached a constant value of approximately $0.0033 \text{ m}^3/\text{min}$ which equalled the inlet flow of 200 l/h ($0.0033 \text{ m}^3/\text{min}$).

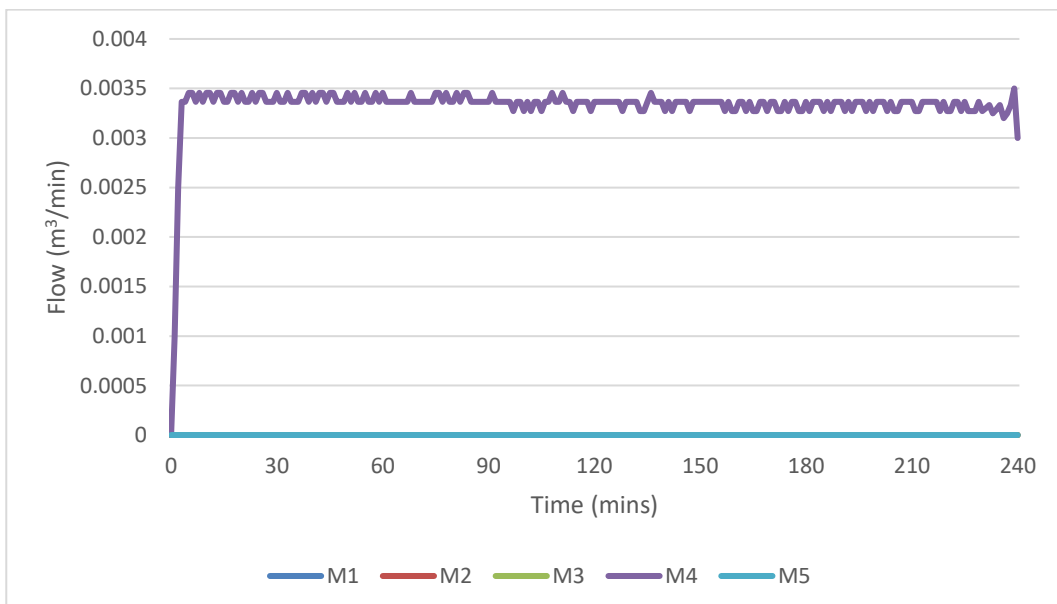


Figure 4-13: Leakage Outflow Readings for 200 l/h

4.2.4 Leak Orientation 180°, Inlet Flow rate: 800 L/h

Figure 4-14 shows the results of the sensors for a flow rate of 800 l/h and leak orientation 180°. The results were slightly similar to the previous experiment with a flowrate of 200 l/h. Only Sensor S1 could read changes in VMC in the tank. All the other sensors did not record any change in VMC and thus, it can be concluded that even at higher a flow rate, for a downward pointing leak, leakage water was flowing to the bottom of the trench. Sensor S1 was recording a constant value of around $0.7 \text{ cm}^3/\text{cm}^3$ VMC throughout the test with fluctuations of $\pm 0.5 \text{ cm}^3/\text{cm}^3$.

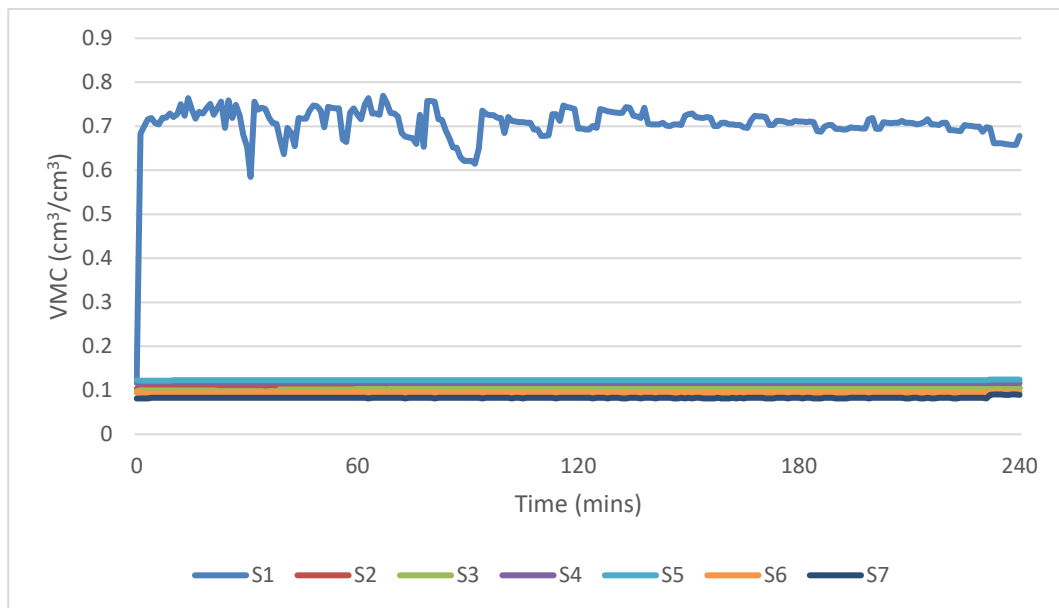


Figure 4-14: Moisture Content Readings for 800 l/h Flowrate

Figure 4-15 shows leakage outflow readings through the different walls of the trench box for 800 l/h and leak orientation 180°. It shows that all meters recorded water flow through their respective pipes and no meter was reading zero. Meters M1, M3 and M4 recorded the highest flow rates in this experiment, which is, $0.0034 \text{ m}^3/\text{min}$, $0.0039 \text{ m}^3/\text{min}$ and $0.0047 \text{ m}^3/\text{min}$ respectively. Meter M2 was reading flow below $0.001 \text{ m}^3/\text{min}$ at the beginning until the 160 mins when it started recording flowrate slightly above $0.001 \text{ m}^3/\text{min}$.

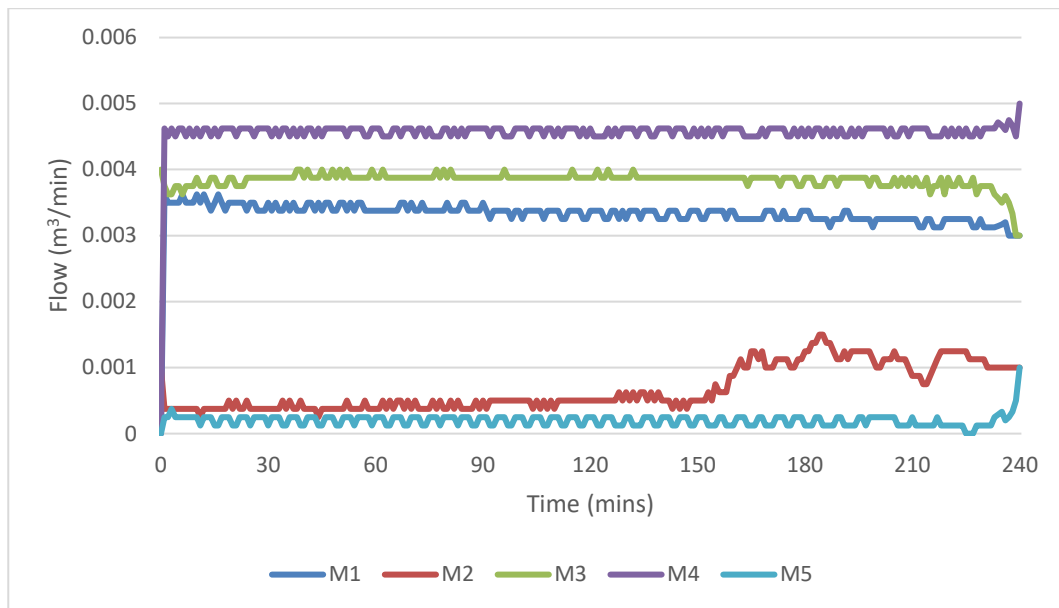


Figure 4-15: Leakage Outflow Readings for 800 l/h

The total outflow was approximated as $(0.0034 + 0.0009 + 0.0039 + 0.0047 + 0.0002) = 0.0131$ m^3/min which equalled to the inlet flow of 800 l/h ($0.0132 \text{ m}^3/\text{min}$).

4.3 Effect of Soil Permeability

The effect soil permeability was determined by aligning the walls of the trench with a thicker textile. Two cases were considered where firstly, the leak orientation was set to the original position of 0° i.e. facing upwards and the soil permeability was changed to a thicker textile all around the trench for one round of tests. The second round of tests had the permeability changed by aligning the shorter side of the trench with the thinner textile and the longer side and bottom walls with the thicker textile, thus the shorter side was more permeable than the longer and bottom sections. Table 4-4 indicates the parameters used in this setup. Flow rates 200 l/h and 400 l/h were used.

Table 4-4: Parameter details for experiments on the effect of soil permeability

Experiment Setup	Parameters		
	Flow Rate (l/h)	Leak Orientation ($^\circ$)	Soil Permeability (l/s/m ²)
(a)	200	0	16
(b)	800	0	16
(c)	200	0	16/77
(d)	800	0	16/77

4.3.1 Soil Permeability 16 l/s/m², Inlet Flow rate: 200 L/h

Figure 4-16 shows the results of the moisture sensors recorded for a flow rate of 200 l/h in and soil permeability 16 l/s/m². Only Sensors S1 and S2 were influenced by leakage flow. S1 showed the greater influence and recorded an increase from 0.15 to 0.5 cm³/cm³ during the test. Sensor S2 also recorded VMC from 0.15 to 0.45 cm³/cm³. The other 5 sensors did not record any VMC measurements and it can be concluded that leakage water did not reach the other sensors in this test. It can be concluded that leakage water was flowing next to the leaking pipe and most definitely not reaching a height close to 300mm above the leak since sensor S3 was not influenced.

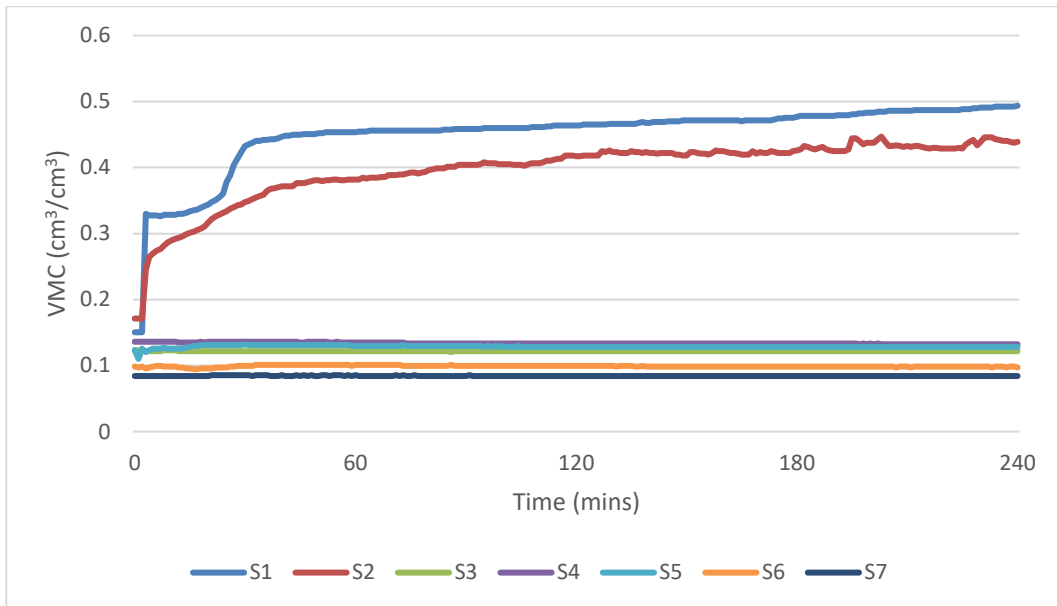


Figure 4-16: Moisture Content Readings for 200 l/h Flowrate

Figure 4-17 shows leakage outflow readings through meters at flow rate 200 l/h and Soil Permeability 16 l/s/m^2 . It shows that only Meter M4 recorded flow and the other meters' readings were zero. Leakage water was only flowing through the bottom of the trench box and there were no flow through the side walls. The reading on the meter reached a constant value of approximately $0.0034 \text{ m}^3/\text{min}$ which equals to the inlet flow of 200 l/h ($0.0033 \text{ m}^3/\text{min}$). Figure 4-17 shows that Meter M4 only started recording after 15 mins and this is probably because of a slow water flow through the thicker textile.

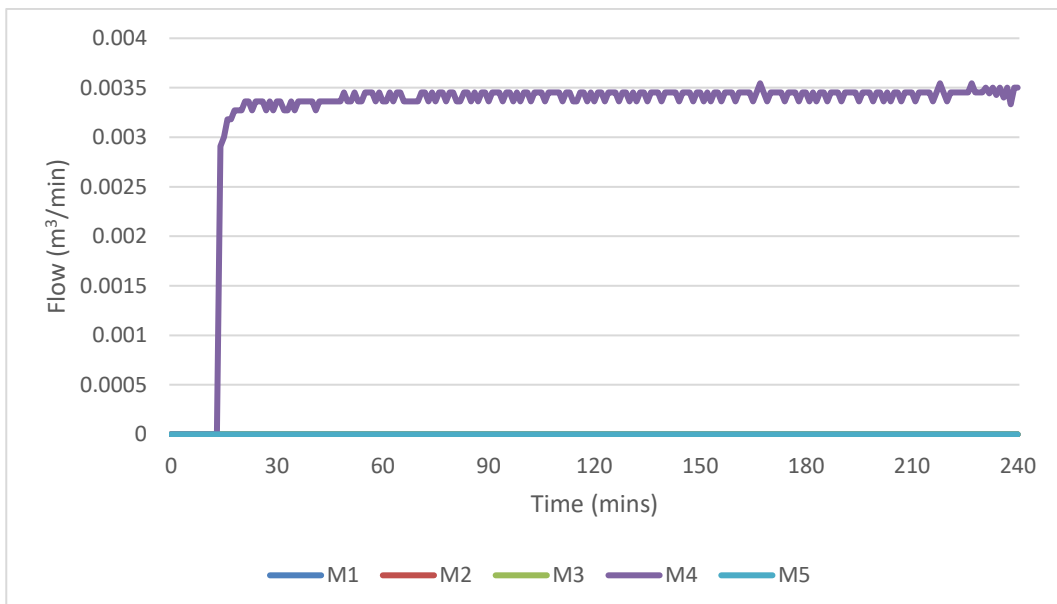


Figure 4-17: Leakage Outflow Readings for 200 l/h

4.3.2 Soil Permeability 16 l/s/m², Inlet Flow rate: 800 L/h

Figure 4-18 shows the results of the sensors for a flow rate of 800 l/h and soil permeability 16 l/s/m². Sensors S4, S6 and S7 did not record any change in VMC. Sensor S1 moisture readings varied between 0.7 and 0.8 cm³/cm³ and Sensor S2 readings varied between 0.5 and 0.7 cm³/cm³ during the test. Sensor S3 started recording VMC after nearly 2 hrs during the test. It is important to point out that when the readings of Sensor S2 started to decrease, the readings of S3 started to increase. This might be due to capillary movements upwards towards Sensor S3 and this was not apparent for the setup with the thinner geotextile. Sensor S5 had a constant value of around 0.4 cm³/cm³ throughout the experiment.

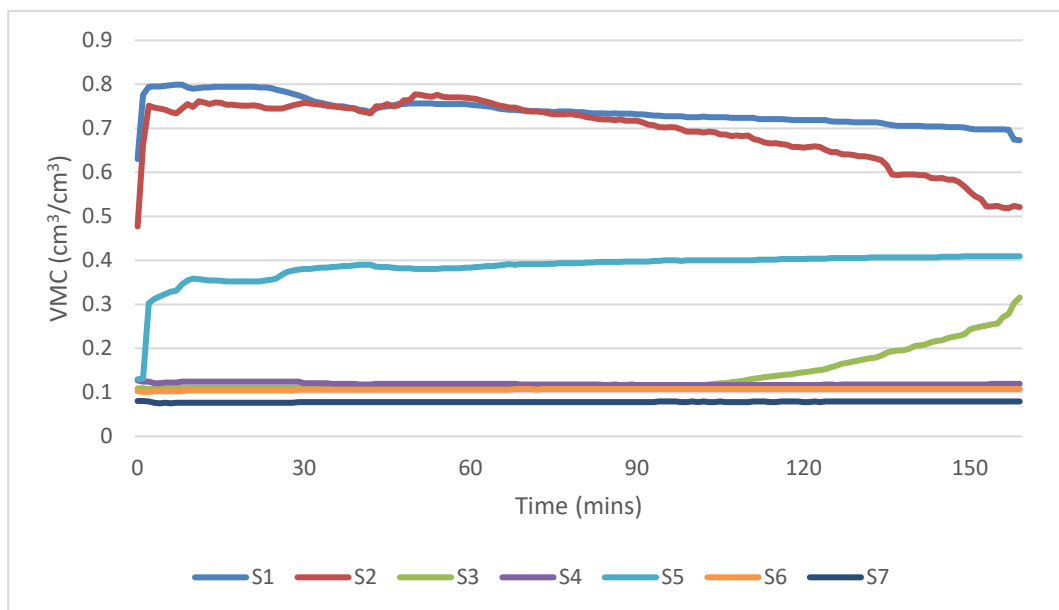


Figure 4-18: Moisture Content Readings for 800 l/h Flowrate

Figure 4-19 shows leakage outflow readings through the different walls of the trench box at a flow rate of 800 l/h and soil permeability 16 l/s/m². It shows that all meters recorded water flow through the pipe and no meter was reading zero. Meters M1, M3 and M4 recorded the highest flow rates in this experiment, that is, 0.0051, 0.0049 and 0.0048 m³/min respectively. Meters M2 and M5 were reading approximately 0.0012 and 0.001 m³/min respectively. The results of this experiment regarding leakage outflow were interesting because Meter M3 recorded relatively high flow rates as compared to previous experiments performed.

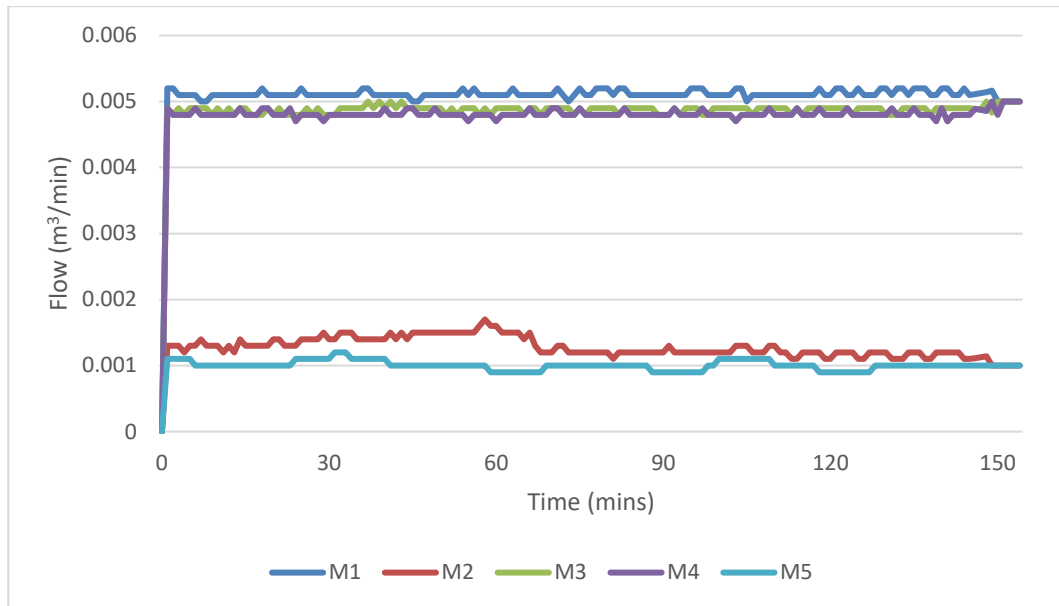


Figure 4-19: Leakage Outflow Readings for 800 l/h

The total outflow was approximated as $(0.0012 + 0.0009 + 0.0049 + 0.0048 + 0.0051) = 0.0139$ m^3/min which equalled to the inlet flow of 800 l/h ($0.0132 \text{ m}^3/\text{min}$).

4.3.3 Soil Permeability of 16 and 77 l/s/m², Inlet Flow rate: 200 L/h

Figure 4-20 shows the results of the sensors for a flow rate of 200 l/h and soil permeability of 16 and 77 l/s/m². It shows that only Sensor S1 was influenced by leakage water during this test. The readings of Sensor S1 varied between 0.7 and 0.8 cm^3/cm^3 throughout the experiment. The other sensors did not record any VMC values and it can be deduced that leakage water did not reach the other sensors in this test. It is suggested that all leakage water was flowing next to the leaking pipe.

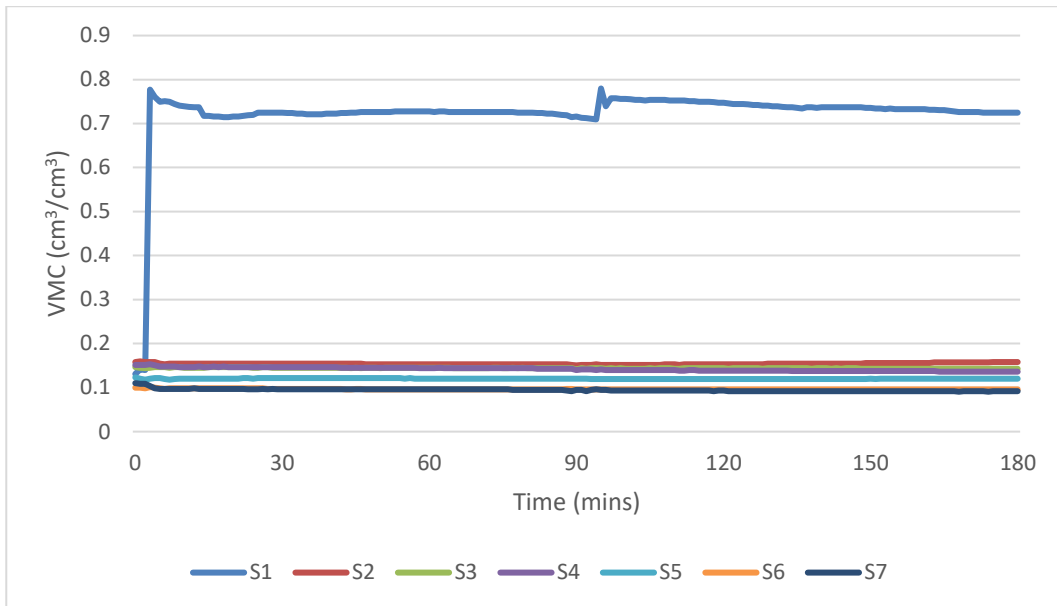


Figure 4-20: Moisture Content Readings for 200 l/h Flowrate

Figure 4-21 shows leakage outflow readings through the meters. It shows that only Meter M4 recorded flow and the other meters' readings were zero. As such, leakage water was only flowing through the bottom of the trench box and there was no flow through the side walls. The reading on the meter was a constant value of approximately $0.003 \text{ m}^3/\text{min}$ for the first 90mins and then, increased to $0.0035 \text{ m}^3/\text{min}$ which roughly equals to the inlet flow of 200 l/h ($0.0033 \text{ m}^3/\text{min}$).

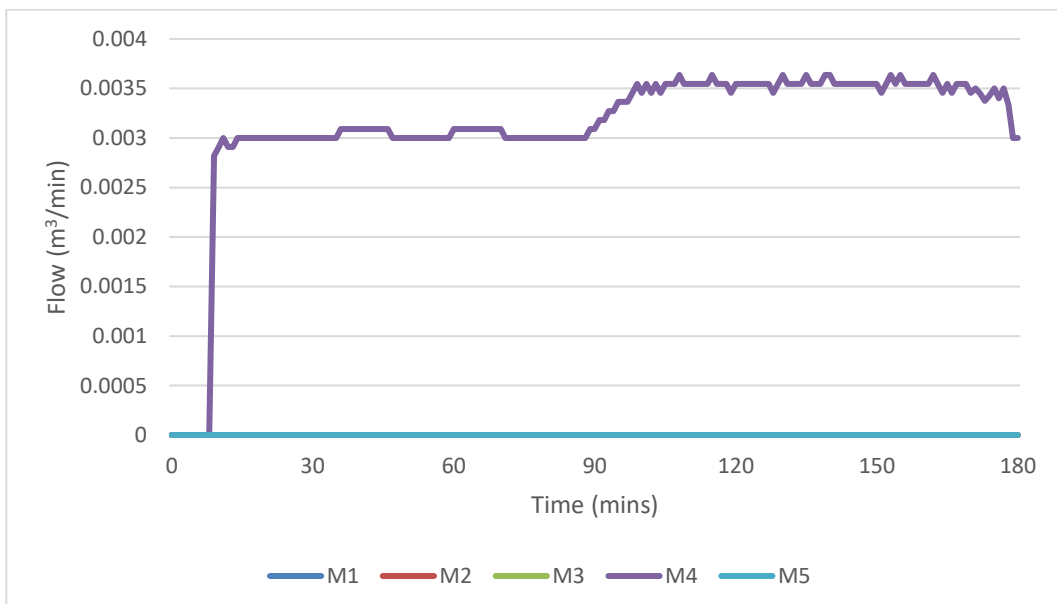


Figure 4-21: Leakage Outflow Readings for 200 l/h

4.3.4 Soil Permeability of 16 and 77 l/s/m², Inlet Flow rate: 800 L/h

Figure 4-21 shows the results of the sensors for a flow rate of 800 l/h. Only Sensors S1, S2 and S5 were influenced by leakage water. Sensors S1, S2 and S5 were recording a VMC of 0.7, 0.8 and 0.3 cm³/cm³ respectively during the test. The other sensors which were close to the sand surface did not record any change in VMC.

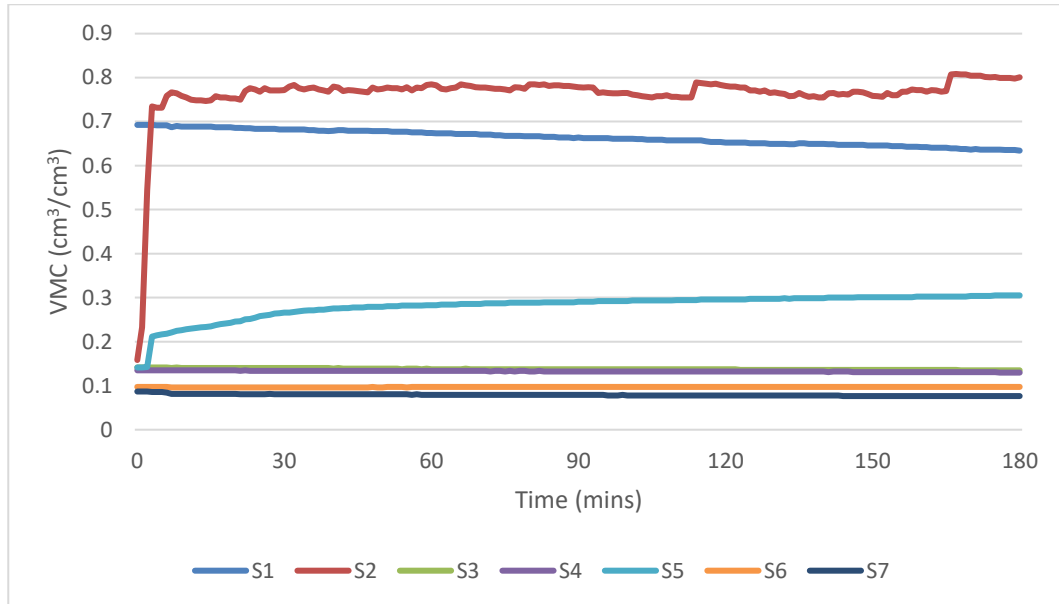


Figure 4-22: Moisture Content Readings for 800 l/h Flowrate

Figure 4-23 shows leakage outflow readings through the different walls of the trench box for 800l/h. It shows that all the meters recorded water flow and no meter was reading zero. Meters M1, M3 and M4 recorded the highest flow rates in this test. The values of the 3 Meters were almost the same and fluctuating between 0.0045 and 0.005 m³/min. Meters M2 and M5 were reading very low flow which can be assumed to be negligible.

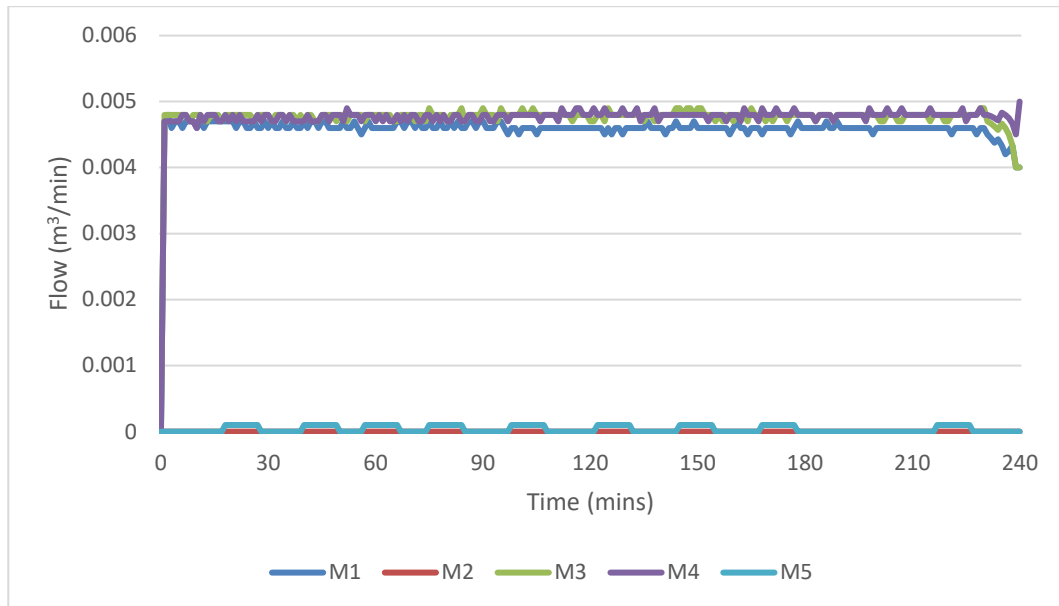


Figure 4-23: Leakage Outflow Readings for 800 l/h

The total outflow was approximated as $(0.0001 + 0.00005 + 0.0047 + 0.0047 + 0.0046) = 0.0134 \text{ m}^3/\text{min}$ which equalled to the inlet flow of 800 l/h ($0.0132 \text{ m}^3/\text{min}$).

4.4 Sensitivity of leakage paths to Influential Factors

The study showed how the three basic factors have an influence on leakage flow paths in a typical trench. The method of measuring volumetric moisture content at different locations in the trench and amount of leakage water flowing through the walls of the trench were used to describe leakage paths in the experiments.

In experiment 1, the flow rate was increased from 200 to 800 l/h to quantify the effect of flow rate on the moisture contents at different locations and flow through the walls with respect to time. The results showed that with an increased flow rate in the pipe, more sensors started recording moisture content readings and implying that leakage water was spreading or diffusing around the tank. At a flowrate of 800 l/h, the water did not reach the surface since the sensors near the surface did not record any volumetric moisture content. With regards to the flow of water through walls, at lower rates, the water was flowing only to the bottom while for a higher flow rate the flow was distributed between the side and bottom walls but still, mostly flowing at the bottom.

For the effects of leak orientations, experiments 1 and 2 can be compared with respect to the different flow rates in the pipe. The results of experiments 1 and 2 would compare an upward, sideway and downward pointing leak jet at a given flow rate. For low flow rate, the results of moisture content around the tank was nearly similar and most flowing at the bottom of the trench. For an increased flow rate, the results differ significantly. The results of tests 1(c) and 2 (b) were almost similar with regards to volumetric moisture content and leakage outflow though the walls.

Experiment 2(d) which had the leak pointing downwards differed by recording moisture content through S1 found next to the pipe and most water was flowing at the bottom of the trench.

The third influential factor studied was in-situ soil permeability in the trench by varying the aligned geotextile permeability. The experiments 1 and 3 can be compared with respect to the flow rate in the pipe. At a low flow rate of 200 l/h, the results of volumetric moisture content and leakage outflow through the walls were almost similar. Only sensors S1 and S2 was recording moisture readings and all water flowing at the bottom of the trench. With an increased flow rate of 800 l/h, there was not any big difference in the results. In both experiment tests 3(b) and 3(d), the meters M1, M3 and M4 recorded flow rates of the same magnitudes.

In conclusion of the above discussion, it can be summarised that influential factors flow rate and leak orientation have the most significant effect on leakage paths in the trench while the influence of the in-situ soil permeability was not really substantial.

4.5 Experimental Observations

A number of interesting observations were made during the testing of the experiments. Some observations were found to be problematic. These observations, as well as their effects and how they were overcome are described in this section.

4.5.1 Damaged EC-5 sensor by water jet

During the running of a trial experiment, the inlet flow rate was increased to 1200 l/h while observing real time readings using the EM 5 data logger of volumetric moisture contents in tank. At some point in time, the Sensor S2 starting to record unrealistic and negative values. When the testing ended and the pipe was being removed from the tank for next experimental Set up, Sensor S2 was found to have broken as shown in Figure 4-24 below.



Figure 4-24: Damaged sensor above leak



Figure 4-26 Minor Leak at the bottom of tank



Figure 4-27: Leakage at drainage outlets

4.5.4 Perforation of Protective Material

During testing of the leak orientation at 90° , a protective piece of uPVC was used to prevent the water from damaging the tank as discussed in Section 3.6.2. At the end of testing with an inlet flow rate of 800 l/h, it was interesting to note how the uPVC board was affected. The water jet from the leak actually perforated the board and started to destroy the aligned geotextile in the first 2 hours. As such, the testing had to be stopped to prevent any further damaged. Figure 4-28 below shows how the material was perforated by the water jet after 2 hours. The hole produced in the 10mm thick uPVC board had an outer diameter of 46mm and inner diameter of 27mm. Figure 4-29 shows how sand started to accumulate in between the inner and outer tank when the geotextile was damaged.

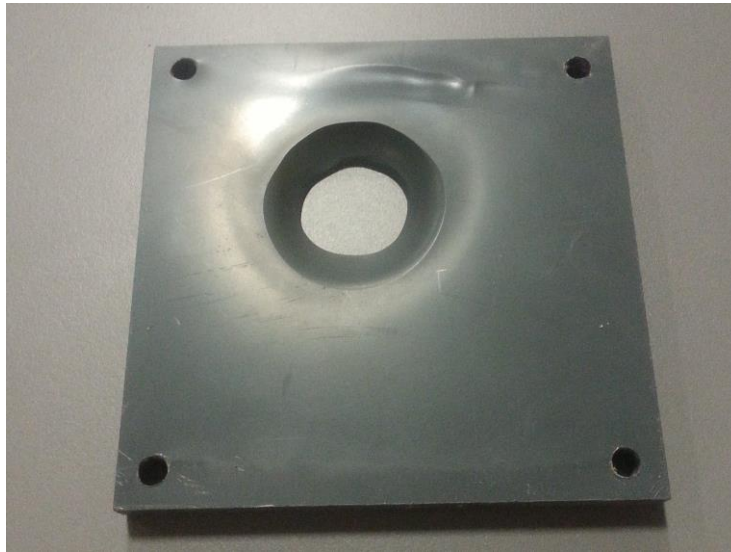


Figure 4-27: PVC board drilled by water jet



Figure 4-28: Accumulated sand

4.5.5 Leak Orientation

It was important to ensure that the leak orientation in the buried pipe stayed the same after the tank was backfilled. During the removal of the pipe sample after the trial test, it was seen that the leak was slightly angled towards one side of the tank while it was supposed to be an upward pointing leak. Figure 4-30 below shows how the leak jet would project if not properly fixed at the bottom and as a result of the tests. As such, the results of the testing would not be reliable. Hence, appropriate measures were taken to ensure the correct leak orientation by hard-pressing the pipe sample into the compacted sand bed during installation.

5. Conclusions and Recommendations

In recent years, many studies in the water distribution systems have been done to investigate the effect of pressure on leakage. However, only a few research have done on the interaction between the pipe and surrounding soil conditions. In this study, an experimental technique was developed to investigate the movement of water leaking from distribution pipes and hence, the interaction of a buried pipe in sand was considered from both a hydraulic and geotechnical point of view.

An inner box was manufactured from perforated metal sheets according to the standard trench dimensions for a 110 mm diameter pipe. The inner box was lined with a geotextile to represent the permeability of the in-situ soil. Water moving through the geotextile and inner box drained down in the gap between the inner and a solid outer box, where it was collected through drainage pipes. The gap between the inner and outer box consisted of a number of isolated chambers that allowed to measure the quantity of water entering through each of the five walls of the inner box.

Three parameters namely flow rate, leak orientation and in-situ soil permeability were varied to understand the movement of the leak flow. The soil moisture levels were measured using EC-5 moisture sensors at different depths to analyse the movement of leakage water and iPERLS smart water meters were used to measure the flow of water through the walls of the trench. The results of the above-mentioned parameters on leakage paths were discussed.

5.1 Key Findings

The study showed that the flow rate has significant influence on the leakage paths in the trench box. The higher the flow rate, the greater the water was spreading in the trench. With a higher the flow rate, the water was moving through the side walls of the tank and not only at the bottom as compared with low flow.

It was found that the leak orientations had a major effect on the flow of leakage in the trench. For an orientation downward pointing leak, volumetric moisture content was only measured at the sensor located next to the pipe sample irrespective of the flow rate and the water was mostly flowing through the bottom of the tank.

The results of the experiments also indicated that the in-situ soil permeability that was replicated with geotextiles had little effect on leakage paths as compared to the other two factors.



5.2 Recommendations for Further Work

This study on leakage flow paths was considered as preliminary work where more time was devoted into designing and manufacturing the experimental equipment. By using the proposed methods of investigation, three parameters were studied based on the literature. As a result, there are a few recommendations to improve the design of equipment and the testing method.

As mentioned in Section 4.7.5, the pipe orientation can be disturbed while filling the tank with backfill and therefore, it is recommended that a proper support mechanism is devised to hold the pipe in the correct orientation during investigation.

An important design modification can be made at the bottom of the tank where there are two draining outlets one above the other. It is noticed that the bottom section of tank tends to receive water quicker than the other compartments. As such, the water fills up the bottom section and overflowing water is likely to be transported to the next compartment. This is a possible reason why meter M1 was recording high flow in some experiments.

The moisture sensors can be made more robust by enclosing the sensors in a manufactured box to support the device. Likewise, the sensors can be more resistant to high velocity jets being projected by the leaks.

In this research, a flow rate was set and readings taken. The same setup was used to get readings for an increased flow rate. It is suggested that a different set up can be used for an increased flowrate and the results can be compared with those obtained in this study.

The tests were performed on unsaturated porous medium and further studies can be done in saturated soils where different parameters can be varied.

The apparatus can be further modified by allowing the pipe sample to be run across the tank instead of using end caps as in this study. As such, the water can be circulated as in real reticulation systems and the difference can be compared.

In this study, only a few basic parameters were tested and therefore, more parameters can be identified from the literature to be tested by the same measuring methods. For example, burial depth can be varied.



- Hlushkou, D., and Tallarek, U. (2006) 'Transition from creeping via viscous-inertial to turbulent flow in fixed beds', *Journal of Chromatography A*, 1126(1–2), pp. 70–85.
- Lambert, A. (2001) 'What do We Know about Pressure Leakage Relationship in Distribution Systems?', in *Proceedings of IWA Specialised Conference: System Approach to Leakage Control and Water Distribution Systems Management*. Brno, pp. 89–96.
- Ledwith, C., Weisman, R. N. and Lennon, G. P. (1990) 'Selection of Hole size for Fluidisation Pipes', *American Society of Civil Engineers*, pp. 933–938.
- Ma, C. H. (2011) *Internal Fluidisation due to Horizontal Seepage – A Laboratory Study*. University of Southampton.
- Marunga, A., Ziykomborero, H. and E., K. (2006) 'Pressure management as a leakage reduction tool: The case of the City of Mutare, Zimbabwe', *Physics and Chemistry of the Earth 31*, pp. 763–770.
- Massimilla, L., Volpicelli, G. and Zenz, F. (1963) 'Flow of fluid particle suspensions from liquid-fluidised beds', *Industrial and Engineering Chemistry Fundamentals*, 2, pp. 194–199.
- Mutikanga, H. . (2012) *WATER LOSS MANAGEMENT: Tools and Methods for Developing Countries*. Delft University of Technology.
- Niven, R. K. (2003) 'Turbulent Flow Through Porous Media', *Ground water*, 39(5), pp. 646–650.
- Niven, R. K. and Khalili, N. (1998) 'In situ fluidisation by a single internal vertical jet', *Journal of Hydraulic Research*, 36(2), pp. 199–228. doi: 10.1080/00221689809498633.
- Pike, S. (2015) *Experimental Investigation of Leakage-Induced Pipe Erosion Outside of Pipe Leaks*.
- Rogers, D. (2014) 'Leaking Water Networks: An Economic and Environmental Disaster', *Procedia Engineering*, 70, pp. 1421–1429. doi: 10.1016/j.proeng.2014.02.157.
- Seago, C., Bhagwan, J. and Mckenzie, R. (2004) 'Benchmarking leakage from water reticulation systems in South Africa', in, pp. 25–32.
- Spangler, M. G. and Handy, R. . (1982) *Soil Engineering*. Harper & Row.
- Taylor, D. W. (1948) *Fundamentals of Soil Mechanics*. New York: John Wiley.
- Terzaghi, K. (1943) *Theoretical Soil Mechanics*. New York: John Wiley and Sons.
- Venkataraman, P. and Rao, P. R. M. (1998) 'Darcian, Transitional, and Turbulent flow through porous media.', *American Society of Civil Engineers*, (9), pp. 840–846.
- Walski, T., Bezts, W., Posluzny, E., Weir, M. and Whitman, B. (2006) 'Modelling Leakage Reduction Through Pressure Control', *Journal of the American Water Work Association*, 98(4), pp. 147–152.
- Walski, T. M., Weir, M., Whitman, B. E. and Bezts, W. (2006) 'Modeling leakage reduction through pressure control', *American Water Works Association*, pp. 147–155.
- Walski, T., Whitman, B., Baron, M. and Gerloff, F. (2009) 'Pressure vs . Flow Relationship for Pipe Leaks', in *World Environmental and Water Resources Congress*. Kansas City: American Society of Civil Engineer, pp. 93–102.
- Ward, J. C. (1964) 'Turbulent Flow in Porous Media', *Journal of Hydraulics Division, ASCE*,



Fibertex geotextiles are used in building and construction works for separation, filtration, drainage, protection, stabilisation and reinforcement. Fibertex geotextiles are manufactured from virgin polypropylene fibres with added UV stabiliser. The basic strength of the Fibertex geotextiles is obtained by needle punching the polypropylene fibres, which provides strong elastic bonding. Fibertex is highly durable and resistant to all natural occurring soil alkalis and acids.

SPECIFICATIONS

Doc No.: FGA COMBINED (SANS) Rev 03 - 04.2016

F_11_7014 REV: 00 Date: 16.03.2016

			F-400M sa	F-500M sa	F-550M sa	F-750M sa	F-1000M sa	F-1200M sa	
Physical Properties									
Thickness	At 2 kPa	mm	3.4	4.2	4.4	5.5	6.5	7.0	SANS 9863:2013
Mechanical Properties									
Static Puncture Strength	CBR Test	N	4 500	6 500	7 100	9 800	12 500	14 000	SANS 12236:2013
Elongation at break		%	>55	>55	>55	>55	>55	>55	SANS 12236:2013
Tensile Strength	MD/CMD	kN/m	25/28	30/38	40.0/40.0	55.0/60.0	70.0/70.0	75.0/75.0	SANS 1525:2013
Elongation at Break		%	>50	>50	>50	>50	>50	>50	SANS 1525:2013
Dynamic Cone Drop		mm	8	4	3	≤1	0	0	SANS 13433:2013
Hydraulic Properties									
Water Flow	50mm Water Head	l/s/m ²	42	38	25	23	16	15	SANS 11058:2013
Permeability	50mm Water Head	m/s	0.04	0.04	0.02	0.02	0.01	0.01	SANS 11058:2013
Permittivity	50mm Water Head	sec ⁻¹	0.85	0.76	0.50	0.47	0.32	0.29	SANS 11058:2013
Pore Size	O _{90%}	micron	70	70	70	70	70	70	SANS 12956:2013
Roll Dimensions									
Widths	Standard	m	5.2						
Length		m	50						
Roll Diameter	Approx.	cm	42		50	58	61	72	

An "M" in the Fibertex product code indicates it is needle punched only, and has not undergone thermal treatment.

Fibertex geotextiles are manufactured to ISO 9001:2008 quality management procedures. The above values represent Typical values based on current production test results.

The information contained in this publication is provided in good faith and to the best of our knowledge is true and accurate.

Fibertex Geotextiles Africa reserves the right to make technical modifications to their products without notice. There is no implied or expressed warranty, and Fibertex Geotextiles Africa does not accept liability for any information supplied, as the conditions of use and installation of the material are out of our control

GAUTENG: (T) +27 (0)11 965 0205
(F) +27 (0)11 965 0231

WESTERN CAPE: (T) +27 (0)21 701 3569
(F) +27 (0)21 701 3381

KWAZULU NATAL: (T) +27 (0)31 736 7100
(F) +27 (0)31 736 7115

APPENDIX B: The following readings are sample data obtained from the EM-5 data logger and H2O utility software for experiment 1(a). The calibration equation was then used to calculate the correct values from the raw data.

EL12937	Port 1 (raw)	Port 2 (raw) EC-5 Soil Moisture m³/m³ VWC	Port 3 (raw) EC-5 Soil Moisture m³/m³ VWC	Port 4 (raw) EC-5 Soil Moisture m³/m³ VWC	Port 5 (raw) EC-5 Soil Moisture m³/m³ VWC
923 records	None				
Measurement Time					
25 Aug 2016 5:20 PM	0	586	556	558	590
25 Aug 2016 5:21 PM	0	584	555	558	590
25 Aug 2016 5:22 PM	0	584	555	558	590
25 Aug 2016 5:23 PM	0	584	555	558	590
25 Aug 2016 5:24 PM	0	584	555	558	590
25 Aug 2016 5:25 PM	0	584	556	559	590
25 Aug 2016 5:26 PM	0	582	557	555	591
25 Aug 2016 5:27 PM	0	583	556	555	590
25 Aug 2016 5:28 PM	0	586	557	557	588
25 Aug 2016 5:29 PM	0	603	559	557	588
25 Aug 2016 5:30 PM	0	601	559	556	589
25 Aug 2016 5:31 PM	0	602	559	555	589
25 Aug 2016 5:32 PM	0	602	558	554	588
25 Aug 2016 5:33 PM	0	602	557	556	590
25 Aug 2016 5:34 PM	0	610	559	559	591
25 Aug 2016 5:35 PM	0	609	559	559	591
25 Aug 2016 5:36 PM	0	610	560	560	592
25 Aug 2016 5:37 PM	0	650	558	561	593
25 Aug 2016 5:38 PM	0	649	558	560	593
25 Aug 2016 5:39 PM	0	649	558	560	593
25 Aug 2016 5:40 PM	0	648	558	560	593
25 Aug 2016 5:41 PM	0	649	558	560	593
25 Aug 2016 5:42 PM	0	649	558	560	593
25 Aug 2016 5:43 PM	0	650	558	560	593
25 Aug 2016 5:44 PM	0	651	558	560	593
25 Aug 2016 5:45 PM	0	652	558	560	593

25 Aug 2016 5:46 PM	0	653	558	560	593
25 Aug 2016 5:47 PM	0	654	558	560	593
25 Aug 2016 5:48 PM	0	655	558	560	593
25 Aug 2016 5:49 PM	0	655	558	560	593
25 Aug 2016 5:50 PM	0	656	558	560	593
25 Aug 2016 5:51 PM	0	657	558	560	593
25 Aug 2016 5:52 PM	0	658	558	560	593
25 Aug 2016 5:53 PM	0	659	558	559	593
25 Aug 2016 5:54 PM	0	660	558	559	593
25 Aug 2016 5:55 PM	0	661	558	559	593
25 Aug 2016 5:56 PM	0	662	558	559	593
25 Aug 2016 5:57 PM	0	663	558	559	593
25 Aug 2016 5:58 PM	0	664	558	559	593
25 Aug 2016 5:59 PM	0	665	558	559	593
25 Aug 2016 6:00 PM	0	666	558	559	593
25 Aug 2016 6:01 PM	0	667	558	559	594
25 Aug 2016 6:02 PM	0	668	558	559	593
25 Aug 2016 6:03 PM	0	668	558	559	593
25 Aug 2016 6:04 PM	0	669	558	559	593
25 Aug 2016 6:05 PM	0	670	558	559	593
25 Aug 2016 6:06 PM	0	671	558	559	593
25 Aug 2016 6:07 PM	0	673	558	559	593
25 Aug 2016 6:08 PM	0	673	558	559	593
25 Aug 2016 6:09 PM	0	676	558	559	593
25 Aug 2016 6:10 PM	0	677	558	559	593
25 Aug 2016 6:11 PM	0	679	558	559	593
25 Aug 2016 6:12 PM	0	682	558	559	593
25 Aug 2016 6:13 PM	0	683	558	559	593
25 Aug 2016 6:14 PM	0	684	558	559	593
25 Aug 2016 6:15 PM	0	685	558	559	593
25 Aug 2016 6:16 PM	0	687	558	559	593
25 Aug 2016 6:17 PM	0	688	558	559	593
25 Aug 2016 6:18 PM	0	689	558	559	593
25 Aug 2016 6:19 PM	0	690	558	559	593
25 Aug 2016 6:20 PM	0	690	558	559	593

25 Aug 2016 6:21 PM	0	690	558	559	593
25 Aug 2016 6:22 PM	0	692	558	559	593
25 Aug 2016 6:23 PM	0	693	559	559	593
25 Aug 2016 6:24 PM	0	694	559	559	593
25 Aug 2016 6:25 PM	0	695	559	559	593
25 Aug 2016 6:26 PM	0	696	559	559	593
25 Aug 2016 6:27 PM	0	697	559	559	593
25 Aug 2016 6:28 PM	0	698	559	559	592
25 Aug 2016 6:29 PM	0	698	559	559	592
25 Aug 2016 6:30 PM	0	698	560	559	592
25 Aug 2016 6:31 PM	0	699	560	558	592
25 Aug 2016 6:32 PM	0	701	561	559	592
25 Aug 2016 6:33 PM	0	703	562	559	592
25 Aug 2016 6:34 PM	0	706	563	558	592
25 Aug 2016 6:35 PM	0	706	564	558	592
25 Aug 2016 6:36 PM	0	707	565	558	592
25 Aug 2016 6:37 PM	0	707	566	558	592
25 Aug 2016 6:38 PM	0	707	567	558	592
25 Aug 2016 6:39 PM	0	707	568	558	592
25 Aug 2016 6:40 PM	0	708	569	558	592
25 Aug 2016 6:41 PM	0	709	570	558	592
25 Aug 2016 6:42 PM	0	712	570	558	592
25 Aug 2016 6:43 PM	0	713	571	558	592
25 Aug 2016 6:44 PM	0	714	571	558	592
25 Aug 2016 6:45 PM	0	715	571	558	592
25 Aug 2016 6:46 PM	0	715	572	558	592
25 Aug 2016 6:47 PM	0	715	572	558	592
25 Aug 2016 6:48 PM	0	717	573	558	592
25 Aug 2016 6:49 PM	0	718	574	558	592
25 Aug 2016 6:50 PM	0	718	574	558	592
25 Aug 2016 6:51 PM	0	718	574	558	592
25 Aug 2016 6:52 PM	0	719	575	558	592
25 Aug 2016 6:53 PM	0	719	575	558	592
25 Aug 2016 6:54 PM	0	719	575	558	592
25 Aug 2016 6:55 PM	0	719	576	558	592

25 Aug 2016 6:56 PM	0	719	576	558	592
25 Aug 2016 6:57 PM	0	720	576	558	592
25 Aug 2016 6:58 PM	0	720	576	558	592
25 Aug 2016 6:59 PM	0	720	577	558	592
25 Aug 2016 7:00 PM	0	722	577	558	591
25 Aug 2016 7:01 PM	0	723	578	558	592
25 Aug 2016 7:02 PM	0	723	578	557	591
25 Aug 2016 7:03 PM	0	724	578	557	591
25 Aug 2016 7:04 PM	0	725	579	557	591
25 Aug 2016 7:05 PM	0	725	579	557	591
25 Aug 2016 7:06 PM	0	725	579	557	591
25 Aug 2016 7:07 PM	0	726	580	557	591
25 Aug 2016 7:08 PM	0	727	580	557	591
25 Aug 2016 7:09 PM	0	728	581	557	591
25 Aug 2016 7:10 PM	0	728	581	557	591
25 Aug 2016 7:11 PM	0	728	582	557	591
25 Aug 2016 7:12 PM	0	729	582	557	591
25 Aug 2016 7:13 PM	0	729	583	557	591
25 Aug 2016 7:14 PM	0	729	584	557	591
25 Aug 2016 7:15 PM	0	729	584	557	591
25 Aug 2016 7:16 PM	0	729	585	557	591
25 Aug 2016 7:17 PM	0	730	586	557	591
25 Aug 2016 7:18 PM	0	730	586	557	591
25 Aug 2016 7:19 PM	0	731	586	557	591
25 Aug 2016 7:20 PM	0	730	587	557	591
25 Aug 2016 7:21 PM	0	730	588	557	591
25 Aug 2016 7:22 PM	0	730	589	557	591
25 Aug 2016 7:23 PM	0	730	590	557	591
25 Aug 2016 7:24 PM	0	730	590	557	591
25 Aug 2016 7:25 PM	0	730	591	557	591
25 Aug 2016 7:26 PM	0	730	591	557	591
25 Aug 2016 7:27 PM	0	730	592	557	591
25 Aug 2016 7:28 PM	0	732	592	557	591
25 Aug 2016 7:29 PM	0	734	593	557	591
25 Aug 2016 7:30 PM	0	734	594	557	591

25 Aug 2016 7:31 PM	0	734	594	557	591
25 Aug 2016 7:32 PM	0	734	595	557	591
25 Aug 2016 7:33 PM	0	735	595	557	591
25 Aug 2016 7:34 PM	0	735	596	556	591
25 Aug 2016 7:35 PM	0	735	596	557	591
25 Aug 2016 7:36 PM	0	735	597	557	591
25 Aug 2016 7:37 PM	0	734	598	556	591
25 Aug 2016 7:38 PM	0	734	598	556	591
25 Aug 2016 7:39 PM	0	735	598	556	591
25 Aug 2016 7:40 PM	0	735	599	556	591
25 Aug 2016 7:41 PM	0	735	599	556	591
25 Aug 2016 7:42 PM	0	735	600	556	591
25 Aug 2016 7:43 PM	0	736	600	557	591
25 Aug 2016 7:44 PM	0	736	600	556	591
25 Aug 2016 7:45 PM	0	737	601	556	591
25 Aug 2016 7:46 PM	0	738	602	556	591
25 Aug 2016 7:47 PM	0	738	602	556	591
25 Aug 2016 7:48 PM	0	739	602	556	591
25 Aug 2016 7:49 PM	0	739	603	557	591
25 Aug 2016 7:50 PM	0	739	603	556	591
25 Aug 2016 7:51 PM	0	739	604	556	591
25 Aug 2016 7:52 PM	0	739	604	556	591
25 Aug 2016 7:53 PM	0	739	605	556	591
25 Aug 2016 7:54 PM	0	739	605	556	592
25 Aug 2016 7:55 PM	0	738	606	556	592
25 Aug 2016 7:56 PM	0	739	606	556	591
25 Aug 2016 7:57 PM	0	739	606	556	591
25 Aug 2016 7:58 PM	0	739	607	556	591
25 Aug 2016 7:59 PM	0	739	607	556	592
25 Aug 2016 8:00 PM	0	740	608	556	591
25 Aug 2016 8:01 PM	0	740	608	556	592
25 Aug 2016 8:02 PM	0	740	608	556	591
25 Aug 2016 8:03 PM	0	740	608	556	591
25 Aug 2016 8:04 PM	0	740	608	556	591
25 Aug 2016 8:05 PM	0	740	608	556	591

25 Aug 2016 8:06 PM	0	740	609	556	591
25 Aug 2016 8:07 PM	0	740	609	556	592
25 Aug 2016 8:08 PM	0	740	609	556	591
25 Aug 2016 8:09 PM	0	740	609	556	591
25 Aug 2016 8:10 PM	0	741	609	556	592
25 Aug 2016 8:11 PM	0	741	609	556	591
25 Aug 2016 8:12 PM	0	741	610	556	592
25 Aug 2016 8:13 PM	0	741	610	556	592
25 Aug 2016 8:14 PM	0	741	610	556	592
25 Aug 2016 8:15 PM	0	741	610	556	591
25 Aug 2016 8:16 PM	0	741	610	556	591
25 Aug 2016 8:17 PM	0	741	610	556	592
25 Aug 2016 8:18 PM	0	741	610	556	592
25 Aug 2016 8:19 PM	0	740	611	556	592
25 Aug 2016 8:20 PM	0	740	611	556	592
25 Aug 2016 8:21 PM	0	740	611	556	592
25 Aug 2016 8:22 PM	0	740	611	556	592
25 Aug 2016 8:23 PM	0	741	611	556	591
25 Aug 2016 8:24 PM	0	740	611	556	592
25 Aug 2016 8:25 PM	0	740	611	556	592
25 Aug 2016 8:26 PM	0	741	611	556	591
25 Aug 2016 8:27 PM	0	742	611	556	591
25 Aug 2016 8:28 PM	0	744	611	556	591
25 Aug 2016 8:29 PM	0	745	612	556	592
25 Aug 2016 8:30 PM	0	745	612	556	591
25 Aug 2016 8:31 PM	0	745	612	556	591
25 Aug 2016 8:32 PM	0	744	612	556	591
25 Aug 2016 8:33 PM	0	744	612	556	592
25 Aug 2016 8:34 PM	0	744	612	556	592
25 Aug 2016 8:35 PM	0	745	612	556	592
25 Aug 2016 8:36 PM	0	745	612	556	592
25 Aug 2016 8:37 PM	0	745	612	556	592
25 Aug 2016 8:38 PM	0	745	612	556	592
25 Aug 2016 8:39 PM	0	745	612	556	592
25 Aug 2016 8:40 PM	0	745	612	556	592

25 Aug 2016 8:41 PM	0	746	612	556	592
25 Aug 2016 8:42 PM	0	746	613	556	592
25 Aug 2016 8:43 PM	0	746	613	556	592
25 Aug 2016 8:44 PM	0	746	613	556	592
25 Aug 2016 8:45 PM	0	746	613	556	592
25 Aug 2016 8:46 PM	0	746	613	556	592
25 Aug 2016 8:47 PM	0	747	613	556	592
25 Aug 2016 8:48 PM	0	747	613	556	592
25 Aug 2016 8:49 PM	0	747	613	556	592
25 Aug 2016 8:50 PM	0	747	613	556	592
25 Aug 2016 8:51 PM	0	747	613	556	592
25 Aug 2016 8:52 PM	0	747	613	556	592
25 Aug 2016 8:53 PM	0	748	614	556	592
25 Aug 2016 8:54 PM	0	749	614	557	592
25 Aug 2016 8:55 PM	0	749	614	556	592
25 Aug 2016 8:56 PM	0	749	614	556	592
25 Aug 2016 8:57 PM	0	749	614	556	592
25 Aug 2016 8:58 PM	0	749	614	556	592
25 Aug 2016 8:59 PM	0	749	614	556	592
25 Aug 2016 9:00 PM	0	749	614	556	592
25 Aug 2016 9:01 PM	0	750	614	556	592
25 Aug 2016 9:02 PM	0	750	614	556	592
25 Aug 2016 9:03 PM	0	750	614	556	592
25 Aug 2016 9:04 PM	0	750	614	556	592
25 Aug 2016 9:05 PM	0	751	614	556	592
25 Aug 2016 9:06 PM	0	751	614	556	592
25 Aug 2016 9:07 PM	0	750	614	556	592
25 Aug 2016 9:08 PM	0	750	614	556	592
25 Aug 2016 9:09 PM	0	750	614	556	592
25 Aug 2016 9:10 PM	0	750	614	556	592
25 Aug 2016 9:11 PM	0	750	614	556	592
25 Aug 2016 9:12 PM	0	750	615	556	592
25 Aug 2016 9:13 PM	0	750	615	556	592
25 Aug 2016 9:14 PM	0	750	615	556	592
25 Aug 2016 9:15 PM	0	750	615	556	592

25 Aug 2016 9:16 PM	0	751	615	556	592
25 Aug 2016 9:17 PM	0	752	615	556	592
25 Aug 2016 9:18 PM	0	752	615	556	592
25 Aug 2016 9:19 PM	0	752	615	556	592
25 Aug 2016 9:20 PM	0	751	615	556	592
25 Aug 2016 9:21 PM	0	751	615	556	592
25 Aug 2016 9:22 PM	0	750	615	556	592
25 Aug 2016 9:23 PM	0	750	615	556	592
25 Aug 2016 9:24 PM	0	750	615	556	592
25 Aug 2016 9:25 PM	0	750	615	556	592
25 Aug 2016 9:26 PM	0	749	615	556	592
25 Aug 2016 9:27 PM	0	749	616	556	592
25 Aug 2016 9:28 PM	0	749	616	556	592
25 Aug 2016 9:29 PM	0	749	616	556	592
25 Aug 2016 9:30 PM	0	750	616	556	592
25 Aug 2016 9:31 PM	0	750	616	556	592
25 Aug 2016 9:32 PM	0	751	616	556	592
25 Aug 2016 9:33 PM	0	752	616	556	592
25 Aug 2016 9:34 PM	0	752	616	556	592
25 Aug 2016 9:35 PM	0	752	616	556	592
25 Aug 2016 9:36 PM	0	753	616	557	592
25 Aug 2016 9:37 PM	0	754	616	557	592
25 Aug 2016 9:38 PM	0	754	617	557	592
25 Aug 2016 9:39 PM	0	754	617	557	592
25 Aug 2016 9:40 PM	0	754	617	557	592
25 Aug 2016 9:41 PM	0	754	617	557	592
25 Aug 2016 9:42 PM	0	754	617	557	592
25 Aug 2016 9:43 PM	0	754	617	557	592
25 Aug 2016 9:44 PM	0	755	617	557	592
25 Aug 2016 9:45 PM	0	755	617	557	592
25 Aug 2016 9:46 PM	0	755	618	557	592
25 Aug 2016 9:47 PM	0	755	618	557	592
25 Aug 2016 9:48 PM	0	755	618	557	592
25 Aug 2016 9:49 PM	0	755	618	557	592
25 Aug 2016 9:50 PM	0	755	618	557	592

25 Aug 2016 9:51 PM	0	755	618	557	592
25 Aug 2016 9:52 PM	0	755	618	557	592
25 Aug 2016 9:53 PM	0	755	618	557	592
25 Aug 2016 9:54 PM	0	755	618	557	592
25 Aug 2016 9:55 PM	0	755	618	557	592
25 Aug 2016 9:56 PM	0	754	618	557	592
25 Aug 2016 9:57 PM	0	754	618	557	592
25 Aug 2016 9:58 PM	0	754	618	557	592
25 Aug 2016 9:59 PM	0	754	618	557	592
25 Aug 2016 10:00 PM	0	755	618	557	592
25 Aug 2016 10:01 PM	0	755	618	557	592
25 Aug 2016 10:02 PM	0	755	618	557	592
25 Aug 2016 10:03 PM	0	755	618	556	592
25 Aug 2016 10:04 PM	0	755	618	557	592
25 Aug 2016 10:05 PM	0	755	618	557	592
25 Aug 2016 10:06 PM	0	754	618	557	592
25 Aug 2016 10:07 PM	0	754	618	557	592
25 Aug 2016 10:08 PM	0	755	618	557	592
25 Aug 2016 10:09 PM	0	754	618	557	592
25 Aug 2016 10:10 PM	0	755	618	557	592
25 Aug 2016 10:11 PM	0	755	618	556	592
25 Aug 2016 10:12 PM	0	755	618	556	592
25 Aug 2016 10:13 PM	0	755	618	557	592
25 Aug 2016 10:14 PM	0	755	618	557	592
25 Aug 2016 10:15 PM	0	756	618	556	592
25 Aug 2016 10:16 PM	0	757	618	556	592
25 Aug 2016 10:17 PM	0	757	619	557	592
25 Aug 2016 10:18 PM	0	757	618	557	592
25 Aug 2016 10:19 PM	0	757	619	557	592
25 Aug 2016 10:20 PM	0	756	619	557	592
25 Aug 2016 10:21 PM	0	757	619	557	592
25 Aug 2016 10:22 PM	0	757	619	557	592
25 Aug 2016 10:23 PM	0	757	619	556	592
25 Aug 2016 10:24 PM	0	756	619	557	592